Molecular analysis of the decision making process in NK cells

presented by

Diplombiologin Doris Urlaub

born in: Würzburg

Dissertation
submitted to the
Combined Faculties for the Natural Sciences and for Mathematics
of the Ruperto-Carola University of Heidelberg, Germany
for the degree of
Doctor of Natural Sciences

presented by
Diplombiologin Doris Urlaub
born in: Würzburg
Oral-examination: _____

Molecular analysis of the decision making process in NK cells

Referees: PD Dr. M. Mayer

Prof. Dr. C. Watzl

Acknowledgments

First of all I'd like to thank Prof. Dr. Carsten Watzl. Thank you for excellent supervision, for always taking the time for helpful discussions. Your optimism and support extremely motivated me.

Furthermore I highly appreciate that PD Dr. Matthias Mayer agreed to represent this work in the Faculty of Natural Science of the University Heidelberg.

I would also like to thank my cooperation partners from the Division of Theoretical Bioinformatics at the DKFZ, Roland Eils, Hauke Busch and especially Sven Mesecke. Your questions and ideas made working on this project so interesting.

I want to thank all past and present members of the Watzllab: Philipp Eißmann, Johanna Endt, Stephan Meinke, Maren Claus, Kristine Kohl, Stefanie Margraf-Schönfeld, Sabine Wingert, Birgitta Messmer, Rauf Bhat, André Cohnen, Stephan Gütgemann, Patrick Rämer and Mina Sandusky. Thank you for teaching me so much, for all the productive discussions and for your friendship.

Additionally, I would like to thank all members in the Institute for Immunology. I've been supported wherever I asked for help.

Last but not least I want to thank the persons in my private life: my mother for always supporting me, my brothers for encouraging me to study and all my friends for backing me up.

Thank you very much!

Summary

Natural killer (NK) cells are a subpopulation of lymphocytes that are involved in the control of different tumors and infections. Unlike T and B cells, NK cells belong to the innate part of the immune system. NK cells carry on their surface a multitude of activating and inhibitory receptors. The regulation of NK cell activation depends on a balance of positive and negative signals initiated by various receptors. Triggering of activating receptors leads to Src family kinase mediated Vav1 phosphorylation, whereas inhibitory receptors dephosphorylate Vav1 via the phosphatase SHP-1. This makes Vav1 the first point where negative signals can intercept the activating signaling cascade. In cooperation with computational biologists we established a mathematical model describing these early signaling events to gain insight into the integration of positive and negative signals on a molecular level. In quantitative mathematical models each equation refers to identifiable processes and parameters have physical interpretation (such as concentration, binding affinity and reaction rate). Therefore we quantified the concentrations of involved molecules. The predictions from the model and our experimental data show that engagement of activating receptors results in a rapid switch-like increase of Vav1 phosphorylation. Similarly, engagement of inhibitory receptors induces a switch-like dephosphorylation of Vav1 that is dominant over activating signals. Comparing experimental results to predictions derived from a family of simplified models shows that kinase association with the NK cell receptors and the enhanced activity of SHP-1 bound to inhibitory receptors is essential to simulate such a physiological response. Interestingly, other concepts of immune receptor signaling such as phosphatase segregation and kinase autophosphorylation were dispensable for our model. The cytotoxic activity of NK cells induced by a combination of activating and inhibitory signals correlates with the switch-like Vav1 phosphorylation. Our data are consistent with a central role of Vav1 in the decision making process of NK cells and enable a novel insight into the integration of positive and negative signals during lymphocyte activation.

Zusammenfassung

Natürliche Killerzellen (NK Zellen) sind eine Lymphozytenpopulation, die dazu beiträgt verschiedenste Krebserkrankungen und Infektionen zu kontrollieren. Anders als T und B Zellen gehören NK Zellen zum angeborenen Immunsystem. NK Zellen exprimieren auf ihrer Oberfläche eine Vielzahl aktivierender und inhibierender Rezeptoren. Die Regulation der Aktivität von NK Zellen beruht auf einem Zusammenspiel der Signale die von den verschiedenen Rezeptoren ausgelöst werden. Die Stimulation aktivierender Rezeptoren bewirkt die Phosphorylierung von Vav1 durch Kinasen der Src Familie, wohingegen Signale der inhibierenden Rezeptoren Vav1 durch die Phosphatase SHP-1 dephosphorylieren können. Dadurch ist Vav1 der erste Schritt der aktivierenden Signalkaskade, der von inhibierenden Signalen beeinflusst werden kann. Um einen Einblick in die Signalverarbeitung auf molekularer Ebene zu bekommen, haben wir in einer Kooperation mit Bioinformatikern ein mathematisches Modell aufgestellt, das diese frühen Signalprozesse beschreiben kann. In quantitativen mathematischen Modellen steht jede Gleichung für einen definierten Prozess und jeder Parameter hat eine physikalische Bedeutung (wie Konzentration, Bindungsaffinität und Reaktionsgeschwindigkeit). Deshalb haben wir die Konzentrationen der beteiligten Proteine quantifiziert. Vorhersagen des Modells und unsere experimentellen Ergebnisse zeigten, dass zunehmende Stimulation der aktivierenden Rezeptoren einen rapiden Anstieg der Vav1 Phosphorylierung verursacht. Wenn gleichzeitig inhibierende Rezeptoren stimuliert werden erfolgt eine Hemmung der Vav1 Phosphorylierung, die über die aktivierenden Signale dominiert. Der Vergleich experimenteller Ergebnisse mit den Berechnungen des Modells zeigt, dass zwei Konzepte essentiell sind um die physiologische Reaktion der Vav1 Phosphorylierung zu erzeugen: die Assoziation der Kinase mit den Rezeptoren und die Verstärkung der SHP-1 Aktivität wenn diese an inhibierende Rezeptoren gebunden ist. Andere Prinzipien der Signalverarbeitung, wie Segregation von Phosphatasen von der Synapse und Kinase Autophosphorylierung, waren in unserem Modell für eine physiologische Reaktion entbehrlich. Wenn NK Zellen durch eine Kombination aktivierender und inhibierender Signale stimuliert werden zeigt die zytotoxische Aktivität das gleiche schalterartige Verhalten wie die Vav1 Phosphorylierung. Unsere Ergebnisse sprechen für eine zentrale Rolle von Vav1 bei der Entscheidungsfindung der NK Zellen. Durch das mathematische Modell wird ein neuer Einblick in die Verarbeitung aktivierender und inhibierender Signale während der Aktivierung von Lymphozyten ermöglicht.

1. Introduction

1.1. An introduction to NK cells

Natural killer (NK) cells are a subset of lymphocytes that were first described in 1975 as having the ability to lyse allogenic tumor cells in mice without prior sensitization (Herberman *et al*, 1975a; Herberman *et al*, 1975b; Kiessling *et al*, 1975a; Kiessling *et al*, 1975b). This defined the term 'natural cytotoxicity' but later on it became clear that this is not the only function of NK cells. Additionally, these cells can secrete proinflammatory cytokines, play an important role in the defense against various pathogens and also have important immunoregulatory functions. Human NK cells are defined as $CD56^+$ and $CD3^-$ but recently the marker NKp46 has been described to be more convenient over species barriers (Walzer *et al*, 2007a; Walzer *et al*, 2007b).

NK cells develop from a common lymphoid progenitor in the bone marrow and represent therefore a third subpopulation of lymphocytes in addition to T and B cells (Colucci *et al*, 2003). Unlike T and B cells, NK cells rely on germ line encoded receptors. Due to the lack of somatic recombination of receptor genes and the ability to carry out effector functions without sensitization NK cells are defined as a part of the innate immune system. They share a bipotential progenitor with T cells, but their development is independent of the thymus. The development of NK cells, including the formation of the receptor repertoire, the acquisition of self tolerance and effector functions, takes place in the bone marrow. The effector mechanisms of NK cells are similar to cytotoxic T lymphocytes, and many receptors that were first described on NK cells are also expressed on different subsets of T cells.

NK cells constitute about 5-15 % of all peripheral blood lymphocytes (PBL), represent 5 % of the lymphocyte population in lymph nodes and are also present in all other secondary lymphoid organs. They circulate through other organs like lung and liver. Two distinct subsets of mature NK cells have been described that are specialized in cytokine production and cytotoxicity. Cytokine production is mainly performed by $CD56^{high}$ $CD16^-$ cells while $CD56^{dim}$ $CD16^+$ cells are thought to be more cytotoxic (Colucci *et al*, 2003). A specialized subtype of NK cells is found in the decidua during pregnancy, probably performing regulatory and antiviral functions (Tabiasco *et al*, 2006). In mucosa-associated lymphoid tissues a recently discovered subset of NK cells is essential for mucosal homeostasis (Malmberg and Ljunggren, 2009).

Under certain conditions the amount and distribution of NK cells in the body can change. Viral infections result in an expansion of the NK cell population (Dokun *et al*, 2001) and NK cells are recruited to the sites of infection (Salazar-Mather *et al*, 1998) or tumor challenge (Smyth et al, 2000). Human NK cells have a turnover time in blood of about 2 weeks and proliferation rates appear to fall with ageing (Zhang *et al*, 2007). In an adoptive transfer experiment in mice, NK cells were detectable in the circulation for about five weeks (Ranson *et al*, 2003).

1.2. NK cell functions

Morphologically NK cells are characterized as large granular lymphocytes. These granules contain perforin and members of the family of granzyme proteases. NK cells form conjugates with target cells, resulting in a highly organized structure at the contact site called immunological synapse (IS) (Davis, 2002). Formation of an activating IS causes polarization of the lytic granules towards the target and degranulation of these granules into the synaptic cleft. Subsequently the target cell membrane becomes permeable and granzymes can induce apoptosis (Lieberman, 2003). The ability to kill target cells by this mechanism is of importance for the clearance of transformed cells and during the response to various viral infections (Cerwenka and Lanier, 2001). NK cells also eliminate cells by triggering death receptors on susceptible target cells. They express the tumor necrosis factor (TNF) related apoptosis inducing ligand (TRAIL) and Fas ligand (CD178) both belonging to the TNF superfamily. If these ligands trigger the respective death receptors they induce a signaling cascade that can lead to apoptosis of the target cell (Chavez-Galan *et al*, 2009). But NK cells are also necessary during other infectious diseases like bacterial infections (e.g. Listeria monocytogenes and mycobacteria) (Kaufmann, 1993), fungal infections (e.g. Cryptococcus) (Murphy and McDaniel, 1982) and parasites (e.g. Leishmania and Toxoplasma) (Korbel *et al*, 2004).

The second important effector mechanism of NK cells is the production and release of cytokines, mainly interferon (IFN)-γ, TNF-α and granulocyte-macrophage colony-stimulating factor (GM-CSF) (Biron *et al*, 1999). In addition to their major role in the defense against certain viral infections, NK cell released IFN-γ and TNF-α are also important for the development of a protective T cell mediated immunity against intracellular pathogens and cancer (Cooper *et al*, 2004; Moretta, 2002). Such 'helper' activity of NK cells is mediated, at least in part, by crosstalk with dendritic cells (DC), either by cytokines or direct cell contact (Degli-Esposti and Smyth, 2005). NK cells therefore not only act as effector cells, but they also serve an important immunoregulatory role (Ferlazzo and Munz, 2004). Despite the expression of the lytic machinery, decidual NK cells are less cytotoxic than blood NK cells. Their functions are not completely understood, but they play a role in controlling extravillous invasion, control of uterine vascular remodeling, and local antiviral activity through the productions of large amounts of cytokines (Tabiasco *et al*, 2006). In mucosa-associated lymphoid tissues a subset of NK cells expressing the transcription factor RORγt has been described recently. These cells have been identified in mice (Luci *et al*, 2009; Sanos *et al*, 2009) and human (Cella *et al*, 2009), produce interleukin (IL)-22 and are essential for mucosal homeostasis and tissue repair.

1.3. NK cell recognition: 'missing' and 'induced' self

The discovery of NK cells in the 1970's was based on their ability to lyse allogenic tumor cells without prior activation (Herberman *et al*, 1975a; Herberman *et al*, 1975b; Kiessling *et al*, 1975a; Kiessling *et al*, 1975b). The phenomenon of F1 hybrid resistance was also established as an NK cell mediated process. But the mechanism

how NK cells recognize their targets stayed mysterious until the 'missing-self' hypothesis was postulated. Based on the observation, that tumor cells resistant to T cell killing were NK susceptible and vice versa, it was hypothesized that NK cells detect if major histocompatibility complex (MHC) class I is missing on the target and attack these cells with low or no MHC class I expression (Karre *et al*, 1986; Ljunggren and Karre, 1985). This hypothesis was supported by the identification of receptors on NK cells that bind to self-MHC class I and are responsible for NK cell inhibition (Karlhofer *et al*, 1992; Moretta *et al*, 1993). Downregulation of MHC class I expression on the cell surface is a common mechanism of many viruses to evade T cell recognition and transformed cells often loose MHC class I expression completely. These cells therefore are susceptible to NK cell recognition. Transplanted grafts that display a different MHC class I pattern than the host are also not able to deliver inhibitory signals to NK cells (Ljunggren and Karre, 1990). For several years the missing-self hypothesis was the only explanation for NK cell activation and specificity. But NK cells also have activating receptors that recognize various ligands on target cells. Some of these ligands are upregulated under certain conditions and then NK cells can be activated in the presence of inhibitory signals, a phenomenon referred to as 'induced-self' (Watzl, 2003). The regulation of NK cell function is therefore better characterized as a fine balance of activating and inhibitory signals (Fig. 1).

1.4. Inhibitory NK cell receptors

The first inhibitory NK cell receptors described were the C-type lectin like Ly49 receptors in the mouse (Karlhofer et al, 1992) now also called killer cell lectin-like receptor family a (Klra). Ly49 receptors are a family of type II transmembrane proteins that recognize MHC class I proteins. Some family members have inhibitory function as they carry an immunoreceptor tyrosine-based inhibition motif (ITIM) in their cytoplasmic tail. Other Ly49 receptors instead interact via a charged amino acid in the transmembrane domain with the immunoreceptor tyrosine-based activation motif (ITAM) containing adapter molecule DNAX activation protein (DAP)12. These receptors therefore are activating, and their ligands are not restricted to MHC class I but they can also recognize MHC class I homologue viral ligands (Daniels *et al*, 2001; Lee *et al*, 2001). The recognition of the mouse cytomegalovirus protein m157 leads to control of the viral infection in mice expressing the respective receptor Ly49H (Kielczewska *et al*, 2007). The first inhibitory receptors characterized on human NK cells were type I transmembrane receptors of the Immunoglobulin (Ig)-superfamily (IgSF), named killer cell Ig-like receptors (KIR) (Wagtmann *et al*, 1995a; Wagtmann *et al*, 1995b).

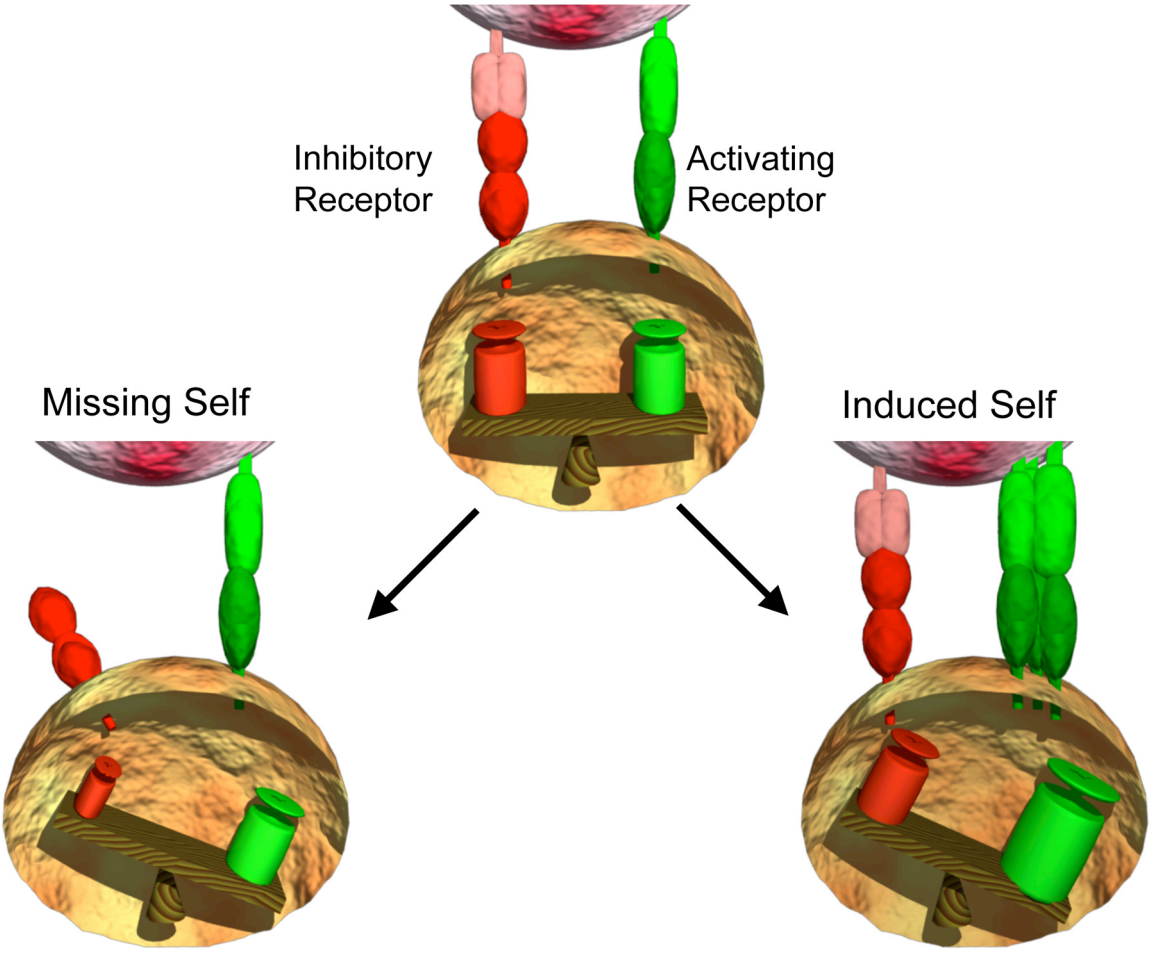

Figure 1: Illustration of missing and induced self. The NK cell (bottom) can bind with activating and inhibitory receptors to the attached target cell (top). The fine balance of inhibitory and activating signals can be shifted towards NK cell activation by the loss of inhibitory ligands (missing self) or by enhanced expression of activating ligands (induced self) on the target cell.

The KIR receptors can be divided in two groups, based on their extracellular domains: they either contain two (KIR2D) or three (KIR3D) Ig-like domains (Fig. 2). Furthermore, similar to Ly49 receptors, they are distinguished by the length of their cytoplasmic tail. Those with a long (L) cytoplasmic tail (KIR2DL and KIR3DL) contain an ITIM and function as inhibitory NK cell receptors, while those with a short (S) cytoplasmic tail (KIR2DS and KIR3DS) deliver activating signals by coupling to DAP12. KIR receptors specifically recognize certain human leukocyte antigen (HLA)-A, -B or -C allotypes, but unlike T cells, this is not peptide specific although the peptide contributes to KIR binding (Rajagopalan and Long, 1997). NK cells also express inhibitory receptors of the C-type lectin-like family, which are conserved between mice and human: NKG2 members forming heterodimers with CD94. The NKG2/CD94 complex specifically binds the non-classical MHC class I molecule HLA-E. The peptides presented by HLA-E are derived from the leader sequence of other MHC class I molecules. Only if it binds a peptide, HLA-E is expressed on the cell surface. The expression of HLA-E is therefore a marker for the overall expression of MHC class I molecules. This receptor complex also comes in inhibitory and activating forms: NKG2A and B contain an ITIM in their cytoplasmic domain whereas NKG2C

and E couple to DAP12 and can deliver activating signals. The sialic-acid-binding immunoglobulin-like lectins (Siglecs) are thought to regulate adaptive and innate immune cells. The Siglec receptors 7 and 9 are expressed on NK cells and have inhibitory properties (Avril *et al*, 2004). Probably Siglecs are necessary in regulating the tolerance of NK cells towards MHC class I low or negative cells, like cells of the nervous system (Crocker *et al*, 2007). Human NK cells also express one inhibitory receptor of the leukocyte immunoglobulin like receptor (LILR) family. LILRB1 binds to a conserved region of HLA class I and can inhibit NK cell activation, but the KIR and NKG2/CD94 receptors seem to play a more dominant role towards MHC class I expressing targets.

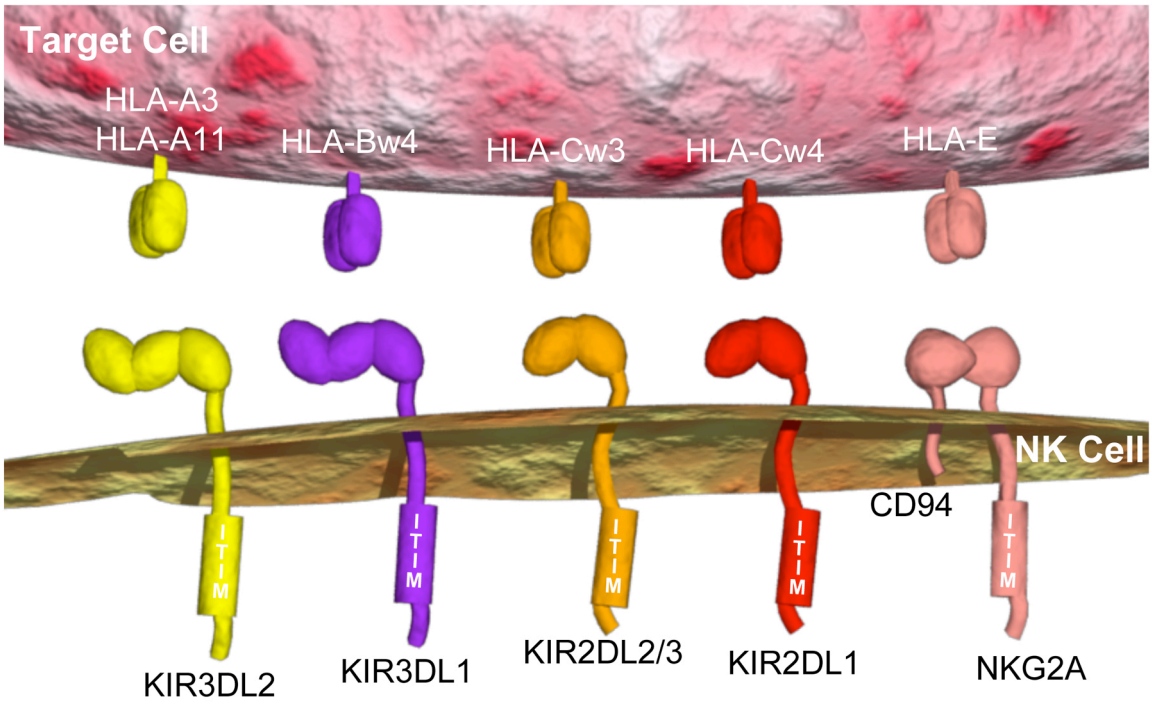

Figure 2: Overview of the human inhibitory receptors and their ligands. Inhibitory KIRs and NKG2/CD94 complexes carry an ITIM in their cytoplasmic domain. KIRs are receptors of the IgSF that bind to different HLA allotypes, while NKG2/CD94 receptors belong to the C type lectin like family and recognize HLA-E.

1.5. Activating NK cell receptors

The activating NK cell receptors are much more heterogeneous than the inhibitory receptors. They cover many different families, use different signaling strategies and recognize various ligands. Some of the activating human NK cell receptors do not have homologue receptors in the mouse and vice versa, or the homologue receptors exhibit distinct signaling properties. This makes it very difficult to compare results gained in the two species. The receptors for the 'natural' cytotoxicity (Fig. 3) recognize cellular ligands that can be ubiquitously expressed, also on healthy cells, or so called induced-self ligands that are upregulated upon cellular stress. The low affinity Fc receptor CD16 (FcγRIII) has a unique role in NK cell activation, as it does not recognize cellular ligands but antibodies bound to target cells. Engagement of CD16 results in antibody-dependent cellular cytotoxicity (ADCC), a mechanism

enabling NK cells to support the antigen-specific adaptive immune response (Trinchieri and Valiante, 1993). ADCC therefore is not part of the 'natural' cytotoxicity. Through this mechanism NK cells also support therapies with monoclonal antibodies, e.g. the B-cell non-hodgkin lymphoma targeting antibody rituximab (Anderson *et al*, 1997; Reff *et al*, 1994) as they help eliminating the cells that are recognized by this antibody.

The receptors responsible for natural cytotoxicity include the family of signaling lymphocyte activation molecule (SLAM) related receptors (SRR) of which NK cells express 2B4 (CD244), CD2-like receptor-activating cytotoxic cells (CRACC/CS1) (CD319) and NK, T- and B-cell antigen (NTB-A) (Claus *et al*, 2008). CRACC and NTB-A are homophilic, but 2B4 binds CD48 a glycophosphatidylinositol (GPI) anchored protein also expressed on NK cells. SRR have in their cytoplasmic tail so called immunoreceptor tyrosine-based switch motifs (ITSM) that can couple to activating and inhibitory signaling pathways. But at least in humans the activating function of SRR is dominant. Another important group of activating receptors are the natural cytotoxicity receptors (NCR) consisting of NKp30 (CD337), NKp44 (CD336) and NKp46 (CD335). NKp30 and NKp46 are expressed on all human NK cells, currently NKp46 is the most specific marker for human and mouse NK cells (Walzer *et al*, 2007a; Walzer *et al*, 2007b). NKp44 is expressed on activated human NK cells only. Despite their importance for NK cell function, the cellular ligands for NKp44 and NKp46 are still unknown. Viral hemagglutinin is recognized by NKp46 and NKp44, resulting in enhanced lysis of infected cells (Arnon *et al*, 2001; Mandelboim *et al*, 2001). Human leukocyte antigen-B-associated transcript 3 (Bat3) has been identified as cellular ligand for NKp30 (Pogge von Strandmann *et al*, 2007) and the consequences of this interaction are currently under investigation. The NKp30 ligand B7-H6 has been described recently and is expressed selectively on tumor cells (Brandt *et al*, 2009). The main tegument protein of human cytomegalovirus (pp65) also interacts with NKp30 but results in suppression of NK cell activity (Arnon *et al*, 2005), representing an immune evasion strategy by this important pathogen. NCRs have no signaling motifs and couple with the ITAM containing adapter molecules CD3ζ (NKp30, NKp46), FcεRI-γ (NKp46) and DAP12 (NKp44) (Moretta *et al*, 2001). The receptor NKp80 activates NK cells if it is bound to its ligand activation-induced C-type lectin (AICL; also called CLEC2B) (Welte *et al*, 2006), but the signaling via the atypic tyrosine motifs of NKp80 is not understood yet. DNAX accessory molecule 1 (DNAM-1) binds the molecules poliovirus receptor (PVR) (CD155) and Nectin-2 (CD112) and also activates NK cells (Gilfillan *et al*, 2008). The C-type lectin like receptor NKG2D has an important role among the activating receptors. The ligands identified so far are MHC class I related chain (MIC) molecules A and B and the UL-16 binding proteins (ULBP). These ligands are of special interest as they are upregulated during cellular stress like infection and transformation (Eagle and Trowsdale, 2007). While mouse NKG2D is also able to bind DAP12, human NKG2D only associates with the DAP10 adapter molecule, which contains an YxNM motif instead of an ITAM. The multitude of these receptors is able to activate NK cells on

their own, but in a physiological context it is hard to discriminate the contribution of a single receptor.

Integrins like lymphocyte function-associated antigen (LFA)-1 play a special role in NK cell activation, as they are necessary for stable adhesion of NK cells to their targets. Interaction of LFA-1 with its ligand ICAM-1 is already sufficient to induce polarization of granules, but does not trigger NK cell degranulation (Bryceson *et al*, 2005).

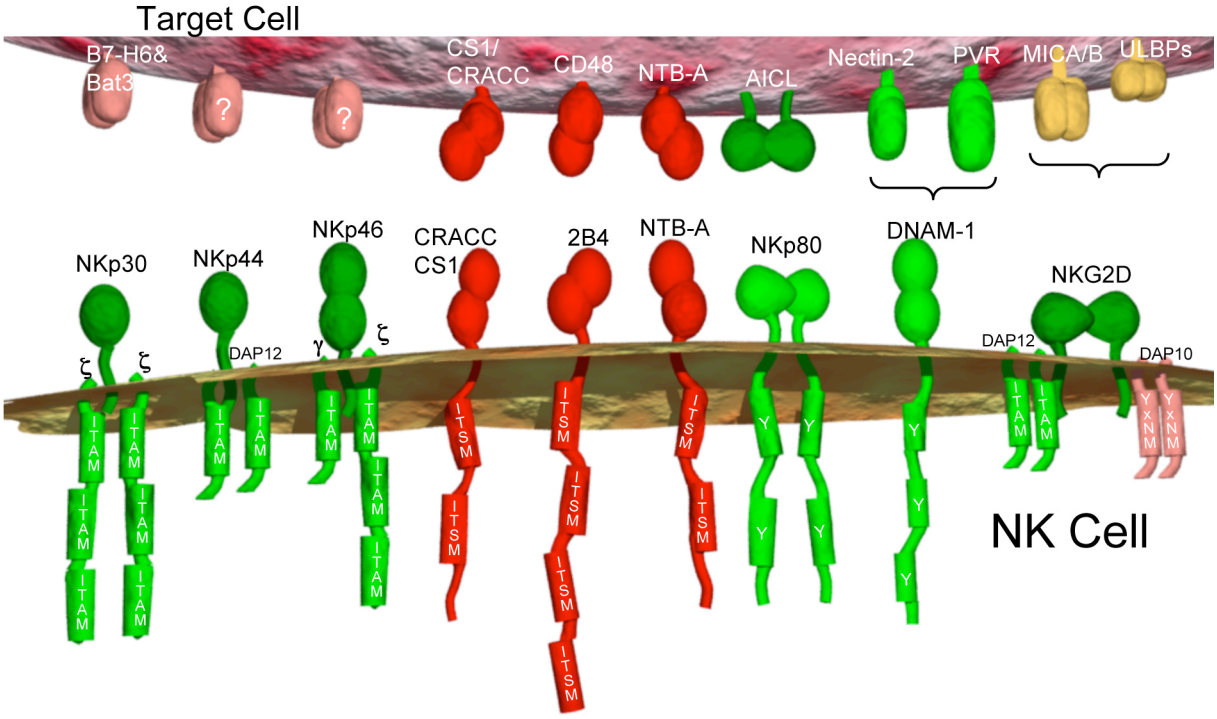

Figure 3: Overview of activating receptors and their ligands. Signaling motifs of the receptors or their respective adapter chains are indicated. CD3ζ is symbolized by ζ and FcεRI-γ by γ. NKG2D interacts only with DAP10 on human NK cells.

1.6. NK cell 'licensing'

The inhibitory receptors are expressed in a seemingly random manner on NK cells, although there is emerging evidence that expression of KIRs is not completely stochastic (Andersson *et al*, 2009) and NKG2A can be upregulated upon NK cell activation (Saez-Borderias *et al*, 2009). As inhibitory receptors were thought to be necessary to maintain self-tolerance, the hypothesis was that every NK cell has to express 'at least one' self-specific KIR or NKG2A (Valiante *et al*, 1997). But in humans and mice lacking the expression of MHC class I or associated proteins, NK cells are not autoreactive, despite the absence of inhibitory ligands (Bix *et al*, 1991; Hoglund *et al*, 1991). In contrast, they are hyporesponsive to MHC class I deficient or mismatched target cells. In humans the subset of mature NK cells, which does not express at least one inhibitory receptor is also hyporesponsive (Anfossi *et al*, 2006). These findings led to the hypothesis, that NK cells need to be 'educated' by stimulation of inhibitory receptors. Either NK cells are non- or hyporesponsive and need the inhibitory signal to become activated (arming model) or they are initially

autoreactive, but get anergic in the absence of inhibitory signal (disarming model) (Yokoyama and Kim, 2006). Recently it has been demonstrated in mice with various MHC class I backgrounds, that this education of NK cells even is dose-dependent. The more MHC class I alleles are expressed in the host, the higher is the reactivity of these NK cells towards allogenic targets with low or no MHC class I expression (Brodin *et al*, 2009b). Therefore NK cell education has been described to be more like a 'tunable rheostat' instead of an on-off switch (Brodin *et al*, 2009a). One possible mechanism for the varying activity of NK cells has been proposed to be the cis-interaction of inhibitory receptors with matching MHC class I on the same cell (Chalifour *et al*, 2009). The complete process that matches NK reactivity to self MHC class I is only poorly understood and it cannot be excluded, that unknown receptor-ligand interactions also play a role.

1.7. Signaling pathways

The signaling of inhibitory and activating NK cell receptors is depending on tyrosine phosphorylation of signaling motifs in the cytoplasmic part of the receptors themselves or their adapter proteins. ITAM motifs are phosphorylated by Src family kinases (SFK) and then can recruit the kinases Syk and ZAP70. The ITAM initiated signals are quite similar to T cell receptor signaling but in contrast to T cells, NK cell development is not abrogated in the absence of Syk and ZAP70, and only some receptor specific functions are affected (Colucci *et al*, 2002). Similar observations have been made with NK cells lacking all the ITAM containing adapter molecules. The receptors belonging to the SRR carry ITSMs that have unique signaling properties. Upon phosphorylation ITSMs can recruit the SLAM-associated protein (SAP) family of adapters, including SAP, Ewing's sarcoma-activated transcript-2 (EAT-2), and in mice additionally EAT-2-related transducer (ERT). By binding to SAP, SRR are coupled to the Src kinase FynT, which can phosphorylate the receptors as well as transmitting the activating signal to downstream effectors. ITSMs can also exhibit an inhibitory function by recruiting the SH2 containing protein tyrosine phosphatases (SHP)-1, SHP-2 and the inositol phosphatase SHIP (Eissmann *et al*, 2005). If triggering of SRR results in activation or inhibition is critically dependent on the adapter molecules accessible (Wahle *et al*, 2007), but the mechanism is only partially understood (Veillette, 2006). The adapter molecule DAP10, which associates with NKG2D, carries an YxNM motif that is typical for costimulatory receptors e.g. CD28, but NKG2D engagement alone is sufficient for NK cell activation. After NKG2D triggering DAP10 binds the p85 subunit of phosphatidylinositol-3-kinase (PI3K), but PI3K alone cannot initiate the full signal necessary for effector functions. Additionally DAP10 can recruit complexes of the adaptor molecule growth factor receptor-bound protein (Grb)2 and Vav1, leading to Vav1 activation (Upshaw *et al*, 2006). There are functional redundancies between the Vav family members Vav1, 2 and 3. In NK cells Vav proteins are indispensable for ADCC and natural cytotoxicity initiated by distinct NK cell receptors (Cella *et al*, 2004; Colucci *et al*, 2001). To release Vav1 from its autoinhibitory conformation regulatory tyrosines in the acidic region have to be phosphorylated (Aghazadeh *et al*, 2000).

First, the N-terminal Y142 and Y160 are phosphorylated, to enable SFKs to bind to Vav1 and phosphorylate Y174 blocking the Dbl homology (DH) domain (Amarasinghe and Rosen, 2005). If these tyrosines are phosphorylated the DH domain is accessible and Vav1 can perform its function as a guanine exchange factor (GEF) for the small Rho family guanosine triphosphatase (GTPases) Rac1 and Cdc42 (Billadeau *et al*, 1998; Galandrini *et al*, 1999). Like all members of the Dbl family, Vav proteins also contain a Pleckstrin-homology (PH) domain that can bind PI3K generated lipid products. The mechanism by which the PH domain influences the GEF activity of Vav is controversial. Activation of the small GTPases has multiple downstream effects, e.g. the reorganization of the actin cytoskeleton. The induction of actin reorganization is essential for the formation of the IS. The actin driven clustering of activating receptors at the contact area between NK and the target cell (Orange, 2008) can enhance the activating signal. The process of activating receptor clustering is paralleled by clustering of cholesterol-enriched membrane microdomains (lipid rafts) at the IS (Fassett *et al*, 2001; Lou *et al*, 2000). The recruitment of activating receptors such as NKG2D or 2B4 to membrane microdomains seems to be crucial for the phosphorylation and function of these receptors (Endt *et al*, 2007; Watzl and Long, 2003). SFKs are also enriched in membrane microdomains through the post-translational addition of a lipid anchor (Shenoy-Scaria *et al*, 1993). The activity of these kinases can be enhanced by phosphorylation of a tyrosine in the activation loop and inhibited by phosphorylation of a C-terminal tyrosine. The phosphatase CD45 is required for dephosphorylation of this inhibitory tyrosine (McNeill *et al*, 2007), thereby maintaining a pool of active SFKs. But CD45 may also play a role in dephosphorylating the activating tyrosines of receptors, adaptors and signaling molecules. As postulated by the kinetic-segregation model (Davis and van der Merwe, 2006), CD45 and other bulky phosphatases such as CD148 are excluded from the close contact in the IS. This would further enhance the phosphorylation of activating NK cell receptors and their downstream mediators.

Inhibitory receptors can regulate the activity of a variety of activating receptors coupling to diverse signaling pathways. Therefore the question arises if they employ different inhibitory mechanisms for different receptor signaling pathways or if they interfere with a central signaling event common to all activating receptors. Upon engagement with MHC class I molecules, inhibitory receptors get tyrosine phosphorylated on ITIMs in their cytoplasmic tails. The phosphatases SHP-1 and SHP-2 are recruited to these ITIMs (Long *et al*, 2001). The binding increases the activity of the phosphatases (Hof *et al*, 1998), which might further be stabilized by phosphorylation (Lu *et al*, 2001). Active SHP-1 can interfere with early events of NK cell activation. Vav1 has been identified as a direct target for SHP-1 when recruited by an inhibitory NK cell receptor (Stebbins *et al*, 2003), and may represent the first step at which activating and inhibitory signals converge. Dephosphorylation of Vav1 would block the actin dependent recruitment of activating receptors to specialized membrane domains (Watzl *et al*, 2003). Thereby they stop the activating feedback loop initiated by the phosphorylation of activating receptors followed by Vav1

phosphorylation, recruitment and phosphorylation of more activating receptors (Watzl *et al*, 2000). This process of NK cell inhibition is spatially restricted to the site of the inhibitory IS, enabling NK cells to recognize and attack target cells lacking inhibitory ligands while being inhibited by other contacts (Eriksson *et al*, 1999).

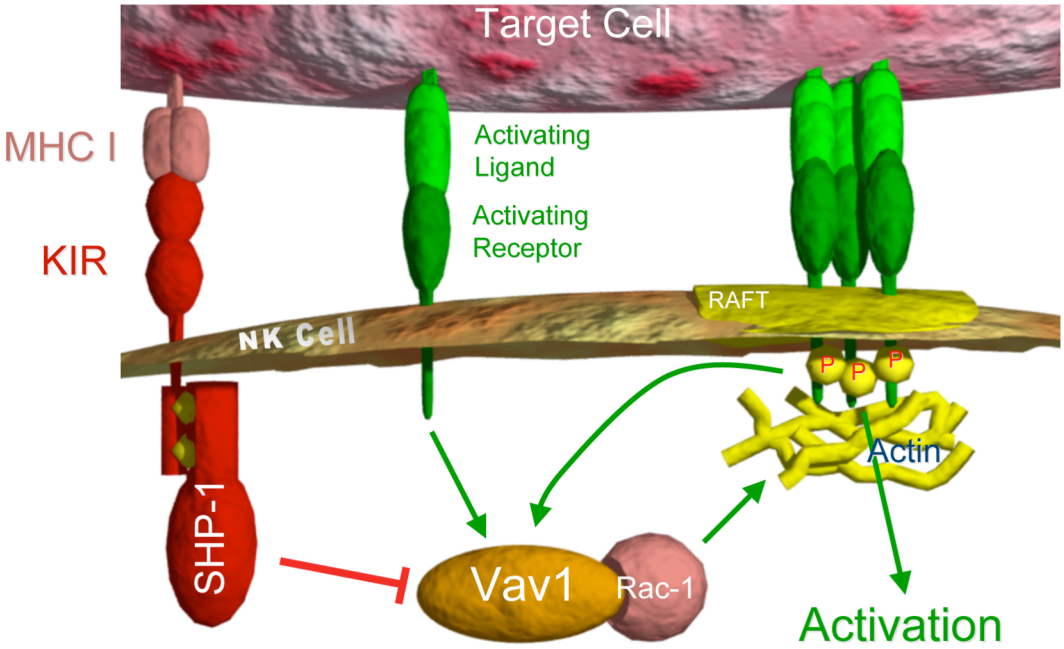

Figure 4: Crosstalk between activating and inhibitory signals. Upon triggering of activating receptors Vav1 gets phosphorylated and initiates a positive feedback loop of actin reorganisation and recruitment of more activating receptors. Inhibitory receptors can block phosphorylation of Vav1 via the phosphatase SHP-1.

If the inhibitory signal cannot overcome the activating signal, downstream mediators get initiated. Phosphoinositide 3-kinase (PI3K) can be activated directly upon NKG2D triggering by interacting with DAP10, or via Syk or ZAP70 after triggering of receptors that use ITAMs. Active Vav1 acts as a GEF and activates Rac1 (Galandrini *et al*, 1999). As Vav1 and PI3K both interact with DAP10 and are activated directly upon NKG2D triggering, it is hard to differentiate the sequence of events. In mice lacking Vav1 it has been shown, that Akt phosphorylation is impaired, indicating that Vav1 is required for PI3K activation upon NKG2D stimulation (Graham *et al*, 2006). The p21-activated kinase (PAK1) acts downstream of Rac1 and is responsible for the initiation of the mitogen activated protein kinase (MAPK) cascade including MAPK kinase (MEK) and extracellular signal-regulated kinase (ERK). Phosphatidylinositol-specific phospholipase C-γ (PLC-γ) enzymes are indispensable components of signal transduction complexes downstream of a number of immune receptors. PLC-γ cleaves phosphatidylinositol (PI) 4,5-bisphosphate (PI4,5P2) into inositol 1,4,5-trisphosphate (IP3) and 1,2-diacyl-glycerol (DAG). IP3 induces the opening of intracellular Ca^{2+} stores leading to a rise in intracellular Ca^{2+} concentration, whereas DAG activates the protein kinase C (PKC) and the Ras pathways. The Ca^{2+} release by PLC-γ is necessary for the secretion of cytotoxic granules, but not for conjugate formation and polarization of actin and the microtubule-organizing center (MTOC) towards the target cell (Caraux *et al*, 2006). The Ca^{2+} signal and the MAPK cascade

are essential for the initiation of effector functions of NK cells, but probably not involved in the primary integration of activating and inhibitory signals.

Given the importance of regulating immune cell responses by a balance of positive and negative signals, it is mandatory to better understand the integration of these opposing signals on a molecular level. NK cell activation is strictly dependent on such a balance of positive and negative signals mediated by many different surface receptors.

1.8. Revealing signaling dynamics by mathematical modeling

Systems biology is an integrative discipline combining modeling approaches and experiments. With classical methods like biochemistry many aspects of the signaling of immune cells have been studied. But as the network is so complex the impact of a single molecule or one defined protein interaction is hard to estimate. Used appropriately, mathematical models can represent pathways in a physically and biologically realistic manner. Therefore a mathematical model could support the understanding of the decision making process of NK cells.

The methods that can be applied to construct a model are very diverse. Depending on the biological system, the question that has to be solved and the data available, different models can be generated. Qualitative molecular reactions and signaling pathways modeled as static networks or boolean networks are often used to get an overview in large systems, when little or no quantitative information is available. But as in these systems every element exists only in two states (yes/no) concentration dependent dynamics and kinetics cannot be simulated. As the decision making of NK cells is critically depending of the strength of two opposing signals, these qualitative models are not suitable to solve our question. In quantitative mathematical models each equation refers to identifiable processes (such as catalysis and assembly) and parameters have physical interpretation (such as concentration, binding affinity and reaction rate). These models work best with pathways that are well studied, as information about molecule concentrations and reaction parameters are necessary (Aldridge *et al*, 2006). As the quantitative approach is able to reveal dose-responses and kinetics, it is appropriate to describe the balance of NK cell activation. When limited mechanistic knowledge or conflicting hypotheses hamper the development of predictive mechanistic models, ‘ensemble modeling’ can be performed (Kuepfer *et al*, 2007). As several concepts have been proposed to influence the signaling of immune receptors, ensemble modeling can be useful to distinguish between the effects of these concepts. In addition to one core model several optional reaction modules can be included. The effects of these optional modules on the simulation results can elucidate which reactions are of special importance for a physiologic response of the system.

2. Aim of the thesis

The signal integration of NK cells is able to transform the gradual signal input through a variety of activating and inhibitory receptors into a decision to kill or spare the target cell. The mechanisms regulating this balance of positive and negative signals are only poorly understood. To gain better insight into the signal integration on the molecular level, we chose a systems biology approach. In cooperation with the group of Roland Eils of the division of Theoretical Bioinformatics from the DKFZ we wanted to create a mathematical model describing the receptor proximal signal transduction network of NK cells. By comparing the simulation results of this model with experimental data we aimed to reveal the mechanisms of the decision making of NK cells.

We propose a model, which integrates the activating and inhibitory signals on the level of the GEF Vav1, as it is an early target of both pathways. By using 'ensemble modeling' we created a family of simplified models. Each module of the model family addresses one concept of immune receptor signaling, that has been proposed to be important for signal regulation. Among these different concepts we aimed to identify the reactions that play key roles during the integration of activating and inhibitory signals. As we wanted to establish a mathematical model based on differential equations we needed to quantify concentrations of the proteins involved in the reactions of the model. Based on these quantifications and information from the literature we were able to simulate the phosphorylation of Vav1 with the model family. Then experimental data about the Vav1 phosphorylation was compared to the simulation results derived from the models containing the reactions that addressed the different signaling concepts. This analysis should reveal the key concepts necessary for a physiological response of the model on the level of Vav1. With the model containing the essential reactions we could make additional predictions concerning manipulations and perturbances of the system. Testing these predictions experimentally could show the validity and the reliability of our simulations. Furthermore we wanted to investigate the cytotoxic activity of NK cells differentially stimulated via activating and inhibitory receptors, to uncover how the signal integration on the level of Vav1 contributes to a reliable killing decision of the NK cell.

3. Materials and Methods

3.1. Materials

3.1.1. Mouse monoclonal antibodies

Name	Source, Reference
IgG control, MOPC21	Sigma, Taufkirchen, Germany
anti-NKG2D (149810)	RnD Systems, Minneapolis, USA
anti-NKG2D (3.1.1.1)	(Endt *et al*, 2007)
anti-NKG2A/CD159a (Z199)	Beckman Coulter, Fullerton, USA
anti-CD94 (HP-3B1)	
anti-KIR2DL1 (EB6)	
anti-KIR2DL2/3 (GL183)	
anti-2B4 (C1.7)	
anti-Vav1 (VAV-30)	Abcam, Cambridge, USA
anti-Vav	Millipore, Billerica, USA
anti-SHP-1	BD Transduction Laboratories, Franklin Lakes, USA
anti-non-phospho-Src (7G9) (Tyr416)	Cell Signaling Technologies, Danvers, USA
anti-Fyn (25)	BD Transduction Laboratories
anti-Lck	Abnova

3.1.2. Rat monoclonal antibodies

Name	Source, Reference
anti-human DAP10 (4E1)	a gift of E. Vivier, Centre d'Immunologie de Marseille-Luminy, France

3.1.3. Rabbit polyclonal antibodies

Name	Source, Reference
anti-phospho Vav1 pY 160	Biosource, Camarillo, CA
anti-Actin	Sigma
anti-Fyn	Cell Signaling Technologies
anti-phospho-Src family pY416	Cell Signaling Technologies
anti-Lck	a gift of A. Veillette, Clinical Research Institute of Montreal, Canada

3.1.4. Secondary antibodies

Name	Source, Reference
goat-anti-mouse IgG unlabeled	Jackson ImmunoResearch Laboratories, West Grove, PA
goat-anti-mouse IgG PE / Cy3	
goat-anti-mouse IgG HRPO	
goat-anti-rat IgG HRPO	
goat-anti-rabbit IgG HRPO	Santa Cruz Biotechnology, Heidelberg, Germany

3.1.5. Recombinant Proteins

Name	Tag, Size	Source
Lck	GST, full length, 85 kDa	Abnova
SHP-1	GST, full length, 95 kDa	Millipore
N-Vav1	His, N terminal 58 kDa	this work

3.1.6. Bacteria

E.coli strain	Use	Source
TOP10	amplification of plasmids	Invitrogen, Carlsbad, CA
BL21 (DE3) pLys	expression of proteins	Invitrogen

3.1.7. Cells (eukaryotic)

All media were purchased from Gibco (Invitrogen, Carlsbad, CA); Fetal calf serum (FCS), Non essential Amino Acids and Pyruvate was from Gibco, human serum from PromoCell (Heidelberg, Germany), PHA-P from Sigma and purified human IL-2 from Hemagen Diagnostics (Columbia, USA). If not indicated otherwise all cells were grown with 10 % (v/v) FCS and 1 % (v/v) Penicillin/Streptomycin (Gibco, Invitrogen).

Cell type	Origin	Culture medium
NKL	human NK cell line	RPMI, 100 U/ml IL-2
human peripheral blood lymphocytes	isolated from whole blood or buffy coats	
primary human NK cell populations (NK pop)	isolated from human peripheral blood lymphocytes	NK pop medium: IMDM, 10 % (v/v) human serum, 10 % (v/v) Non essential Amino Acids, 10 % (v/v) Pyruvate, 100 U/ml IL-2

primary human NK cell clones	expanded from primary human NK cell populations	cloning medium: IMDM, 10 % (v/v) human serum, 10 % (v/v) Non essential Amino Acids, 10 % (v/v) Pyruvate, 100 U/ml IL-2, 10 % (v/v) purified human IL-2, 1 µg/ml PHA-P
JY	B cell lymphoblastoid cell line	RPMI, 50 µM 2-Mercaptoethanol
P815	mouse mastocytoma cell line	IMDM

3.1.8. Buffers

Triton X-100-lysis buffer:	150 mM	NaCl
	20 mM	Tris-HCL, pH 7.4
	10 % (v/v)	Glycerol
	0.5 % (v/v)	Triton X-100
	2 mM	EDTA
	10 mM	NaF
	1 mM	PMSF
	1 mM	Na-orthovanadate (for studies on protein phosphorylation)
Brij58-lysis buffer:	150 mM	NaCl
	20 mM	Tris-HCL, pH 7.4
	10 % (v/v)	Glycerol
	0.5 % (v/v)	Brij58, AppliChem, Darmstadt
	2 mM	EDTA
	10 mM	NaF
	1 mM	PMSF
	1 mM	Na-orthovanadate (for studies on protein phosphorylation)
	200 Kunitz Units	DNase (Sigma)
PBS (pH 7.4):	137 mM	NaCl

	8.1 mM	Na_2HPO_4
	2.7 mM	KCl
	1.5 mM	KH_2PO_4
PBST:	1 x	PBS
	0.05 % (v/v)	Tween 20
PBST/NaCl:	1 x	PBS
	0.05 % (v/v)	Tween 20
	0.5 M	NaCl
Blocking Buffer for western Blot:	1 x	PBST
	5 % (w/v)	nonfat dry milk powder, Saliter, Obergünzburg
PBS/pervanadate:	1 x	PBS
	10 mM	H_2O_2
	200 µM	Na-orthovanadate
Western blot transfer buffer:	24 mM	Tris
	129 mM	Glycin
	20 % (v/v)	MeOH
Reducing sample buffer (5 x):	10 % (w/v)	SDS
	50 % (v/v)	Glycerol
	25 % (v/v)	2-Mercaptoethanol
	0.1 % (w/v)	Bromphenol Blue
	0.3125 mM	Tris-HCL, pH = 6.8
Stripping buffer (pH 2.2) for western Blot:	200 mM	Glycin
	0.1 % (w/v)	SDS
	1 % (v/v)	Tween 20

DNA-sample buffer (6 x):	0.25 % (w/v)	Bromphenol Blue
	0.25 % (w/v)	Xylene Cyanol FF
	30 % (v/v)	Glycerol in H_2O
Protein purification:		
Lysis buffer pH 8	6 M	Guanidin Hydrochlorid
	0.1 M	Na_2HPO_4
Elution buffer pH 4	6 M	Guanidin Hydrochlorid
	0.1 M	Na_2HPO_4
Ca^{2+} assay:		
wash medium	2.5 mM	Probenicide (500 mMin 1 M NaOH)
	5 mM	HCl
	10 % (v/v)	FCS
	1 % (v/v)	Penicillin/Streptomycin
		in IMDM
assay medium	500 mM	Probenicide (in 1 M NaOH)
	5 mM	HCl
	10 mM	HEPES
		in HBSS
loading medium	4.8 µM	Fluo4
	0.16 % (v/v)	Pluronic acid
		in wash medium

MOPS buffer (20 x) Invitrogen

TAE (10 x) Invitrogen

3.1.9. Reagents

Agarose, Gibco, Paisley, Scotland

Ampicillin, Roth, Karlsruhe, Germany

BSA, Serva, Heidelberg, Germany

5-Bromo-4-chloro-3-indoxyl-β-D-galactoside (X-Gal), Roth

Choleratoxin B subunit (Alexa488), Calbiochem, Beeston, England

Chromium-51, Hartmann Analytik, Braunschweig

Complete protease inhibitor mix, Roche, Mannheim, Germany

DNA ladder (100 bp and 1kb), Invitrogen

Dynabeads Protein G, Dynal, Invitrogen

Inhibitors (Piceatannol, PP1, Wortmannin, Cytochalasin D, Latrunculin, PD-98059, SB-202190, U73343, U73122), Biomol, Hamburg, Germany

Isopropyl-β-D-thiogalactopyranoside (IPTG), Roth

Kanamycin, Roth

LB broth, Invitrogen

LSM solution, PAA, Pasching, Germany

Ni^{2+}-NTA Agarose Qiagen, Hilden, Germany

Poly-L-Lysine, Sigma

Precision Plus Protein Standard, BioRad, Hercules, CA

Protein G agarose, Invitrogen

Streptavidin-HRPO, Jackson ImmunoResearch Laboratories

SuperSignal West Pico and Dura, Thermo

X-ray films, Perbio/Pierce, Rockford, IL

3.1.10. Vectors

Name	Use	Source
pCR2.1-TOPO	subcloning of PCR products	Invitrogen
pRSetB	expression of His tagged proteins	Invitrogen

3.1.11. Enzymes

Name	Use	Source
restriction endonucleases	DNA digest	New England Biolabs, Frankfurt, Germany
T4 DNA ligase	DNA ligation	
Taq DNA Polymerase	PCR	
AMV reverse transcriptase (RT)	RT-PCR	First strand cDNA synthesis kit, Roche Diagnostics

All enzymes were used in buffers provided by the manufacturer.

3.1.12. Oligonucleotides

Name	Use	Sequence (5'-3')
Vav N fw	amplification of N-Vav1	ggatccagagctgtggcgccaatg
Vav N rev		gaattctcactcggtctcctgaagagtc

3.1.13. Kits

Isolation of RNA: RNeasy Mini Kit, Qiagen

Plasmid DNA purification: Plasmid Mini Kit, Plasmid Midi Kit, Qiagen

DNA Fragment Purification: Gel Extraction Kit, Qiagen

Quantification of surface receptors: Qifikit, Dako

Quantification of SHP-1 activity: DuoSet IC, Human/Mouse/Rat Active SHP-1 Activity Assay, R&D

Quantification of protein concentration: EZQ Protein Quantitation Kit, Molecular Probes, Invitrogen

3.2. Methods

3.2.1. Molecular biology

Isolation of RNA

RNA was isolated from IL-2 expanded primary human NK populations using the RNeasy Mini Kit according to the manufacturers instructions.

Reverse Transcription

RNA was transcribed to cDNA using the First strand cDNA synthesis kit. 1 µg or 2µg RNA were used as template, the reaction was performed according to the manufacturers instructions.

Polymerase chain reaction (PCR)

PCR was used to amplify DNA fragments from cDNA. The conditions were fit to the respective need.

Isolation of Plasmid DNA

Bacteria were grown in 1 x LB medium with the appropriate selective antibiotic at 37°C over night. After harvesting the bacteria by centrifugation at 3500 g for 5 min, DNA was isolated according to the manufacturers instructions, using either the Plasmid Mini or Midi Kit from Qiagen.

Ligation of DNA

The insert and the vector DNA were mixed at a ratio of approximately 3:1 in ligation buffer. The mixture was incubated with 2U T4 DNA ligase for 1h at room temperature or overnight at 16°C and used for the transformation of competent bacteria.

Transformation of bacteria

All bacteria were chemically competent. Transformation was done according to the manufacturers instructions. Bacteria were grown on LB-agar plates at 37 °C for 24h and selected with the appropriate antibiotic.

Agarose gel electrophoresis

The DNA solution was mixed with DNA sample buffer before loading the gel. 1 % gels were used for optimal separation of the fragments (TAE, agarose, 0.00001 % Ethidiumbromide). The correct size of the DNA fragment was controlled using a DNA ladder.

DNA digest

Between 1 and 2 µg of DNA were incubated with 2 U of the respective restriction endonuclease for at least 1h at 37°C. Conditions of the reaction were set according to the manufacturers instructions. The DNA fragments were separated by agarose gel electrophoresis.

Isolation of DNA fragments from agarose gels

DNA fragments were excised from the agarose gel and the DNA was extracted using the Qiagen gel extraction kit according to the manufacturers instructions.

3.2.2. Cell biology

Cell culture

All cells were grown at 37°C and 5 % CO_2 in a humidified incubator under sterile conditions. Cells lines were split on a regular basis every two to three days. Cell culture flasks were exchanged every week. Cells were frozen in FCS containing 10 % DMSO at -75°C and stored in liquid nitrogen. Cell lines were thawed on a regular basis. FCS and human serum were heat inactivated by incubation on 56°C for 30 min prior to use.

NK cell isolation

Human polyclonal NK cells were isolated from whole blood or buffy coats. First peripheral blood mononuclear cells (PBMC) were purified by density centrifugation over LSM solution. Then NK cell were isolated using the NK cell negative isolation kit from Dynal (Invitrogen). NK cells were between 90 % and 99 % $NKp46^+$, $CD3^-$ and $CD56^+$. After isolation NK cells were plated on 96 well round bottom plates at $1x10^6$-$2x10^6$ cells/ml with $5x10^5$ cells/ml irradiated JY cells. Growing cells were expanded 1:1 with NK pop medium.

Expansion of NK cell clones

NK clones were generated by limiting dilution of fresh NK cells in cloning medium containing $5x10^5$ cells/ml irradiated feeder cells (1:1 ratio of JY cells and allogenic PBMC). After 7 days clones were re-stimulated with 50 % fresh cloning medium and feeder cells. Growing clones were expanded 1:1 with NK pop medium.

Cell stimulation

Antibody crosslinking

Cells were resuspended at $2x10^7$ cells/ml in medium supplemented with 100 U/ml recombinant IL-2. Samples were incubated at room temperature (RT) for 10 min after adding the respective amounts of primary antibody. Samples were washed with 500 µl medium, pelleted by centrifugation for 5 min at 500 g at RT, and again resuspended at $4x10^7$ cells/ml in medium containing IL-2. Cells were then transferred to 37°C and the same volume of prewarmed 10 µg/ml solution of secondary antibody in medium was added for the indicated times. Stimulation was stopped by putting the cells immediately on ice and washing with 500 µl ice cold medium. Cells were pelleted by centrifugation for 5 min at 500 g at 4°C and lysed.

Bead stimulation

Dynabeads were washed 3 times with medium and resuspended in the initial volume. Human-anti-mouse coupled Dynabeads contained $4x10^5$ beads/µl. Then the indicated amount of mouse antibody was added and incubated for 1 h at room temperature. After 3 washes, the Dynabeads were resuspended at $4x10^7$ beads/ml in medium supplemented with 100 U/ml recombinant IL-2. Cells were also resuspended at $4x10^7$ cells/ml. Cells were then transferred to 37°C and the same volume of prewarmed Dynabeads suspension was added for the indicated times. After stimulation cells were immediately chilled on ice and washed with 500 µl ice cold medium. Cells were pelleted by centrifugation for 5 min at 500 g at 4°C and lysed.

Inhibitor pretreatment

To inhibit signaling processes cells were treated for 30 min at 37°C with the respective inhibitors at $2x10^7$ cells/ml in medium supplemented with 100 U/ml. Unless indicated otherwise, the following concentrations were used: 50 µM Piceatannol, 10 µM PP1, 100 nM Wortmannin, 20 µM PD-98059, 100 nM SB-202190 and 1 µM U-73122. During the following stimulation of these cells the inhibitor concentration was kept constant. Protein phosphorylation was induced by using the phosphatase inhibitor pervanadate. Cells were resuspended at $2x10^7$ cells/ml in PBS/pervanadate solution and incubated for 10 min at 37°C.

Cell lysis

For western blot analysis $1\text{-}4x10^7$ cells/ml were lysed to obtain the required protein concentrations. Pelleted cells were resuspended in 0.5 % Triton X-100 lysis buffer supplemented with 1 mM PMSF and if necessary 1 mM Na-orthovanadate and

incubated on ice for 20 min. Lysates were clarified by centrifugation for 15 min at 20000 g and 4°C.

Chromium-release assay

The medium was always supplemented with recombinant IL-2 to a final concentration of 100 U/ml. Cell lines were grown to mid log phase, primary NK clones were used at 3-4 weeks age. Antibody dilutions were prepared in medium on a 96 V-well plate. Usually $5x10^4$ NKL or $1x10^4$ primary NK cells per well were mixed with the prepared antibody dilutions. 5 $x10^5$ P815 target cells were labeled in 100 µl medium with 100 µCi ^{51}Cr (3,7 MBq) for 1 h at 37°C. Cells were washed twice in medium and resuspended at $5x10^4$ cells/ml in medium. 5000 target cells/well were used in all assays. Maximum release was determined by incubation of target cells in 1 % Triton X-100. For spontaneous release, targets were incubated without NK cells in medium alone. All samples were done in triplicates. Plates were incubated for 4 h at 37°C, 5 % CO_2. Supernatant was harvested and ^{51}Cr release was measured in a gamma counter. Percent specific release was calculated as ((experimental release - spontaneous release) / (maximum release - spontaneous release)) x 100. When the inhibitor PP1 was used effector cells were pre-incubated with the inhibitor for 30 min at 37°C, 5 % CO_2 before target cells were added.

Ca^{2+} measurement

NKL cells were resuspended at $1x10^7$ cells/ml in loading medium and incubated for 30 min at 37°C, washed twice with wash medium, rested for 30 min at 37°C in wash medium and were washed again. Cells were resuspended at $1x10^6$ cells/ml in wash medium and preincubated with the indicated primary antibodies for 10 min at RT on a 96 V-well plate and washed to remove excess antibody. Cells were mounted in assay medium and transferred to a 96 well flat bottom plate. The plate was measured immediately in a plate reader (Wallach Victor^2, 1420 Multilabel Counter, Perkin Elmer) at 488 nm excitation and 525 nm emission to obtain the baseline of the Ca^{2+} signal. Then crosslinking antibody was added to all wells to a final concentration of 5 µg/ml, mixed gently and measured again in the plate reader. All samples were done in triplicates.

Flow cytometry

Cell staining

Surface staining of cells was performed in 96 V-well plates. About $2x10^5$ cells were resuspended in 50 µl fluorescence-activated cell sorting (FACS)-buffer (PBS containing 2 % FCS) containing 10 µg/ml of the respective primary antibody and incubated on ice for 20 min. After washing with FACS-buffer cells were resuspended in 50 µl PE conjugated goat-anti-mouse secondary antibody diluted 1:200 in FACS-buffer. Cells were incubated on ice for 20 min in the dark to protect the fluorophore, washed again and resuspended in FACS-buffer containing 2 % formaldehyde. Samples were analyzed on a BD FACScan or BD FACScalibur and results were evaluated using the FlowJo Software from Treestar.

Quantification of surface molecules

Surface molecules were quantified using the Qifikit (Dako) according to the manufacturers instructions. In brief, cell staining was performed as described but additionally calibration beads were stained with the same solution of secondary antibody. Based on the mean fluorescence intensity (MFI) of the calibration bead populations a standard curve was generated and used to calculate molecule numbers on the stained cells.

Confocal microscopy

Imaging of cells stimulated by receptor crosslinking

NKL cells were resuspended at $2x10^7$ cells/ml in medium supplemented with 100 U/ml recombinant IL-2. Cells were stimulated as described, but for receptor crosslinking 7 µg/ml Cy3 conjugated goat-anti-mouse antibody were used and cells were incubated for 5 min on ice with the secondary antibody prior to crosslinking. After stimulation cells were immediately fixed by adding the equal volume of 4 % Paraformaldehyde solution and incubation for 15 min at RT. Cells were washed once with PBS and resuspended at $1.5x10^5$ cells/ml in PBS. 200 µl of this solution (=30 000 cells) were centrifuged onto Poly-L-Lysine (PLL) (Sigma) coated coverslips. Coverslips were incubated for 5 min in 0,1 TritonX-100 solution to permeabilize the cells. Then the coverslips were washed twice with FACS buffer, with 10 min incubation to block unspecific binding in the following staining. Cells were incubated with Alexa488 conjugated phalloidin (Molecular Probes) for 20 min at RT, washed 3 times in PBS and finally in H_2O. When the coverslips were dry, they were mounted using Mowiol (Calbiochem) and imaged on a Leica DMRBE.

Imaging of cell-bead conjugates

Antibody coated Dynabeads were prepared as described and mixed at a 1:1 ratio with NKL cells at a concentration of $2x10^6$ cells/ml. 100 µl of this mix (=$2x10^5$ cells) were incubated for 30 min at 37°C on PLL coated coverslips. Cells were fixed as described above and stained with Alexa488 conjugated CTX for 20 min at RT. Then cells were washed, permeabilized and blocked as described. Finally cells were stained with TRITC labeled phalloidin, washed and mounted as above.

3.2.3. Protein biochemistry

Production of recombinant protein

To produce a His-tagged N-terminal part of Vav1 (amino acids 2-462) we amplified the respective sequence using cDNA from primary human NK cells and sub-cloned it into the pRSet B Vector (Invitrogen). The Vector was transformed into E. coli BL21 (DE3) pLys (Invitrogen). Bacteria were grown with shaking at 37°C to OD_{600} 0.7, induced with 0.5 mM IPTG and incubated for additional 3 h. Then bacteria were pelleted and 500 ml culture were lysed in 100 ml protein purification lysis buffer (pH 8) for 60 min with agitation at RT. Lysates were clarified by 30 min centrifugation at 20000 g. 2 ml Ni^{2+} NTA agarose beads were washed two times with lysis buffer,

added to the lysates and incubated with agitation for 2 h. The beads were extensively washed with lysis buffer and applied to a PolyPrep chromatography column (Biorad). Proteins were eluted by adding 5 ml protein purification elution buffer (pH 4) to the column and fractions were collected. Fractions containing the maximum yield were pooled and dialyzed against 10 mM Tris (pH 8.8). If necessary, precipitated protein was dissolved by adding SDS to a final concentration of 0.1 %. For storage, 1 mM PMSF was added, and protein solution was frozen in aliquots at -20°C.

Protein quantification

Protein concentration was determined using a customized BSA standard and the EZQ Kit according to the manufacturers instructions. The membrane was analyzed on a FLA-2000 (Inter Departmental Equipment, Haifa, Israel) using 473 nm excitation wavelength and 580 nm emission filter.

Immunoprecipitation

For immunoprecipitations stimulated cells were lysed in Brij58-lysis buffer at a concentration of $2x10^7$ cells/ml. The non-clarified lysates were incubated with gentle agitation with 5 µg/ml goat-anti-mouse for 20 min at 4°C, then 12.5 µl Protein G Dynabeads (Invitrogen) were added for 2 h at 4°C. Beads were washed at least 5 times with lysis buffer. Proteins were eluted from the beads with 50 mM glycine (pH 2) and the eluates were neutralized with 1 M NaOH prior to SDS-PAGE.

SDS-Polyacrylamid gel electrophoresis (SDS-PAGE)

After adding reducing sample buffer, samples were boiled for 5 min at 95°C and centrifuged for 1 min at 20000 g. Samples to a maximal volume of 25 µl and 5 µl of Precision Plus Protein Standard (BioRad) were loaded on 10 % or 4-12 % NuPage gels (Invitrogen) and separated for 1 h 15 min at 150 V in 1 x MOPS buffer.

Western Blot

After SDS-PAGE proteins were transferred to a polyvinylidene difluoride (PVDF) membrane (Millipore) for 1.5 h at 200 mA in western blot transfer buffer. PVDF membranes were activated with methanol and washed with transfer buffer prior to use. After western blotting, membranes were incubated for 1 h at RT in blocking buffer and washed for at least 3 times in PBST. Membranes were incubated with the primary antibody for 1 h at RT or overnight at 4°C. The membrane was washed at least three times with PBST/NaCl and incubated with the appropriate horseradish-peroxidase (HRPO)-conjugated secondary antibody for 1 h at room temperature. Secondary antibodies were diluted 1:5 000-1:40 000 in blocking buffer. After incubation with the secondary antibody, the membrane was extensively washed with PBST and developed using either SuperSignal West Pico or Dura and X-Ray films. The films were quantified using a densitometer (GS 800, Biorad).

Coomassie staining

Gels were washed three times for 5 min in deionized water, incubated for 30 min or longer with SimplyBlue Safe stain (Invitrogen) or Imperial stain (Pierce) for higher

sensitivity on a shaking incubator and washed again. Gels were scanned on a densitometer (GS 800, Biorad).

4. Results

4.1. Establishing the experimental and the mathematical system

4.1.1. Vav1 phosphorylation induced by NKG2D triggering

As we wanted to test the signal integration of activating and inhibitory receptors on the level of Vav1, we needed a suitable experimental system to test our simulation-derived predictions. Expression of the receptors on primary human NK cells is very heterogeneous between different donors and among the cell population of one donor. We chose the activating receptors NKG2D and 2B4 for stimulation of the cells, as these receptors are expressed on all primary human NK cells and the NK cell line NKL and they are known to be strong activators of cytotoxicity. The inhibitory receptor complex NKG2A/CD94 is more frequently expressed on primary human NK cells than KIR receptors, and also expressed on NKL cells. In contrast to stimulating the NK cells with ligand expressing target cells, antibody crosslinking offers the possibility to trigger defined receptors, and it is possible to titrate the respective stimulus. To establish our experimental system we stimulated NKL cells by crosslinking of NKG2D and visualized Vav1 phosphorylation by western blotting with specific antibodies against Vav1 phosphorylated at tyrosine 160 and total Vav1. By pretreating the cells with chemical inhibitors we blocked specific signaling steps during NK cell activation (Fig. 5). The inhibitors used were Piceatannol that competes with substrates of Syk, PP1 that blocks SFKs (especially Lck and Fyn) by binding in the ATP pocket, Wortmannin covalently binding to PI3K, PD-98059 preventing the activation of MEK, SB-202190 that blocks p38 MAP kinase by binding in the ATP pocket and U-73122, a PLC inhibitor. Only the SFK inhibitor PP1 shows a significant effect, the Vav1 phosphorylation in PP1 treated cells is even lower than the background phosphorylation in unstimulated cells. In the quantification the effect of the unspecific PLC inhibitor U-73122 also looks relevant, but as the inactive control U-73343 shows the same reduction of pVav1 this could be due to toxic effects of these substances. In this experiment we confirmed the specific phosphorylation of Vav1 upon NKG2D triggering by antibody crosslinking, which is only depending on the functionality of SFKs.

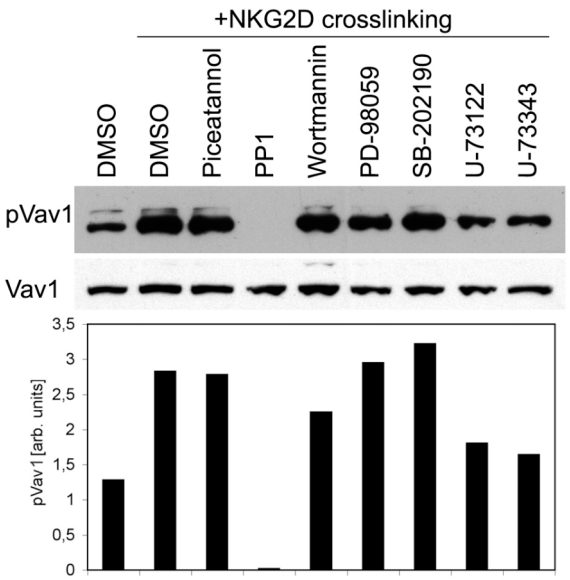

Figure 5: Influence of inhibitors on Vav1 phosphorylation. NKL cells were preincubated for 30 min at 37°C with indicated inhibitors (see text for explanations) and DMSO as solvent control. Cells were incubated with anti-NKG2D and stimulated with crosslinking antibody for 1 min on 37°C and immediately lysed. One sample of DMSO treated cells was kept on ice as unstimulated control. Vav1 phosphorylation was determined by western blotting with antibodies specific for pVav1 (Y160) and total Vav1. For the quantification films were scanned with a densitometer and pVav1 [arbitrary units] was calculated as pVav1 density divided by total Vav1 density. The result is representative for two independent experiments.

4.1.2. Mathematical model of the receptor proximal signaling network

To investigate the hypothesis that the signals from activating and inhibitory NK cell receptors are integrated at the level of Vav1 phosphorylation (Fig. 6b), we constructed a mathematical model describing this process (Fig. 6a) in cooperation with the division of Theoretical Bioinformatics (DKFZ). This model is based on (bio-) chemical reaction kinetics, i.e. bimolecular reaction kinetics for associations, unimolecular reaction kinetics for dissociations and Michaelis-Menten kinetics for enzymatic reactions. To introduce the required spatial heterogeneity into the mathematical model two distinct compartments, 'cytoplasm' and 'immunological synapse (IS)' were assumed. Receptor-ligand interactions are restricted to the IS. The other reactions can occur in the cytoplasm as well as in the IS. In this model the activating receptor NKG2D (exemplified by its associated signaling chain DAP10) can interact with MICA on the target cell within the IS of the NK cell. Furthermore DAP10 as well as Vav1 can be tyrosine-phosphorylated by SFKs. Phosphorylated DAP10 can serve as a binding site for Vav1. To simplify the mathematical model we excluded the adaptor molecule Grb2 from the system, which is justified for fast pDAP10-Grb2 and Grb2-Vav1 binding reactions. Inhibitory receptors (exemplified by the CD94/NKG2A complex) can interact with their MHC class I ligand (HLA-E) in the IS, resulting in the phosphorylation of NKG2A by SFKs and the recruitment of SHP-1, which can also be phosphorylated by SFKs. All phosphorylation events are counteracted by the activity of phosphatases (exemplified here by CD45). The activating and inhibitory receptor signaling cascades communicate through SHP-1-mediated dephosphorylation of Vav1.

In order to address several important concepts in immune receptor signaling we performed 'ensemble modeling' (Kuepfer *et al*, 2007) and included several optional reaction modules in our model (Fig. 6c). (a) pVav1-triggered Actin reorganization, leading to increased recruitment of activating receptors (DAP10) in the IS (Graham *et al*, 2006). (b) Following the kinetic segregation hypothesis we excluded the phosphatase CD45 from the IS (phosphatase segregation) (Davis *et al*, 2006). In module (c) we assumed an association of SFKs with the phosphorylated receptors (kinase association) (Cerny *et al*, 1997). (d) SFKs can mediate intermolecular autophosphorylation resulting in enhanced activity (kinase autophosphorylation) (Cooper and MacAuley, 1988), (e) which could be counteracted by SHP-1-mediated dephosphorylation (Chiang and Sefton, 2001). (f) Finally, we assumed that SHP-1 may only be active when it is bound to the phosphorylated NKG2A receptor (SHP-1 association) (Hof *et al*, 1998). Combination of the core model and all putative modules and considering that module (e) requires module (d) generates 48 different potential models of the proximal NK cell signal transduction network.

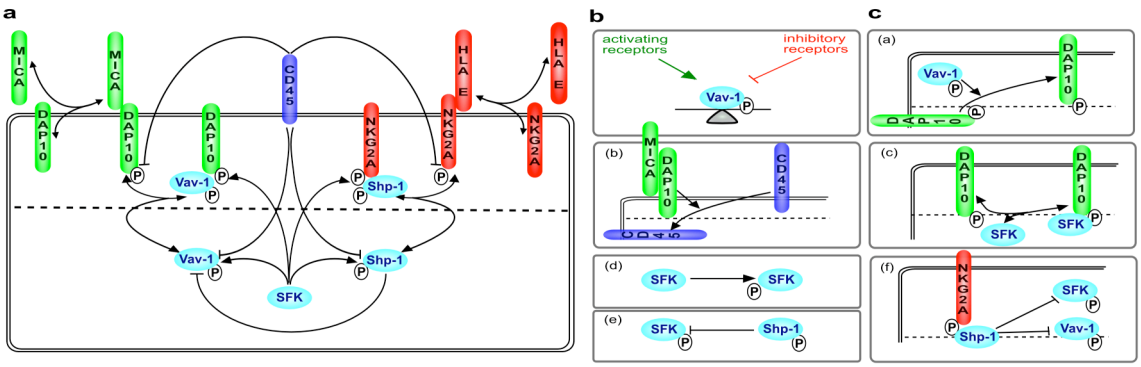

Figure 6: Modeling the proximal NK cell signal transduction network. a: Graphical representation of the mathematical core model. Activating receptor and ligands are shown in green, inhibitory receptors and ligands are shown in red. Arrows represent interaction and phosphorylation events. Blunt arrows represent dephosphorylation events. The immunological synapse is separated from the cytoplasm by the dashed line. b: Graphical representation of the basic hypothesis that activating and inhibitory receptor signals are integrated at the level of Vav1 phosphorylation. c: Optional modules used to expand the core model with additional reactions as described in the text: (a) actin reorganization, (b) phosphatase segregation, (c) kinase association, (d) kinase autophosphorylation, (e) SHP-1 mediated kinase dephosphorylation, (f) SHP-1 association

4.1.3. Spatial dimensions of the cells

As our model is quantitative, based on ordinary differential equations, we needed exact values for the spatial dimensions of NK cells. We used the NK cell line NKL and primary NK cells that were expanded with IL-2. The volumes of each cellular compartment were calculated based on measurements of the cell diameter and literature values (see images in McCann *et al*, 2007; Vanherberghen *et al*, 2004) for the size of the IS and the nucleus (Fig. 7). These volumes were then used to calculate the concentrations of proteins in the compartments.

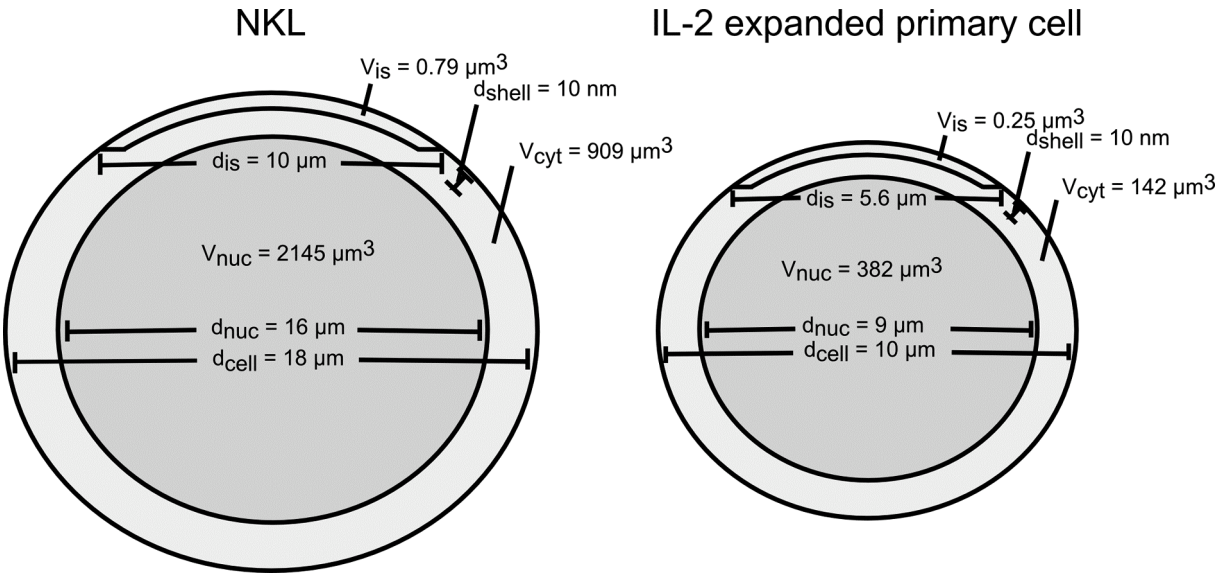

Figure 7: Cellular dimensions. The dimensions of the NK cell line NKL (left) and IL-2 expanded primary human NK cells (right) used for modeling are indicated. Diameter of cells was determined using a Casy cell counter (Innovatis). The volumes of each compartment were calculated from microscopic images from the literature based on the measured dimensions of the cells. V_{is}, volume immunological synapse; d_{shell}, diameter of plasma membrane; V_{cyt}, volume cytoplasm; d_{is}, diameter immunological synapse; V_{nuc}, volume nucleus; d_{nuc}, diameter nucleus; d_{cell}, diameter cell.

4.1.4. Quantification of surface molecules

For running simulations with our model we needed to calculate the concentrations of the molecules involved. The surface molecules NKG2D, NKG2A and CD45 were quantified with a FACS based assay using commercially available calibration beads (Qifikit). These beads are a mixed population, each carrying a defined amount of mouse Fc epitopes on their surface. After preincubation of the cells with monoclonal mouse antibody against the respective molecule, cells and beads were stained with a fluorescent-labeled anti-mouse antibody. With the measured mean fluorescence intensity (MFI) of the bead populations and cells the total amount of molecules on the cell surface was calculated according to the manufacturers instructions. In combination with the cellular dimensions (Fig. 7) we could calculate the concentrations for these molecules. A representative staining of the beads and NKL cells is shown in Fig. 8 and a summary of the results for NKL and primary NK cells in table 1.

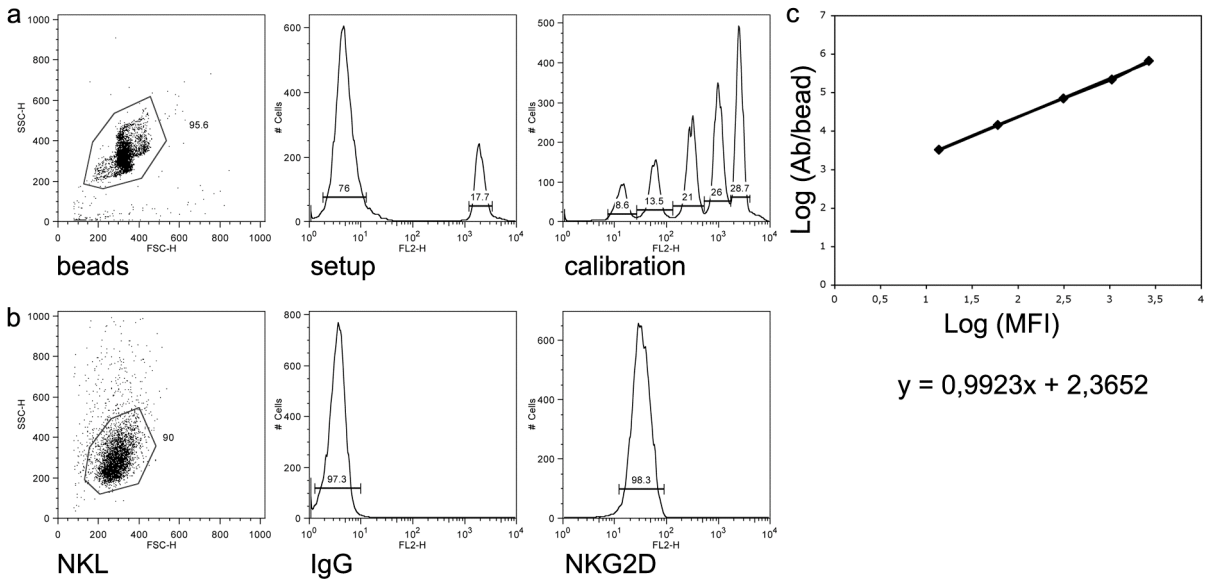

Figure 8: Representative example for the quantification of surface molecules. a: FACS plots of the setup and calibration beads (Qifikit). The setup beads are a mixture of empty beads and beads with the maximal amount of epitopes to adjust the settings of the cytometer. The calibration beads consist of five populations of beads, each with a defined amount of epitopes. b: FACS plots of NKL cells, stained with isotype control or NKG2D specific antibody c: With the information about the amount of epitopes on the calibration beads provided by the manufacturer and the MFI of the bead populations measured with the staining shown in (a) a calibration curve and function were generated to calculate the amount of epitopes on the cells.

Table 1: Summary of the quantification of surface molecules. Numbers are representative for 3 experiments with NKL cells; quantification with primary NK cells has been done with cells from 4 different donors. DAP10 numbers, needed for the simulation, were taken as four times the measured NKG2D numbers to incorporate the stoichiometry of the NKG2D/DAP10 complex.

	NKL		IL-2 expanded primary NK cells	
protein	MFI	molecules/cell	MFI range (mean)	molecules/cell range (mean)
IgG	6	0	2.97-5.61 (4)	0
NKG2D	65	8400	7.39-15.1 (11)	2 648-5284 (3980)
CD94	390	55000	66-128 (94)	8061-16497 (12787)
CD45	807	120000	44-96 (78)	5100-16753 (11756)

4.1.5. Production of recombinant Vav1

For the quantification of cytoplasmic proteins we needed a recombinant standard for the detection by western blotting. The commercially available recombinant Vav1 was not detectable with our preferred antibodies. So we produced a His-tagged N-terminal part of Vav1 (amino acids 2-462) by amplifying the respective sequence using cDNA from primary human NK cells and sub-cloned it into the pRSet B Vector. The protein was over-expressed in *E. coli* BL21-DE3 PLysS and purified under denaturing conditions. Purity was assessed by SDS-PAGE and Coomassie staining (Fig. 9a) and total protein concentration was determined using the EZQ Protein Quantitation Kit (Fig. 9b) according to the manufacturers instructions. Although the recombinant Vav1 was only 15 % pure, detection by western blot did not show unspecific binding of Vav1 antibodies or control antibodies to contaminating proteins. The concentration of Vav1 less contaminations was calculated and used for the following quantification of Vav1 in NKL and primary NK cells.

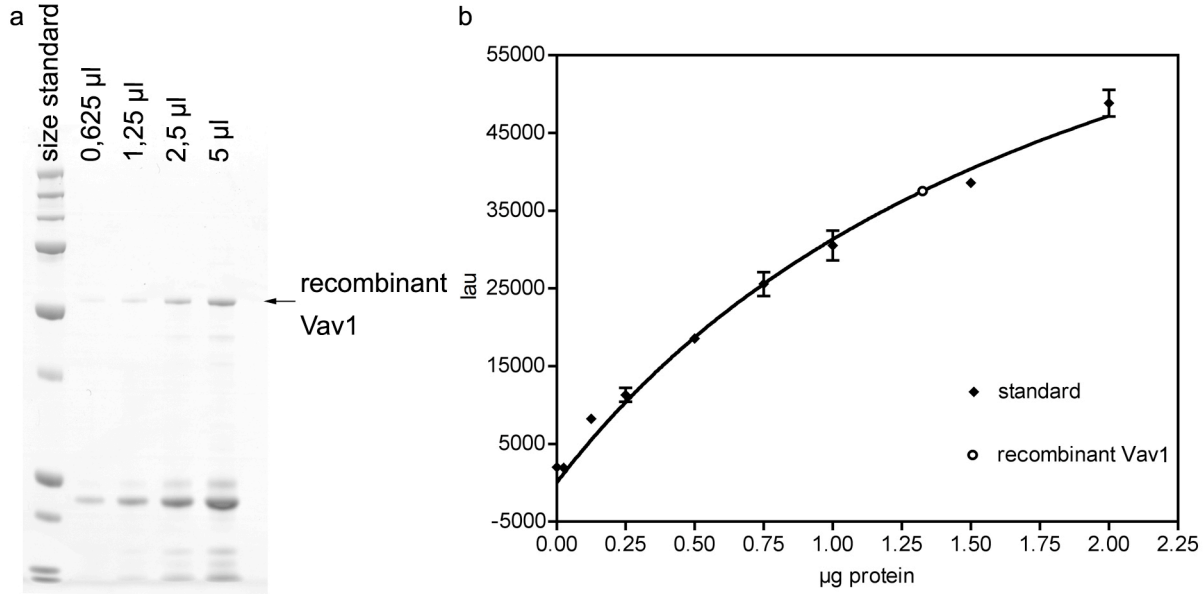

Figure 9: Production of His-tagged N-terminal partial Vav1. a: The purity of the recombinant protein was assessed by coomassie staining and densitometric analysis, Vav1 is 15 % of the total protein. b: Concentration of total protein was determined with the EZQ Kit in comparison to a customized BSA standard. The EZQ assay membrane was scanned with a FLA-2000, measuring linear arbitrary units (lau). The purification contains 1300 ng/µl total protein.

4.1.6. Quantification of intracellular molecules

Cytoplasmic proteins were quantified by western blotting using the purified His-tagged N-terminal partial Vav1 and commercially available recombinant proteins (GST-tagged full length LCK, GST-tagged full length SHP-1) as standards. As the recombinant proteins differed in size from the endogenous proteins a dilution of the standard proteins in constant amounts of cell lysates was subjected to SDS-PAGE and western blotting. Representative blots for NKL with quantifications are shown in Fig. 10 and a summary of the results for NKL and primary NK cells in table 2.

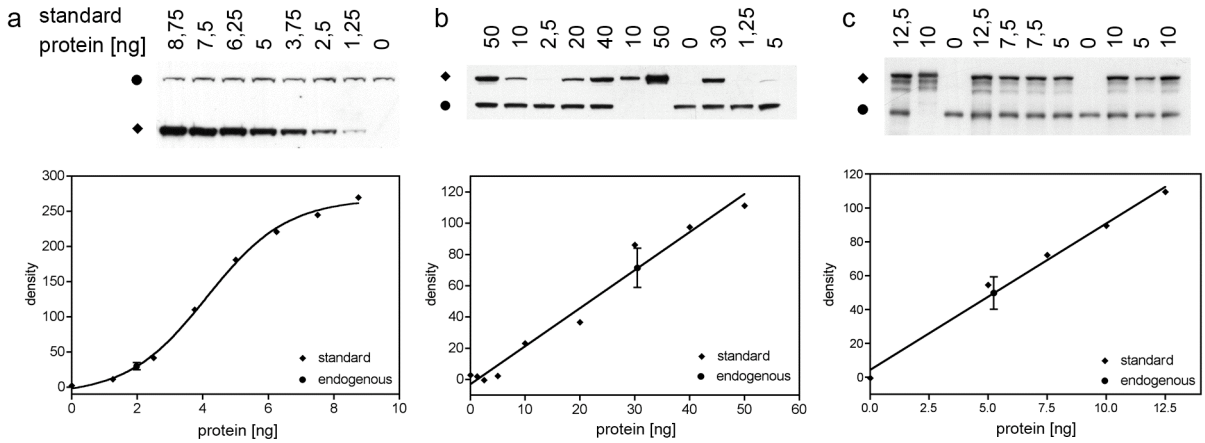

Figure 10: Representative example for the quantification of cytoplasmic proteins. a: Vav1, b: SHP-1 and c: Lck. Blots were analyzed by densitometrical scanning and a standard curve was created for the recombinant protein (indicated in the standard curve and next to the blots by diamonds) and compared to the signal of the endogenous protein (indicated by circles). The amount of endogenous protein per cell was calculated using the following formula: (measured amount of endogenous protein per lane / molecular weight of recombinant protein) * (particles per mol / amount of cells loaded per lane). Representative experiments are shown. Results of all quantifications are summarized in table 2.

Table 2: Summary of the quantification of cytoplasmic proteins. For NKL the mean of at least 3 independent experiments and for primary NK cells the range and mean of at least 5 different donors is shown.

	NKL		IL-2 expanded primary NK cells	
protein	molecules/cell	concentration [nM]	molecules/cell range (mean)	concentration [nM] range (mean)
Lck	710000	1300	553000-1256000 (760000)	6460-14680 (8880)
Vav1	104000	190	79000-359000 (197000)	920-4200 (2300)
SHP-1	1900000	3470	405000-648000 (535000)	4730-7570 (6250)

4.2. Comparing simulation results with experimental data

4.2.1. Initial simulation results

We now used the protein quantification data and kinetic parameters derived from the literature (Mesecke *et al*, 2009, in revision) and calculated the steady state phosphorylation of Vav1 after target cell contact for different activating (MICA) and inhibitory ligand (HLA) concentrations. The ligand concentrations used as an input to the models refer to the concentrations in the target cell sub-compartment directly in contact with the NK cell.

As we wanted to display the response depending on activating and inhibitory stimulus in one graph, we use a three-dimensional coordinate system. The concentrations of the ligands are displayed on the xy-plane, for better visibility the MICA concentration on the y-axis is inversed. The 48 different models basically generate two different response behaviors: Models containing only the modules actin reorganization (a), phosphatase segregation (b), kinase autophosphorylation (d) and SHP-1 mediated kinase dephosphorylation (e) generate a 'valley'-behavior. Activating and inhibitory ligands alone have hardly any effect on the Vav1 phosphorylation, whereas both stimuli together decrease the pVav1-concentration below unstimulated levels (Fig. 11a). The same behavior but with a sharper response appears when we additionally include the SHP-1 association module (f) (Fig. 11b). However, the kinase association module (c) changes the behavior: increasing amounts of activating ligands result in enhanced Vav1 phosphorylation, whereas simultaneous stimulation with inhibitory ligands reduces the level of pVav1, but not to the unstimulated level (Fig. 11c). Again, the inclusion of the SHP-1 association module (f) dramatically increases the steepness of this response. Addition of inhibitory ligand quickly reduces the Vav1 phosphorylation to background level or slightly below and creates a large concentration range of inhibitor dominance (Fig. 11d).

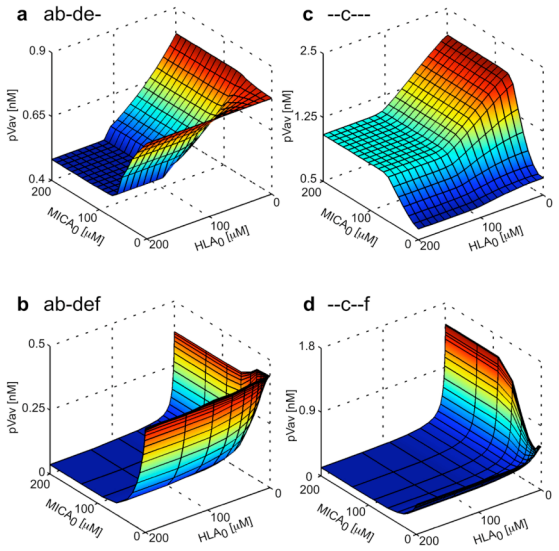

Figure 11: Initial simulations of the Vav1 phosphorylation. Calculations were performed by Sven Mesecke from the Division of Theoretical Bioinformatics (DKFZ). 4 representative pVav1 simulations generated with the 48 different models are shown. The concentration of the NKG2A ligand HLA is displayed on the x-axis, the NKG2D ligand MICA on the y-axis (inversed) and the pVav1 concentration is plotted on the z-axis. The additional modules added to the core model for the simulations shown are indicated above the plots and refer to the numbering in figure 6c.

4.2.2. Confirming activation of NK cells after receptor crosslinking by confocal microscopy

To test the dynamics of Vav1 phosphorylation experimentally, it was necessary to titrate the stimulus directed against activating and inhibitory receptors. As there are no target cells available that express various amounts of ligands for activating and inhibitory receptors and combinations of both we used antibodies to stimulate the cells. As observed by confocal microscopy crosslinking leads to capping of the receptors on one patch of the cell (Fig. 12). NKL cells were coated with primary antibodies directed against activating receptor NKG2D or the inhibitory receptor complex CD94/NKG2A followed by crosslinking with secondary antibody. New

polymerized actin was stained using phalloidin and showed reorganization of actin filaments directed to the site of capping. After 3 and 10 min many cells showed relocalization of receptor and actin (representative cells indicated with white arrows), but the response to the stimulus was very heterogeneous. This observation confirms, that upon receptor crosslinking the NK cells react in a spatially directed manner, like upon encounter with a target cell.

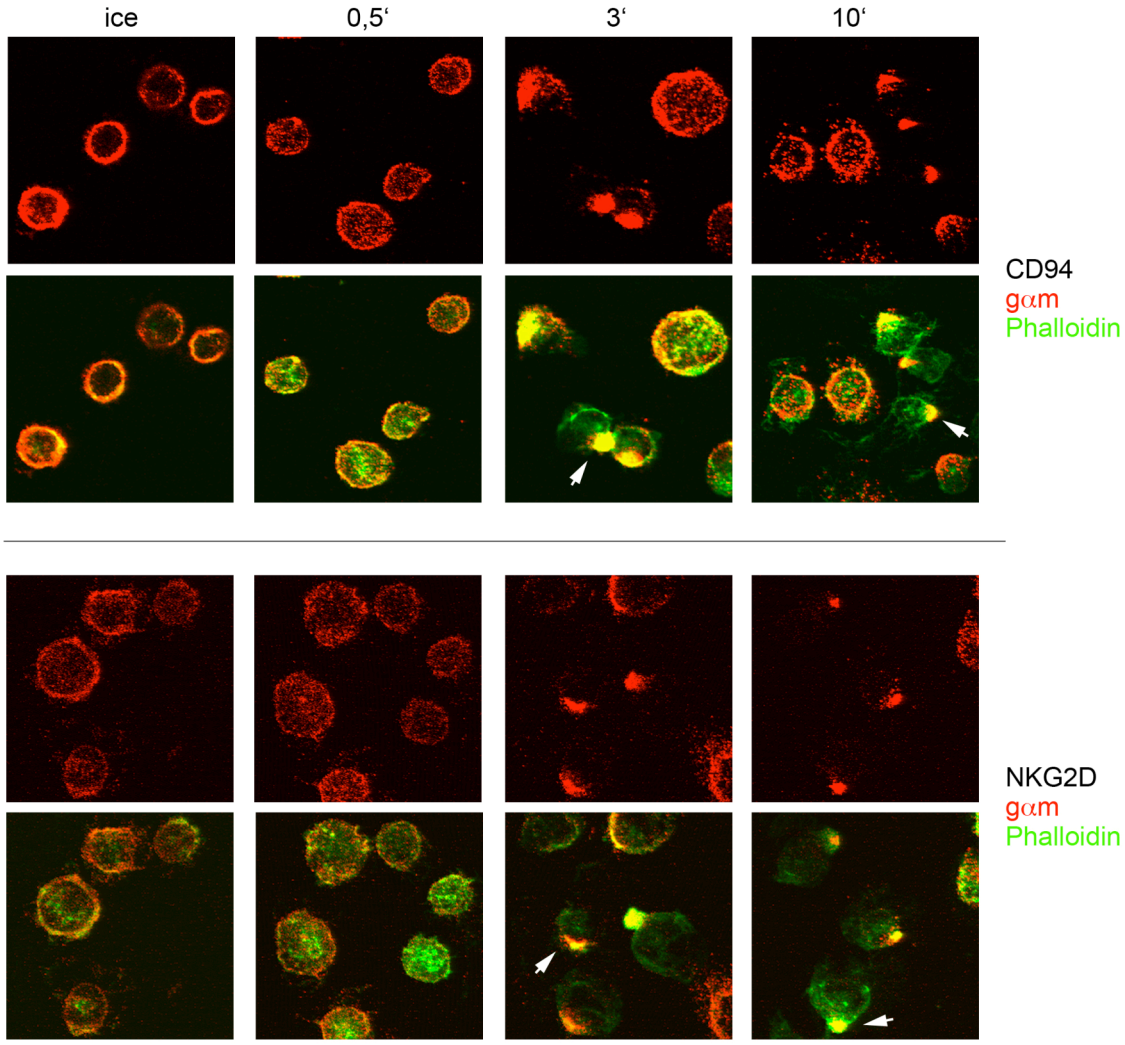

Figure 12: Confocal microscopy of NKL stimulated by receptor crosslinking. NKL cells were first incubated with antibodies against the inhibitory receptor CD94 or the activating receptor NKG2D. Then cells were incubated with Cy3 labeled goat-anti-mouse antibody on ice or for the indicated times on 37°C to crosslink the receptors. After stimulation cells were immediately fixed, permeabilized and stained for actin with Alexa488 labeled phalloidin. Images show the respective receptor and overlays with the phalloidin staining of single sections acquired by confocal microscopy and are representative of three independent experiments. White arrows point to representative cells that show capping of the receptors colocalized with rearranged actin.

4.2.3. Vav1 phosphorylation shows a 2D-sigmoidal response in NKL

To compare the modeling results to the Vav1 phosphorylation in NK cells, we used NKL and triggered the activating receptor NKG2D and/or the inhibitory receptor complex CD94/NKG2A with different concentrations of antibodies followed by crosslinking for 5 min. Vav1 phosphorylation was then determined by quantitative western blotting (Fig. 13b). Increased engagement of NKG2D triggered strong

switch-like induction of Vav1 phosphorylation, which was very effectively counteracted by co-engaging NKG2A. Interestingly, further increasing NKG2D engagement only marginally affected the inhibitory effect of NKG2A. This behavior of Vav1 phosphorylation most closely resembled the simulation results obtained with the model including the kinase association module (c) and SHP-1 association (f) shown in Fig. 13a. The experimental results did not show the same steepness of the inhibitory effect as the simulation results. However, this could be explained by the western blot method used for the determination of Vav1 phosphorylation, which integrates the phosphorylation levels of 100 000 cells. Slight differences in the turning point of Vav1 phosphorylation between individual cells can therefore result in a more blurry response compared to the single cell simulation results. With the reagents available to date it was not possible to measure the Vav1 phosphorylation on a single cell level by FACS analysis.

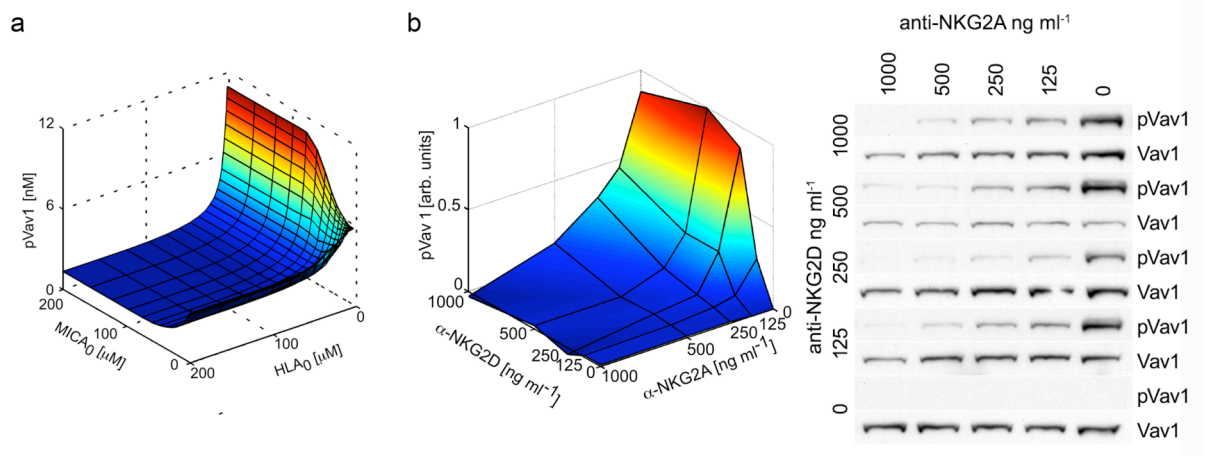

Figure 13: Comparing the experimentally observed Vav1 phosphorylation with the modeling results. a: Simulation of pVav1 with the model including kinase association and SHP-1 association (--c--f). b: Experimental determined Vav1 phosphorylation after stimulation with various amounts of anti-NKG2A and anti-NKG2D and crosslinking antibody for 5 min at 37°C. The Vav1 western blots were quantified like in Fig. 5 and are displayed in a three-dimensional coordinate system. The result is representative for three independent experiments. Module (c) in the simulation was essential to create the dose-response profile matching the experimental observation, module (f) created the steepness and the strong inhibitor dominance.

4.2.4. Vav1 phosphorylation shows a sigmoidal response in primary NK cells

To confirm the physiological relevance of the pVav1 response that we observed in the NKL cell line we wanted to reproduce these findings with primary NK cells. As we need for our experiments large amounts of an NK cell population with homogenous expression of one inhibitory receptor, IL-2-expanded primary human NK cells were analyzed by FACS for the expression of NKG2D (Fig. 14a) and inhibitory receptors. The majority of NK cells from this donor expressed the inhibitory receptor KIR2DL2/3 (Fig. 14b). We stimulated the cells with various amounts of antibodies against NKG2D and KIR2DL2/3 and analyzed the Vav1 phosphorylation. After NKG2D crosslinking alone we observed a steep hyperbolic dose-response of pVav1 (Fig. 14c). When we used a constant amount of anti-NKG2D and titrated the anti-KIR2DL2/3 antibody Vav1 phosphorylation was efficiently reduced almost to

background levels (Fig. 14d). The dominance of the inhibitory signal was even more pronounced than in NKL cells.

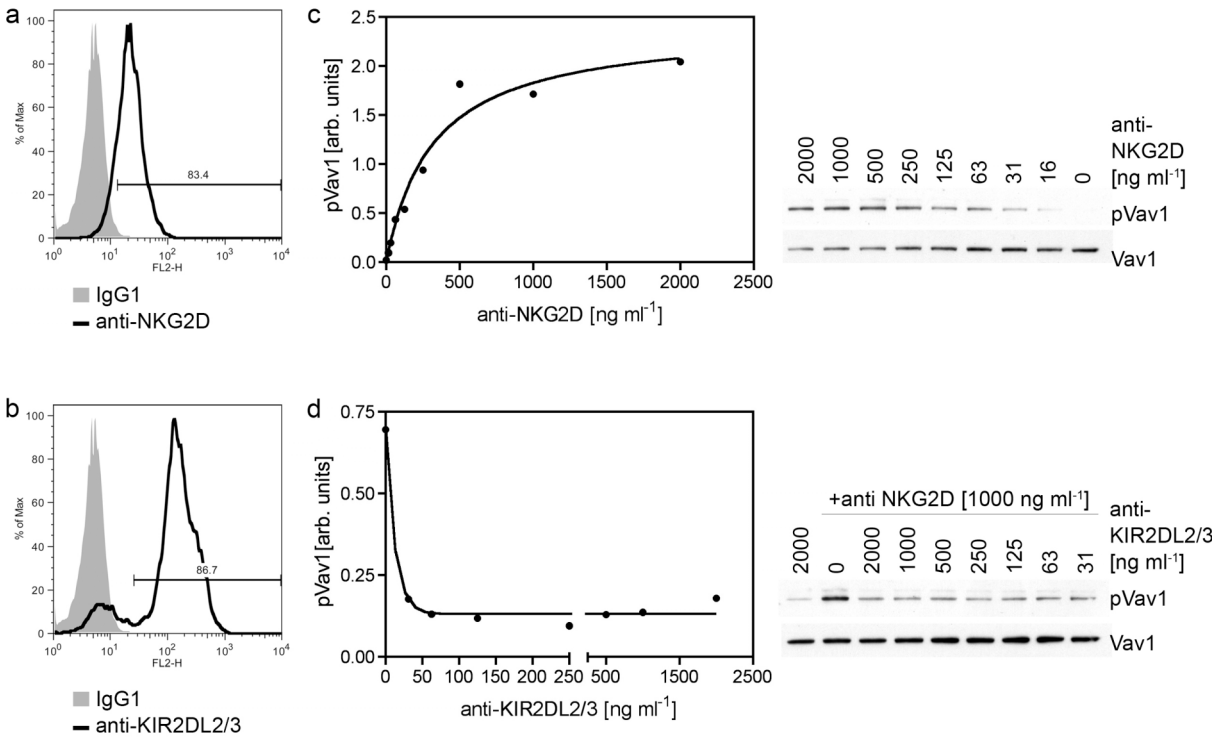

Figure 14: pVav1 response in primary NK cells. FACS staining showing the expression of a: NKG2D and b: the inhibitory receptor KIR2DL2/3. c: NK cells were stimulated with the indicated amounts of an anti-NKG2D antibody followed by crosslinking with goat-anti-mouse antibody for 5 min at 37°C. Cells were then lysed and pVav1 was determined by western blotting. d: NK cells were stimulated with 1000 ng/ml anti-NKG2D plus the indicated amounts of an anti-KIR2DL2/3 antibody followed by crosslinking and analyzed for pVav1. Vav1 phosphorylation was quantified like in Fig. 5.

4.2.5. Confirming the activation of NK cells with antibody coated beads by confocal microscopy

Crosslinking of receptors is one method to stimulate NK cell receptors in a titratable way. But the application of the crosslinking antibody that pulls receptors together from the outside of the cell could lead to artifacts. To stimulate the cells in a more physiological way we also wanted to use antibody coated beads. We first checked for saturating antibody load of the beads by FACS staining (data not shown) and mixed beads that were saturated with antibody with NKL. In a first experiment we confirmed by confocal microscopy that cells formed conjugates with these beads (Fig. 15). Cells were stained with phalloidin to visualize actin reorganization and with Choleratoxin (CTX) subunit B for lipid rafts. With beads that were not antibody coated or incubated with control antibodies (Isotype control, CD56) we observed some background activation of the NK cells. But this activation was not directed towards the control beads (indicated by blue arrows). Only with anti-CD94 and anti-NKG2D we detected actin polymerization that was in most cases directed toward the beads (white arrows). With anti-NKG2D we additionally observed, that actin and the CTX stained membrane wrap around the beads.

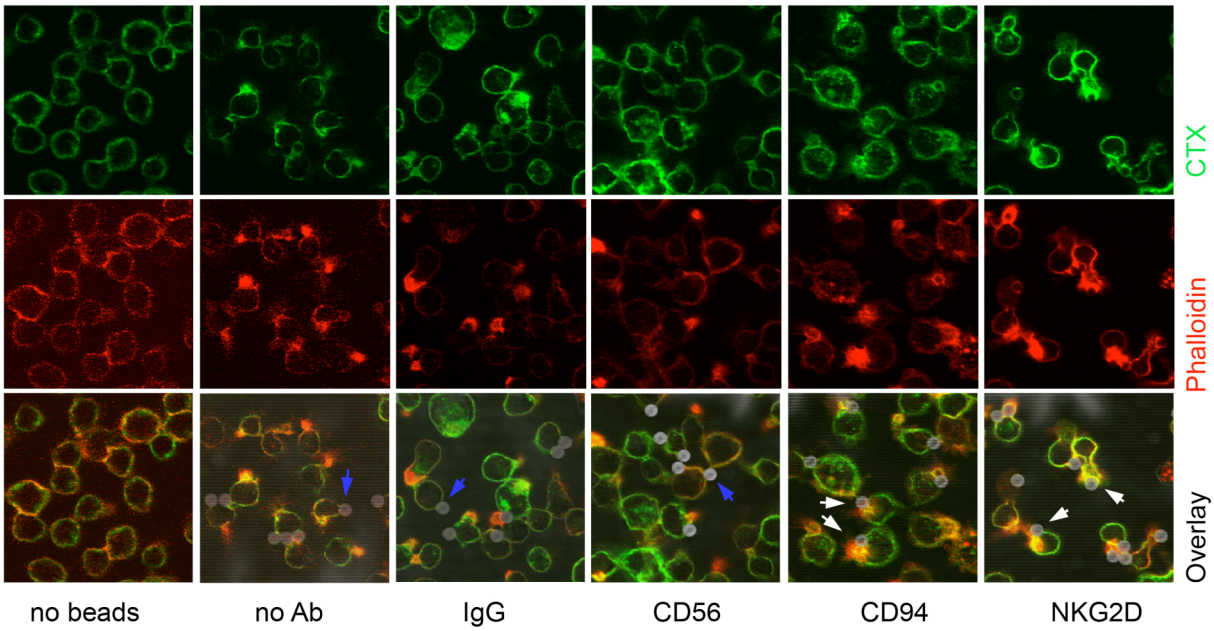

Figure 15: Analysis of NKL-bead conjugates by confocal microscopy. NKL cells were incubated with or without beads on Poly-L-Lysine (PLL) coated coverslips for 30 min. Then cells were stained with Alexa488 labeled CTX, fixed, permeabilized and stained with Tritc labeled phalloidin. Images show single sections acquired by confocal microscopy. To visualize the position of the beads, DIC pictures were acquired, and in inverse color overlaid with the fluorescent images. Blue arrows point to beads attached to cells without, white arrows with, directed actin polymerization.

4.2.6. Vav1 and ERK phosphorylation induced by antibody coated beads

After we confirmed binding of antibody-coated beads to NK cells and observed activation by microscopy we used these beads to stimulate NK cells. We first tested the optimal stimulation time with the beads. In contrast to antibody crosslinking the phosphorylation of Vav1 occurred much slower with an initial lag phase of 4-5 min and reached the maximum after 10-15 min (data not shown). A possible explanation for the slower kinetic is that the antibodies on the beads are immobile, and diffusion can only occur on the NK cell membrane. Starting with the saturating concentration of anti-NKG2D antibody, as determined by FACS, we coated the beads with decreasing amounts of antibody and mixed them at a 1:1 ratio with the NK cells. With this stimulation method we were also able to detect a concentration dependent steep increase of phosphorylated Vav1 (Fig. 16a,b). The MAPK cascade is another signaling event necessary for the cytotoxic response of NK cells, and is induced after activating receptor stimulation. Therefore we also checked for ERK1/2 activation with antibodies specific for double phosphorylated and total ERK1/2 (Fig. 16c,d). Using coated beads we observed a dose-response similar to the response induced by receptor crosslinking.

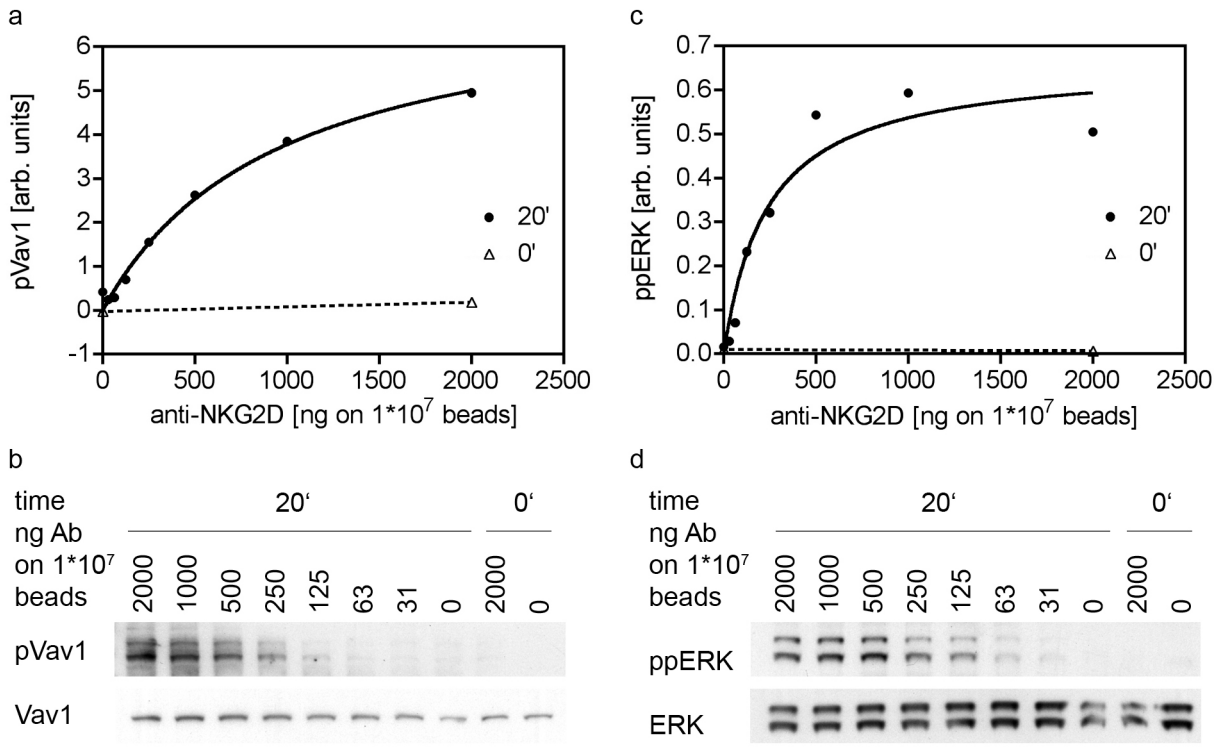

Figure 16: Phosphorylation of Vav1 and ERK1/2 after stimulation with anti-NKG2D coated beads. NKL cells were stimulated for 20 min on 37°C at a 1:1 ratio with beads coated with various amounts of anti-NKG2D. Cells were then lysed and analyzed for b: Vav1 and d: ERK1/2 phosphorylation by western blotting. a,c: Blots were quantified as described in Fig. 5, both proteins show a very steep antibody-concentration dependent increase in phosphorylation. The result is representative for two independent experiments.

4.2.7. Testing the kinetic parameters used in our model

We quantified the concentrations of the molecules involved in our model, but we also needed kinetic parameters for all occurring reactions to run the simulations. So our cooperation partner extracted the necessary values from the literature. These parameters varied in some cases over magnitudes and were measured in different, sometimes quite artificial systems. Using the literature derived parameters for our simulations, the kinase association module (c) was essential to produce a physiologic response, and the SHP-1 association module (f) produced the required steepness (see Fig. 11c,d). Two different methods can be applied to assess kinetic parameters in mathematical models. One possibility is to perform a parameter fit. This method aims at fitting the kinetic parameters to match the simulation to the experimental data. The result of this parameter fit reassured, that the kinase association is essential for our model to create the physiologic response and not only depending on kinetic parameters. All models lacking the kinase association failed and showed a 'valley' behavior (similar to Fig. 11a,b). The steepness of the onset of the inhibitory signal was not only dependent on SHP-1 association with the fitted parameters.

The second possibility to test the kinetic parameters is to perform a parameter scan. The kinetic parameters were randomly varied over 4 log scales to generate 5000 sets of random parameters. For each of these parameter sets the Vav1 phosphorylation was simulated with the 48 models. The resulting simulation profiles were then

classified automatically to 9 different possible shapes; only one of these shapes represents the experimentally observed response. Also with this method we could show that the kinase association module (c) is essential to create a physiological response. With these methods we assured, that module (c) is a critical reaction in our simulation. Our model is very stable and does not depend on a small range of kinetic parameters.

4.2.8. Association of NKG2D with SFKs

Our model suggests that association of SFKs with the activated receptor is absolutely essential for the observed Vav1 response. Most of our experiments were performed by stimulating the NKG2D receptor, direct downstream mechanisms for this receptor are only partially described. So we decided to check for association of this receptor with SFKs in a Co-immunoprecipitation approach (Fig. 17). As harsh detergents disrupt weak protein interactions we lysed the cells in a Brij-58 containing buffer, which is a very mild detergent. The receptor gets recruited to detergent resistant membrane domains after stimulation, so the majority of the receptor gets lost during clarification of the lysates. To avoid this we established an immunoprecipitation protocol from whole cell lysates using magnetic beads. Nevertheless we also noted a slight decrease of recovered receptor in stimulated samples; probably the receptor is less accessible to precipitation after stimulation. The SFKs Fyn and Lck weakly associated with NKG2D in lysates from unstimulated cells, but upon crosslinking of NKG2D we detected high amounts of Fyn and Lck. Additionally Vav1 could be co-precipitated, and this receptor bound Vav1 was strongly phosphorylated. Here we were able to show, that upon receptor crosslinking we find an increase in associated SFKs, which creates a high local concentration of kinases at the stimulated receptors.

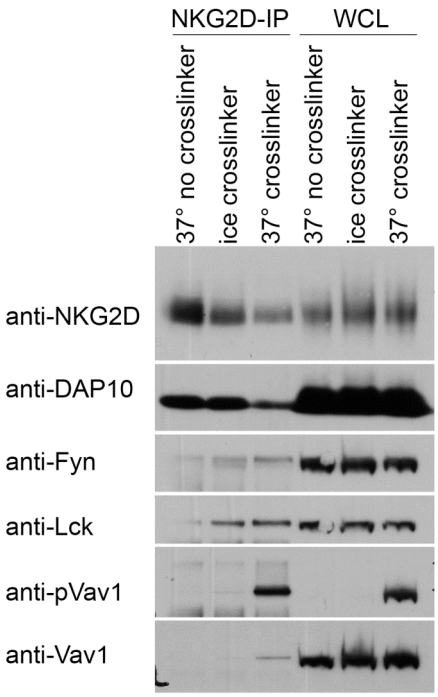

Figure 17: Immunoprecipitation of NKG2D with associating proteins. NKL cells were first incubated with anti-NKG2D. One aliquot was incubated for 3 min at 37°C without crosslinking antibody, one with crosslinker on ice and another with crosslinker at 37°C. Cells were then lysed using the mild detergent Brij-58 and NKG2D was precipitated from whole cell lysates (WCL) using Protein G coated magnetic beads. Proteins eluted from the beads and an aliquot of the WCL were analyzed. We were able to detect the adapter DAP10 in every sample. The amount of SFKs Fyn and Lck that were co-precipitated was strongly increased after receptor crosslinking. Detection of phosphorylated Vav1 confirmed enrichment at the site of stimulation and the activation of the cells. The result is representative for three independent experiments.

4.2.9. SHP activity: Phosphorylation, association or location?

In previous studies it already has been shown that SHP-1 can associate with phosphorylated ITIMs of inhibitory receptors, which we included in our model as module (f). But SHP-1 also could be phosphorylated itself, resulting in increased activity of the phosphatase. In order to distinguish between these two possible regulation mechanisms, we immunoprecipitated SHP-1 and applied a commercially available activity assay. This assay detects free phosphate after cleavage of a SHP specific substrate. We detected specific SHP-1 activity, as we could block phosphate release with the phosphatase inhibitor pervanadate to the same background level we found in a preclear IP that did not contain any SHP-1. The SHP-1 activity did not change from the level of unstimulated cells when we crosslinked the inhibitory receptor NKG2A alone or in combination with NKG2D (Fig. 18a). By western blotting we were able to detect approximately equal levels of SHP-1 in every sample (Fig. 18b), but we could not detect any phosphorylation by using the phospho-tyrosine specific antibody 4G10 (data not shown). This supports the hypothesis, that phosphorylation of SHP-1 is not required, but that the association of SHP-1 with the receptor is essential for the inhibitory function.

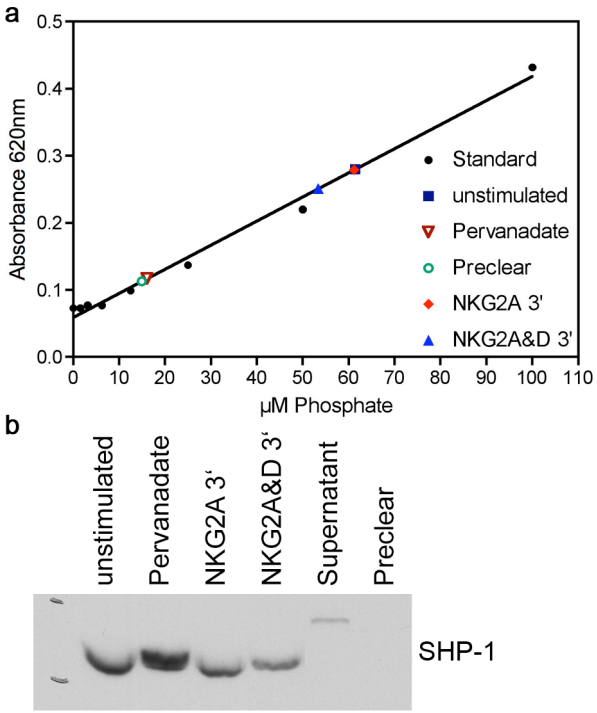

Figure 18: Measuring SHP-1 activity. SHP-1 was first precipitated from lysates of differently stimulated NKL cells, as a negative control Protein G agarose beads without antibody were used. a: These beads were incubated with a phosphorylated SHP specific substrate, to block Phosphatase activity pervanadate was added to one sample during the substrate reaction. As readout free phosphate was measured and compared to a standard. b: Precipitated SHP-1 was further analysed by western blotting which confirmed equal amounts of SHP-1 in the samples. Phosphorylation of SHP-1 was not detected with the 4G10 phosphotyrosine specific antibody (data not shown). The results are representative for at least three independent experiments.

4.2.10. Quantification of Vav1 and SFK phosphorylation levels

Our quantitative model also gives us information about the absolute concentration of phosphorylated signaling molecules; we wanted to confirm this data experimentally. As we could not obtain phosphorylated recombinant standard proteins to quantify the amount directly, we chose a semiquantitative method. By treating cells with the phosphatase inhibitor pervanadate we created a lysate with maximum phosphorylated proteins (100 %) and by incubating cells with the SFK inhibitor PP1 we obtained lysate with the minimal phosphorylation (0 %). The maximum

phosphorylation lysate was then diluted in the minimal phosphorylation lysate and used to create a standard. This standard and lysates of cells stimulated via receptor crosslinking were then analyzed by quantitative western blotting (Fig. 19c,d). We created a standard curve and compared it with the phosphorylation levels of cells stimulated via NKG2D and NKG2A (Fig. 19a,b). About 11 % of Vav1 was phosphorylated after NKG2D crosslinking whereas after NKG2A stimulation Vav1 phosphorylation was not higher than in the medium control. No significant SFK phosphorylation could be detected after receptor crosslinking. Therefore we can exclude, that the kinase autophosphorylation module (d) plays a role in our experimental system. A maximal Vav1 phosphorylation of 11 % corresponds to a concentration of 20 nM pVav1. The simulations with literature derived kinetic parameters predicted a lower phosphorylation level, but after fitting of the parameters our model including (c) and (f) could produce 16 nM of maximal Vav1 phosphorylation.

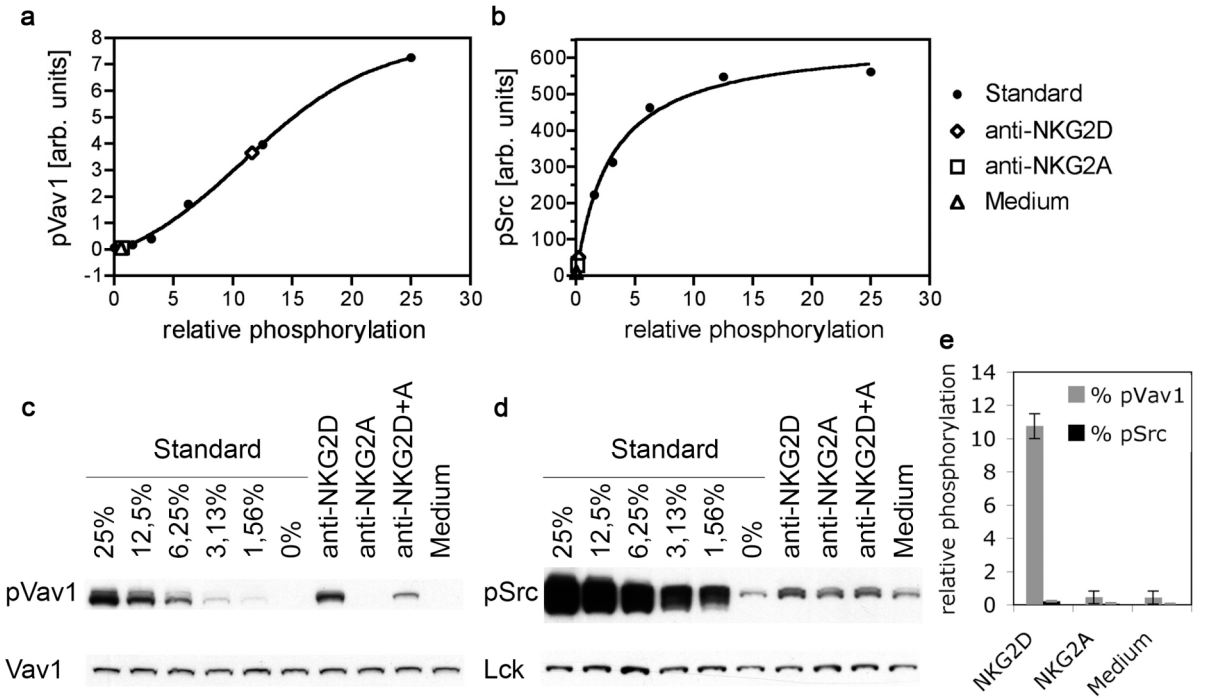

Figure 19: Semiquantitative analysis of Vav1 and SFK phosphorylation. The lysate of pervanadate stimulated cells was diluted in lysate of PP1 pretreated cells to create a standard and compared to lysates from cells activated via receptor crosslinking. Standard curves for a: pVav1 and b: SFK phosphorylation (detected with anti-pSrc) are shown (filled circles) with the respective crosslinked samples (open symbols). The blots quantified are shown in c and d. e: The results of 3 independent experiments are summarized as mean with STD.

4.2.11. Kinetic of Vav1 phosphorylation after NKG2D stimulation

To further validate the physiologic response of the core model containing the kinase association module (c), we calculated the kinetic change in Vav1 phosphorylation upon NKG2D triggering. The model predicted a rapid increase in Vav1 phosphorylation which reached a plateau about 200 seconds after NKG2D receptor engagement (Fig. 20a). While lowering the initial MICA concentration reduced the amplitude of the Vav1 phosphorylation, the time needed to reach the phosphorylation

plateau remained unchanged. To validate these results experimentally we triggered the NKG2D receptor on NK cells and determined the kinetics of Vav1 phosphorylation by western blotting (Fig. 20b). In agreement with the simulation results we observed a rapid increase of Vav1 phosphorylation, which reached its maximum at about 90 seconds after receptor engagement. Reduced engagement of NKG2D with suboptimal antibody concentrations resulted in lower Vav1 phosphorylation with unchanged kinetics, confirming the predictions of the model. However, in contrast to the simulation results, we observed a reduction of Vav1 phosphorylation between 5 and 10 min after receptor engagement. This suggests the presence of negative regulatory signaling pathways to terminate the signal, which are presently not incorporated in our model.

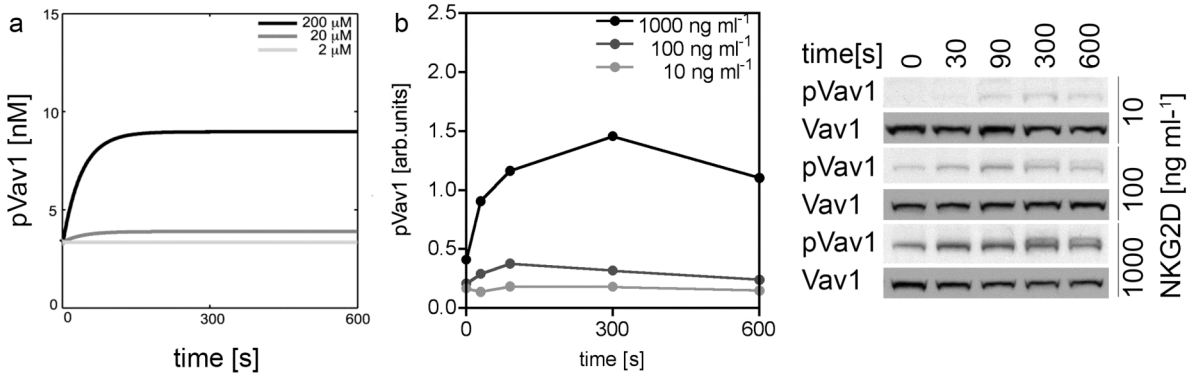

Figure 20: Kinetic of the Vav1 phosphorylation depending on differential engagement of the activating receptor NKG2D. a: The indicated concentrations of the NKG2D ligand MICA were used in the model to calculate the kinetic change in Vav1 phosphorylation. b: Vav1 phosphorylation in NKL cells was then determined experimentally by crosslinking the NKG2D receptor using the indicated concentrations of anti-NKG2D antibody. One representative experiment out of four is shown.

4.2.12. Ca^{2+} flux after stimulation of activating and inhibitory receptors

Additionally to Vav1 phosphorylation we studied Ca^{2+} flux as a very fast responding, receptor proximal signaling event. Our hypothesis is that the activating and inhibitory signals get integrated on the level of Vav1 first and pass this signal on.

We labeled NKL with the Ca^{2+} sensitive dye Fluo4, which increases its fluorescence after Ca^{2+} influx. By using a plate reader we could quantify multiple samples with different stimulation conditions at once and also include kinetic data. Cells were first incubated with various concentrations of antibodies against the activating receptor 2B4 and the inhibitory receptor complex NKG2A/CD94. The baseline of Fluo4 fluorescence was recorded, then crosslinking antibody was added to all wells at the same time and the kinetic Ca^{2+} response was recorded until a plateau was reached. An example for one concentration of anti-2B4 and various anti-CD94 concentrations is shown in Fig. 21. Control antibody did not induce Ca^{2+} flux, but anti-2B4 produces a sharp increase in fluorescence. This signal can be inhibited by anti-CD94 in a dose dependent way. As the data obtained with the plate reader measurement is very noisy and we sometimes observed already different basal fluorescence levels before crosslinking, we decided to quantify the Ca^{2+} flux as area under the curve from the moment of crosslinker addition until the plateau was reached (about 7 min). This

quantification has the additional advantage, that we can compare all combinations of stimulation in one matrix (Fig. 22). In this experiment we observed, that similar to Vav1 phosphorylation the Ca^{2+} signal can be inhibited in a dose dependent way and the inhibitory signal is dominant over the signal from activating receptors.

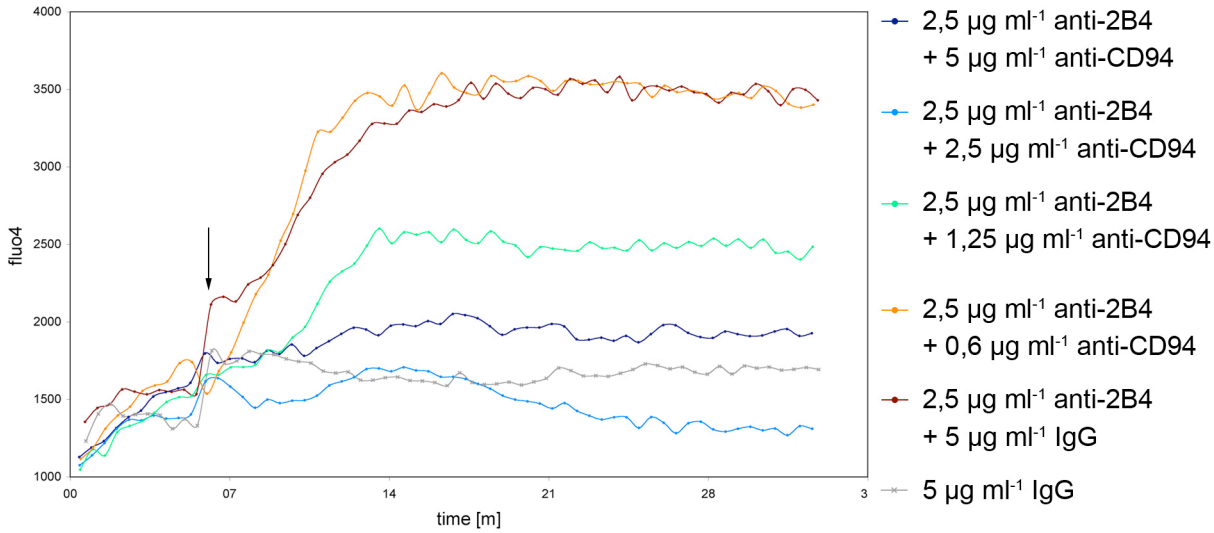

Figure 21: Kinetic of Ca^{2+} flux after stimulation of activating and inhibitory receptors. NKL were labeled with the Ca^{2+} sensitive dye Fluo4 and incubated with 2,5 µg/ml of anti-2B4 and various amounts of anti-CD94. We first recorded the baseline of Ca^{2+} flux; upon crosslinker addition (indicated as black arrow) we noted a strong increase of Fluo4 intensity in the samples incubated with more anti-2B4 than anti-CD94. Samples incubated with equal amounts, more anti-CD94 or control antibody did not show this increase. Mean values of triplicate samples are shown, and are representative for three independent experiments.

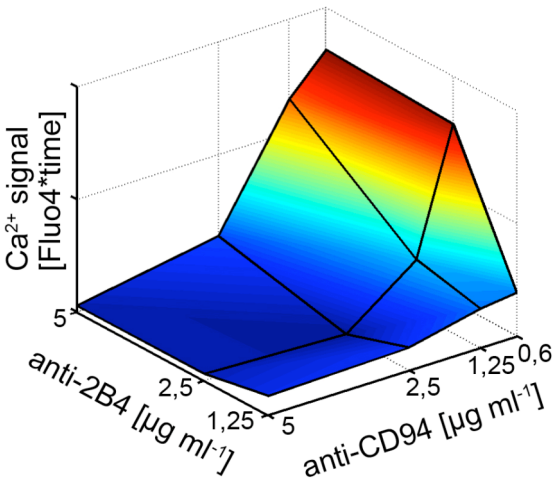

Figure 22: Ca^{2+} signal after various stimulations of activating and inhibitory receptors. To display the Ca^{2+} signal upon various activating and inhibitory signals we recorded the kinetic from the moment of crosslinker addition until the plateau was reached (15 time points, about 7 min) and displayed the result as area under the curve. With this method we can display all combinations of activating and inhibitory stimulus in one matrix. Ca^{2+} signal induced by 2B4 stimulation can be effectively blocked by CD94 triggering.

4.3. Challenging our model

4.3.1. NKG2D clustering is not affected by MEK and SFK inhibitors

So far we confirmed that our model is able to produce physiological endpoint and kinetic simulations for the phosphorylation of Vav1. To further test the reliability of our model we perturbed the signaling cascade by the use of chemical inhibitors. We first

tested the influence of SFK and MEK on the response of NKL cells after receptor crosslinking (Fig. 23). The cells were pretreated for 30 min on 37°C with the respective inhibitors or DMSO as solvent control. We preincubated the cells with anti-NKG2D antibody and crosslinked the receptor for 10 min or incubated a control sample on ice. Cells were immediately fixed, permeabilized and stained for actin. After incubation on ice the NKG2D receptor and actin were distributed homogeneously around the cell, but after incubation on 37°C most of the cells showed capping of the receptor on one site of the cell, which colocalized with polymerized actin. Treatment with inhibitors did not influence the overall morphology of the cells. Receptor capping was not reduced, suggesting that this process is upstream of SFK and MEK activity.

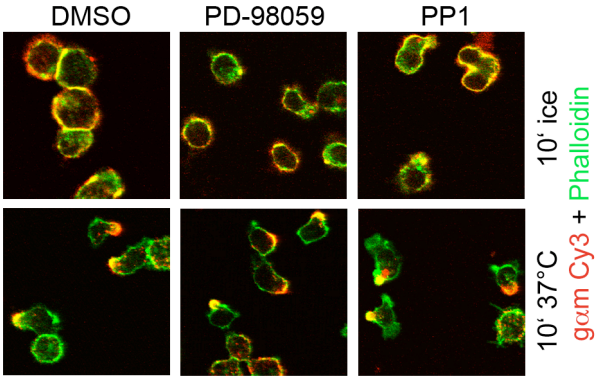

Figure 23: Effect of MEK and SFK inhibition on receptor capping. NKL were pretreated for 30 min on 37°C with the MEK inhibitor PD-98059, the SFK inhibitor PP1 or DMSO as solvent control. We incubated the cells with anti-NKG2D antibody and afterwards incubated with a Cy3 labeled crosslinking antibody for 10 min on ice or at 37°C. After fixation cells were permeabilized and stained with Alexa488 labeled phalloidin. Images show overlays of single sections acquired by confocal microscopy and are representative of two independent experiments.

4.3.2. Effect of reduced SFK activity on the kinetic of Vav1 phosphorylation

As kinase association (c) was identified as crucial step for the phosphorylation of Vav1, we challenged our model by SFK inhibition. We reduced the activity of SFKs in our model and experimentally by PP1 treatment and measured the kinetic of Vav1 phosphorylation. Simulation of the core model containing module (c) with decreased SFK activity predicted a reduced steepness of the Vav1 phosphorylation dynamics and a decrease in the final pVav1 concentration (Fig. 24a). To test these predictions experimentally we measured Vav1 phosphorylation in response to engaging the NKG2D receptor in the presence of different PP1 concentrations (Fig. 24b). Without inhibitor we observed a rapid increase in Vav1 phosphorylation reaching its plateau at about 90 seconds after NKG2D engagement. The presence of increasing PP1 concentrations affected the kinetics, slope and amplitude of Vav1 phosphorylation, essentially confirming our simulation results. As we confirmed before that treatment with PP1 did not affect clustering of the receptor we concluded, that this effect was really due to inhibition of SFK activity.

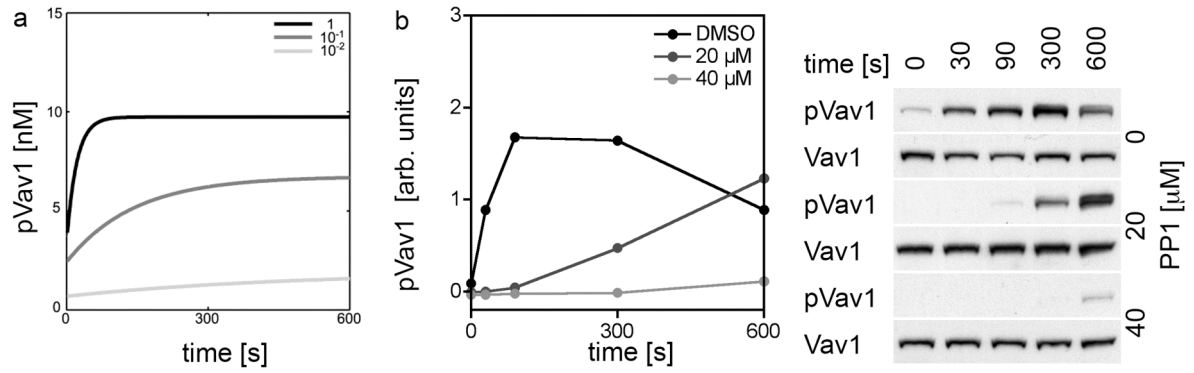

Figure 24: Kinetic changes in Vav1 phosphorylation depending on SFK activity. a: The activity of SFKs was reduced to 10 % or 1 % of the original values and the kinetic changes in Vav1 phosphorylation were calculated after triggering with 200 µM MICA. b: Vav1 phosphorylation was then determined experimentally by crosslinking NKG2D on NKL pretreated for 30 min with the indicated concentrations of PP1 or DMSO as control. Representative data of three independent experiments are shown.

4.3.3. Cytotoxic activity corresponds to Vav1 phosphorylation

If Vav1 phosphorylation is the decision making point for NK cell activation, the decision made at this level is then transmitted to downstream signaling pathways resulting in the cytotoxic activity of NK cells. This hypothesis would therefore predict that the profile of Vav1 phosphorylation upon engagement of activating and inhibitory receptors is paralleled by NK cell cytotoxicity. To test this, we determined the cytotoxic activity of NK cells upon differential triggering of activating and inhibitory receptors in a redirected lysis assay using Fc receptor positive target cells. Increasing the level of NKG2D engagement resulted in a rapid increase of target cell lysis by NKL cells quickly reaching a plateau (Fig. 25a). Co-engagement of the inhibitory CD94/NKG2A receptor very effectively blocked target cell lysis even at very low concentrations and created a large concentration range where the inhibitory signal dominated the response. A similar dose-response was observed when using an NK cell clone expanded from primary human NK cells (Fig. 25b). The profile of cytotoxicity nicely paralleled the Vav1 phosphorylation levels predicted by our mathematical model including all optional modules (Fig. 25c), supporting the hypothesis that pVav1 levels establish a key checkpoint for NK cell cytotoxic activity.

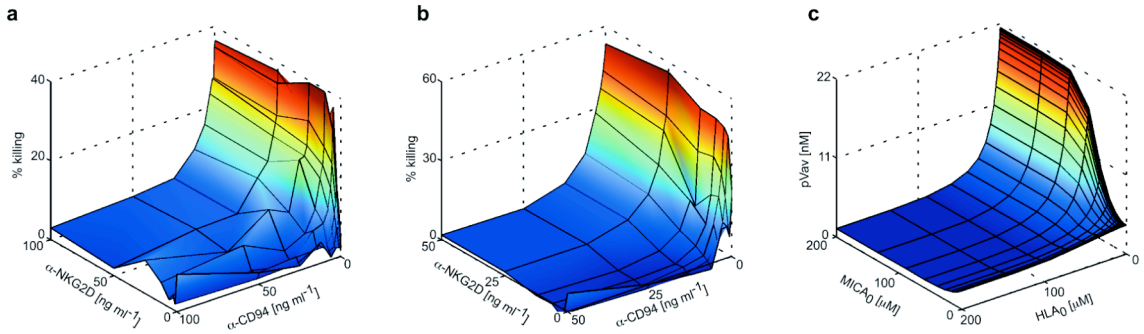

Figure 25: The cytotoxic activity of NK cells correlates with Vav1 phosphorylation. a: NKL cells and b: a primary human NK cell clone expressing the inhibitory CD94/NKG2A receptor were used in a 4h redirected ^{51}Cr release assay. The NKG2D and the CD94 receptor were triggered with the indicated concentrations of antibodies and the resulting lysis of the target cells is indicated. Representative of a: five and b: two independent experiments. c: The calculated pVav1 response upon differentially triggering of activating and inhibitory receptors using the complete mathematical model.

4.3.4. Effect of reduced SFK activity on pVav1 response and cytotoxicity

Additionally to changes in the kinetic of the pVav1 response (shown in Fig. 24), the SFK inhibitor PP1 also reduced the amplitude of the signal. Our model produced physiological endpoint simulations for the phosphorylation of Vav1 (Fig. 13), and the dose-response of cytotoxicity followed the Vav1 phosphorylation. If the decision about NK cell activation is made on the level of Vav1 phosphorylation, disturbing the NK cell activation with PP1 should have the same effect on cytotoxicity as on pVav1. Therefore we checked Vav1 phosphorylation after 5 min of differential engagement of NKG2D and NKG2A/CD94 with and without partial SFK inhibition (Fig. 26c&d). Also in this experiment we noted the decrease in maximal Vav1 phosphorylation, while the overall shape of the response was preserved. This is consistent with the predictions of our model (Fig. 26a&b). To examine the effect of PP1 on cytotoxicity we performed redirected a lysis assay like in Fig. 25a with or without PP1. Reducing the SFK activity only reduced the maximum cytotoxicity, but the profile of the response remained unchanged, further validating our hypothesis.

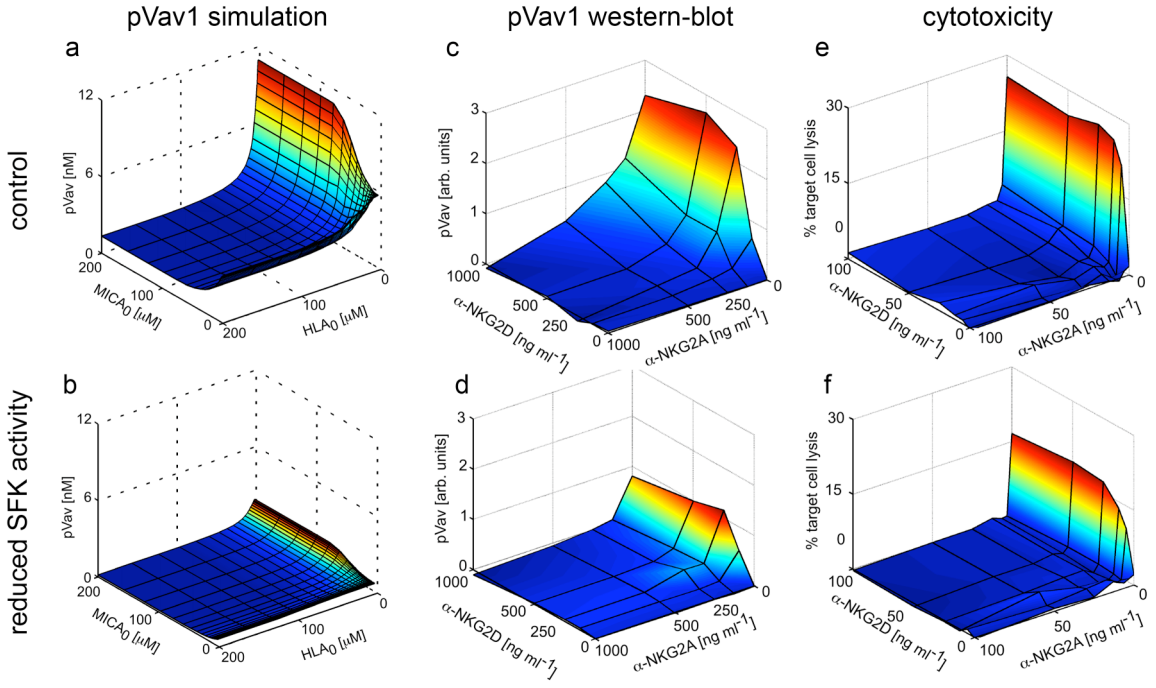

Figure 26: Comparison between predicted and experimentally observed pVav1 and cytotoxic response after reducing SFK activity. Using the core model including module (c) and (f) the phosphorylation of Vav1 for different activating and inhibitory ligand concentrations was simulated with a: full or b: 10 % SFK activity. The human NK cell line NKL was pretreated d: with 5 µM or c: without PP1 for 30 min at 37°C and then incubated with the indicated concentrations of antibodies against the activating receptor NKG2D and the inhibitory receptor NKG2A. After crosslinking with secondary antibodies cells were incubated at 37°C for 5 min. Vav-1 phosphorylation was determined by quantitative western blotting. NKL f: with 5 µM or e: without PP1 were also used in a redirected lysis assay to measure their cytotoxic activity.

5. Discussion

5.1. How are activating and inhibitory signals integrated by NK cells

NK cells receive signals via many activating and inhibitory receptors, that cause a gradual signal input. The cytotoxic response of an NK cell towards a target cell is a yes or no decision. NK cells have to integrate the multitude of incoming signals to decide if they kill or do not kill the target cell. But how do the cells calculate this? The easiest explanation is, that activating and inhibitory signals converge at one point in the signaling cascades initiated by the different receptors. Inhibitory receptors transmit the signal via phosphatases recruited to ITIMs, but different activating receptors initiate different activation cascades and all can be blocked by inhibitory signals. Promising candidates to integrate the signal are the GEFs belonging to the Vav family. Vav1 is a known direct target of the phosphatase SHP-1 and is part of the signals induced by the activating receptors NKG2D and 2B4 studied here.

We therefore propose a model that could describe how activating and inhibitory signals get integrated directly receptor proximal on the level of Vav1 phosphorylation. Mathematical analysis of the possible reactions should reveal if this simple system already provides the possibilities to integrate the signals and to produce a physiological response. Additionally, the gradual activating and inhibitory signal input has to be transformed to permit the cell to come to a reliable killing decision.

The Vav1 phosphorylation upon differential stimulation showed a switch-like behavior towards activation and inhibition. Our simplified model was able to simulate a physiological dose-response of pVav1, but including the association of the kinase with the receptors (c) was absolutely essential. We confirmed this interaction in our system experimentally. With a regular co-immunoprecipitation protocol, we noted high loss in the amount of NKG2D recovered after stimulation, compared to unstimulated controls. We observed that the receptor is found in the nuclear fraction after clarification of the lysates (data not shown). It has been demonstrated before, that NKG2D and other activating NK cell receptors get recruited to GM-1 rich membrane domains (lipid rafts) after stimulation. SFKs are localized constitutively in lipid rafts through posttranslational addition of a lipid anchor (Shenoy-Scaria *et al*, 1993). In conjugates with target cells expressing NKG2D ligands, the NKG2D receptor and GM-1 rich membrane domains cluster at the contact area. Also after stimulation by crosslinking NKG2D is recruited to lipid rafts and clustering of the rafts is induced (Endt *et al*, 2007). If we stimulated the cells with anti-NKG2D coated beads, these beads were often completely surrounded by GM-1 rich membrane, which we did not observe with control or inhibitory antibody coated beads. The lipid rafts are insoluble in cold non-ionic detergents, due to their molecular composition. Clusters of these lipid rafts are lost for immunoprecipitation performing a standard protocol through clarification of the lysates. Therefore we established an immunoprecipitation protocol from non-clarified whole cell lysates, in which lipid rafts are still present and intact. Although we optimized the protocol and kept antibody

concentrations constant in all samples, we recovered less receptor after crosslinking on ice or 37°C. Probably the antigen is less accessible after crosslinking or masked due to the clustering. Nevertheless the amount of the SFKs Lck and Fyn in the precipitates increased in stimulated samples. As we lysed the cells under conditions that did not disrupt lipid rafts, this increase in SFKs could be due to direct protein interaction with the stimulated receptor or to localization of receptor and kinases in close proximity linked through the membrane domains. The importance of lipid rafts as a platform for the signaling of activating receptors has been described before. A disruption of these membrane domains by depletion of cholesterol from the membrane leads to a complete loss of NK cell function (Watzl *et al*, 2003). Especially for Lck we noted a high background association with NKG2D after crosslinking on ice. Probably the induction of the association is so sensitive, that it can occur under these experimental conditions. Activation of the cells occurs specific upon NKG2D crosslinking on 37°C as observed by Vav1 phosphorylation, additionally we observed recruitment of Vav1 to the stimulated receptor. Vav1 precipitated with the stimulated receptor was highly phosphorylated. This suggests that through the association of kinases and Vav1 with the stimulated receptor phosphorylation of Vav1 is facilitated.

Our simulations and experimental results suggest, that the high local concentration of kinases and their substrates is a key mechanism to induce NK cell activation. Semiquantitative analysis revealed, that about 11 % (20 nM) of Vav1 that could be phosphorylated with pervanadate are phosphorylated upon triggering of NKG2D. We could not test how efficient the pervanadate treatment phosphorylated the proteins, but it is unlikely that all Vav1 molecules present in the cell were phosphorylated. Therefore measuring the percentage of pVav1 with this method can lead to an overestimation of the total amount of pVav1. Our simulations produced a much lower phosphorylation level of pVav1 with literature derived kinetic parameters. In the parameter fit we reached a pVav1 level of 16 nM, when we included the kinase- and SHP 1 association modules (c) and (f). Assuming that the experimentally determined 20 nM pVav1 are the upper limit of the possible phosphorylation level, the simulation results would be in a realistic range. We recovered a high amount of phosphorylated Vav1 in the precipitates of stimulated NKG2D compared to total Vav1. Therefore we hypothesize that the magnitude of Vav1 at the activation site gets phosphorylated due to the high local concentration of SFKs, whereas the phosphorylation level in the rest of the cell is lower. This spatially restricted phosphorylation could contribute to a directed activation of the NK cells towards the susceptible target cell.

The second important result from our simulations is, that the steep decrease of pVav1 upon stimulation of inhibitory receptors was depending on the association of the phosphatase SHP-1 with the inhibitory receptors (f). In the simulations without this module, the activity of SHP-1 is increased by phosphorylation, whereas in simulations with (f) the interaction with inhibitory receptors activates the phosphatase and phosphorylation does not contribute to regulate the activity. Induced association of SHP-1 with ITIM bearing receptors and phosphorylation of SHP-1 has been demonstrated before (Hof *et al*, 1998; Lu *et al*, 2001), both resulting in increased

activity of the phosphatase. But which mechanism is responsible for the observed response in our experimental system? We applied an assay that could detect specific SHP-1 activity in NK cells. This activity was completely blocked when the phosphatase inhibitor pervanadate was added to the substrate reaction. But stimulation of activating and/or inhibitory receptors did not change the observed activity of SHP-1 significantly. We could not detect phosphorylation of SHP-1 in precipitates from the SHP-1 activity assay nor in conventional immunoprecipitates (data not shown) after receptor stimulation. This suggests that in our experimental system, phosphorylation of SHP-1 is not responsible for the observed dose-response, which is in agreement with the simulation results. If phosphorylation is not involved in regulating SHP-1 activity, then we would expect, that the interaction with the ITIMs of inhibitory receptors increases the activity. But under experimental conditions that induced this association, we could not detect changes in SHP-1 activity compared to unstimulated controls. One explanation why the measured activity of SHP-1 is unaffected by receptor stimulation is that the assay used is not suitable to detect changes in activity due to conformational changes. Cell lysis and precipitation of SHP-1 could disrupt either the association of receptor and phosphatase or disturb the conformation of the complex necessary for SHP-1 activation. The other possible explanation is, that the activity of SHP-1 does not change significantly upon receptor stimulation in our system, but association of SHP-1 with the receptor and the resulting increased local concentration at the IS is sufficient for the observed effect. Further studies testing the SHP-1 activity in intact cells will be necessary to answer the real contribution of the association to the receptor on the activity of the phosphatase. To distinguish the two functional concepts a membrane-targeted mutant of SHP-1 could help to reveal if the high local concentration at the membrane is of importance and a fluorescence resonance energy transfer (FRET)-probe could visualize conformational changes of the phosphatase.

The other optional modules of our model were not essential to create a physiological response. While phosphatase exclusion (b) has been suggested for the initiation of TCR signaling, it is dispensable in our model. This is consistent with the fact that CD45 is not necessary for NK cell cytotoxicity (Hesslein *et al*, 2006; Huntington *et al*, 2005). The kinase autophosphorylation module (d) assumes, that the background activity of SFKs is enhanced after phosphorylation of an activating tyrosine. In our model this is implemented by increasing the basal SFK activity 5-fold after autophosphorylation. This module was dispensable in the simulations using kinetic parameters from the literature. But it increased the number of random parameter sets in our parameter scan that produced a physiological response. This can be explained by the fact that this module helps creating the physiological response with parameter sets containing lower basal SFK activity. However, we were not able to detect relevant levels of SFKs phosphorylated at the activating tyrosine after receptor engagement, a finding that is consistent with the lack of SFK phosphorylation upon T cell activation (Paster *et al*, 2009). These data suggest that either the

autophosphorylation of SFKs is so transient that we could not detect it experimentally, or what is more likely; the basal SFK activity without autophosphorylation in human NK cells is sufficiently high to induce the observed pVav1 response and cytotoxicity. The additional module (e) hypothesizing SFK dephosphorylation by SHP-1 was only playing a very minor role in improving the simulations. As we exclude the necessity of SFK autophosphorylation, we assume that this process is not involved in the signal integration of NK cells. To our surprise, the pVav1 triggered actin reorganization, which leads to active recruitment of activating receptors to the IS, was also not necessary in our simulations. Blocking the actin rearrangement experimentally leads to a complete abrogation of cytotoxicity and a reduction of Vav1 phosphorylation. How can this discrepancy be explained? In our model without module (a), the clustering of the receptors occurs in a passive way. The receptors can move all over the cell, and get trapped at the IS if their ligand is present on the target cell. Module (a) leads to an acceleration of receptor recruitment to the IS and can also actively retain the receptors in this area. One possibility for the discrepancy is, that we assume in our model a motility of the receptors and signaling proteins that cannot be achieved in cells without the active contribution of the cytoskeleton. In our simulations the cytoplasm and the plasma membrane of the cells are homogeneous solutions of molecules, where the diffusion speed is constant. Whereas in 'real' cells active transport of the proteins might be necessary, as the cytoplasm is crowded with organelles and the plasma membrane has a complex organization. For a functional IS, not only the activating and/or inhibitory receptors are necessary but also adhesion molecules, which we omitted in our simulation, as they do not contribute to the killing decision. Integrins like LFA-1 are crucial for the formation of a stable IS and intimately coupled to regulation of the actin cytoskeleton. We would miss effects caused by relocalization and activation of adhesion molecules to stabilize the synapse in our simulation. The initial pVav1 signal probably is actin independent but without the actin dependent maintenance of the synapse, the conjugate of NK and target cell falls apart and the signal is abrogated. The actin relocalization could be responsible for an increase and an acceleration of the Vav1 phosphorylation but also enable the induction of signaling cascades downstream of Vav1.

While our results demonstrate that SFK and SHP-1 association with the respective receptors are essential for the signal integration of NK cells, it does not exclude the possibility that the remaining optional modules may play a role during the integration of positive and negative signals. None of the remaining modules impaired the simulation results, when they were included additionally.

5.2. Experimental factors influencing the mathematical model

Stimulating cells by antibody crosslinking or with antibodies coated to surfaces is a common but controversial method. We chose this approach, as we needed to titrate the signal to reveal concentration dependent dynamics. Currently there are no target cells available that display the defined various ligand densities on the surface that we

require. Different affinities of the various ligands and of antibodies towards the receptors could influence the quantitative but not the qualitative response of the cell. The receptors do not undergo conformational changes upon ligand binding, but bind as rigid bodies (Boyington *et al*, 2001; McFarland and Strong, 2003). Further quantitative comparisons could answer the question which ligand density on a target is required to induce the response we observed at a certain antibody concentration. After stimulating NK cells with targets, the initiated signals are not well-defined, as other ligands like adhesion molecules contribute to the effects. An alternative would be the expression of the desired ligands in insect cells, as these cells do not express ligands cross-reactive with human NK cell receptors. A titratable and inducible expression system for the ligands is currently in development, to avoid the need for multiple target cell lines expressing various levels of two different ligands. The process of activating receptor clustering at the IS has been shown to be actin dependent whereas the clustering of inhibitory receptors in inhibitory synapses is thought to be independent of actin polymerization (Long, 2008; Watzl *et al*, 2003). We observed actin relocalization with crosslinking of activating and inhibitory receptors, which is contradictory to results with target cells. Surprisingly, PP1 treatment did not affect capping of the NKG2D receptor after crosslinking. In most of the cells showing receptor relocalization we also noted actin enrichment directed to the site of receptor capping. The activation of GTPases by pVav1 is inducing actin cytoskeleton rearrangement. It is possible that the inhibition of SFKs by PP1 is incomplete and the remaining activity is sufficient to induce actin polymerization, although we could not detect pVav1. Another explanation would be that crosslinking of receptors with secondary antibody clusters the receptors from the outside of the cell, and this process is followed by activation independent actin accumulation. As conjugate formation and actin rearrangement are only slightly diminished in NK cells from mice lacking Vav1, there exist mechanisms completely independent of Vav1 (Colucci *et al*, 2001). This mechanism could also be responsible for the clustering in our cells stimulated in the presence of PP1. The observed phenomenon of receptor and actin relocalization in the absence of pVav1 is similar to the response after crosslinking of inhibitory receptors. Despite the actin accumulation, the receptor clusters did not induce activation signals as pVav1 and cytotoxicity were completely abolished at the PP1 concentration used in these experiments. To avoid receptor crosslinking with secondary antibody we stimulated the cells also with antibody-coated beads. The idea is to stimulate one specific receptor, but on a cell shaped and cell sized surface. With this method we wanted to reassure, that the signaling events we observed with receptor crosslinking are not caused by applying an external force pulling the receptors into a cluster. We noted some background actin polymerization with control beads but the actin rearrangement was not directed and phosphorylation of Vav1 or ERK was not induced. We speculate that this background is just due to mechanic disturbance of the cells by the beads. When we used beads coated with antibody against activating or inhibitory receptor the actin polymerization was directed in both cases towards the beads, similar to the observation after crosslinking of these receptors. Despite of the differences in actin rearrangement

after stimulating the cells with soluble antibodies, beads or target cells, the signaling events caused by triggering NK cell receptors were comparable between the stimulation methods. The kinetic of Vav1 phosphorylation after activation by antibody crosslinking occurs very fast and reaches the maximum in less than 3 min, whereas upon stimulation with beads the maximum was reached after 10-20 min. When NK cells get stimulated with target cells the kinetic resembles the one observed after antibody crosslinking (Endt *et al*, 2007). The antibody on the beads is immobile and cannot diffuse like in a target cell membrane or in solution. The NK cells wrap around the beads coated with specific antibody, as they cannot recruit the 'ligands' into a real synapse. This probably causes the slower onset of signaling after stimulation with beads. In target cells NKG2D ligands occur associated with lipid rafts in a clustered form, which is essential for effective activation of NK cells (Eleme *et al*, 2004). The preclustered ligands could facilitate and accelerate clustering of the receptors upon contact of the cells. The structure of an IS is much more complex than a receptor cluster initiated by receptor crosslinking or antibody coated beads. The response is not exclusively triggered by the stimulation of one activating or inhibitory receptor, but is induced by a composition of signals induced by various ligands on the target. We therefore confirmed that the signaling events we wanted to investigate after stimulation with antibody are not distinct from the effects caused by target cells.

As our simulations are based on differential equations that describe the reactions, we needed to determine the concentration of molecules on the cell surface and in the cytoplasm. We first needed to compute the volumes of the relevant cellular compartments. Cells are no smooth spheres, but membrane ruffles can increase the real surface, compared to the volume. In order to simplify the calculation, we assumed a round cell shape. In our model we suppose a compartmentalization of the cytoplasm into the volume involved in synapse formation and the rest of the cell. During formation of the immunological synapse the cells can change their morphology leading to an increase in the size of the contact area (see Graham *et al*, 2006; Vanherberghen *et al*, 2004 for representative images). We tried to take this into account and assumed a diameter of the IS compromising 55 % of the total cell diameter. The volume of the synapse compartment is composed of this area and only the membrane proximal 10 nm of the cytoplasm. The size of individual cells in the population can also differ from the mean values we used for the simulation and we observed donor dependent differences in primary NK cell populations. In NK cells and other lymphocytes the diameter of the whole cell is only a little bit larger than that of the nucleus. We considered this in our calculations but we did not take into account, that some of the proteins localize in or at the membrane, whereas other proteins are cytoplasmic. The volume of the cytoplasm is crowded with organelles and no homogeneous solution of molecules. The volume that is really accessible for a certain molecule might be much smaller than in our simulations. This would increase the relevant concentrations of the proteins, but on the other hand reduce the motility and the diffusion speed, as the proteins have to make long detours.

Quantification of surface molecules by FACS is quite exact and as it is a single cell analysis provides information about the distribution of the expression of a certain molecule in the population. The measurement of cytoplasmic proteins by western blot has higher experimental variability and averages all the cells per sample. Whereas all proteins quantified by FACS are located on the surface and should be in a functional state, western blot acquires all molecules present in the cell. By western blot it is not possible to distinguish between proteins in the relevant location and state and proteins that are already determined for degradation, currently trafficking or newly synthesized, therefore not 'functional'. Due to these uncertainties, the concentrations used for the simulations might not represent physiological relevant values. To reassure that this does not falsify our simulation result, our cooperation partner ran simulations with varied initial protein concentrations. Qualitatively, the simulation results were very robust against these changes.

The results of this work are critically depending on the quantification of western blots. Therefore we were extremely cautious in controlling these results. Two major sources for errors in western blot results are irregularities of the gel and during protein transfer to the membrane. We minimized these problems by using precast gels that provide a higher homogeneity than self cast gels. Additionally we could show that the minigel system used does not produce errors correlated with the position of the sample on the gel, by randomized loading of the samples and/or internal control (Schilling *et al*, 2005). For quantification of protein phosphorylation we always used an appropriate loading control for the unphosphorylated protein or protein family. The signal of unphosphorylated controls was used to normalize the lanes of each blot. The specificity of the phospho-specific antibodies was reassured by using the phosphatase inhibitor pervanadate to induce maximal protein phosphorylation. The pSrc antibody used recognizes SFKs only if the activating tyrosine at position 416 is phosphorylated. Vav1 has three regulatory tyrosines in the acidic region. Phosphorylation of the two N-terminal regulatory tyrosines (Y142, Y160) facilitates the phosphorylation of Y174 and releases the protein from the autoinhibitory conformation. We used an antibody recognizing pY160, as activation of Vav1 goes along with phosphorylation of all three tyrosines. If it was necessary to use more than one blot per experiment due to bigger sample numbers, additional controls were used to normalize the distinct blots. The different methods to develop western blots can also influence the result. The linear range of ECL combined with X-ray films to develop the blot is relatively small, but very sensitive. Acquisition of the ECL signal with a CCD camera provides a bigger linear range, but as we had no access to a suitable acquisition system this was not possible. Another possibility to develop western blots is by using (infrared) fluorescent secondary antibodies for detection. We tried to establish this method, but some of the primary antibodies, which could not be replaced by other products, did not work in this system. We therefore used X-ray films, but always scanned and quantified multiple exposures of every blot to reassure that the signal is not saturated.

When we used recombinant standard protein to quantify absolute protein concentrations these standards were initially controlled for purity and on a regular basis the concentration was monitored. The dilution of the standard was adjusted to produce a linear calibration curve in the concentration range of the cell lysates analyzed. Initial experiments showed, that loading of equal amounts of total protein per lane is crucial for homogeneous protein transfer to the blot membrane. Recombinant standard loaded pure in one lane could not be compared to the same amount of recombinant protein loaded together with cell lysate in one lane. All recombinant standard proteins used, differed in size from endogenous proteins and as neither the standard nor the endogenous protein produced unspecific signals they were always loaded combined in the same lane. This produced the best comparability of both signals. Different scanning and analysis methods have critical influence on the results (Gassmann *et al*, 2009), so we compared analysis of the same film with various methods. In our hands, using the mean optical density of the complete band provided the biggest linear range and the highest sensitivity compared e.g. to peak intensity or volume.

5.3. Heterogeneous response of 'homogeneous' cell populations

We observed in our microscopy experiments that the cells did not respond homogeneously to stimulation. After receptor crosslinking most cells relocalized the receptor and actin to one site of the cell starting within one minute after stimulation with maximum capping after 5-10 min. But some cells did not react to stimulation; the receptor remained homogeneously distributed around the cell, often showing a patchy staining. These patches probably represent small clusters of the receptor, either the receptor is already preclustered in unstimulated cells, or crosslinking with secondary antibody induces these clusters. The heterogeneous response could arise from differences in the cell cycle of the single cells (Rehm *et al*, 2009), as the cultures were not synchronized. Some cells are probably in a phase where they cannot respond to exogenous stimuli. These effects were not included in our model, as we simulated the response of a single cell that is completely responsive. Another reason for heterogeneous responses could be small differences in expression level of relevant molecules in single cells of the population. Previous work has demonstrated, that this variability within a population can have substantial influence on the reactivity towards stimulation (Feinerman *et al*, 2008). The Vav1 phosphorylation determined experimentally by western blot averages the signal of many cells, whereas we simulate the response of a single cell. The experimentally observed pVav1 response is not as steep as in the simulation, especially in the concentration range where activating and inhibitory signals compete. Differences between single cells in the experimental sample could cause this 'blurry' response. From the experimental side, single cell analysis of signaling processes would be necessary to reveal how the reactions of the cells in a population are distributed around the average we measured, but unfortunately there are no suitable reagents available to date, to measure pVav1 e.g. by FACS. An approach to include this heterogeneity in the model and to simulate the behavior of cell populations is to use

stochastic equations that include effects arising from fluctuation around the average. Our cooperation partner chose to control the robustness of our model by variation of initial protein concentrations and analyzed the sensitivity of the response towards changes of multiple parameters at once. The qualitative response of our simulations was stable within a certain concentration range of involved proteins, but the amplitude of pVav1 was affected. These variations in the absolute phosphorylation levels of Vav1 in single cells could be responsible for the slight differences in the experimentally observed compared to the simulated dose-response.

5.4. Signal transduction downstream of Vav1

We focused in our simulations and the experiments on the events integrating the signals on the level of Vav1 phosphorylation. Downstream of pVav1 the signal is transmitted via various pathways. Our initial experiments with chemical inhibitors showed that Syk, PI3K, MEK, p38 and PLC do not influence the Vav1 phosphorylation after stimulation of NKG2D. But PI3K, MEK, and PLC inhibition could completely block NKG2D dependent killing (data not shown). These results and previous work show, that these signaling steps are essential, but either downstream or parallel of Vav1 phosphorylation. In mice lacking Vav proteins it has been shown that the activation of ERK upon receptor stimulation is completely abrogated (Cella *et al*, 2004; Colucci *et al*, 2001). The MAPK pathway is usually activated via Rac-1, PAK signaling after phosphorylation of Vav proteins. We were able to detect double phosphorylated ERK after NKG2D stimulation, but using receptor crosslinking inter experimental variability was extremely high. We noted a high background phosphorylation, as the cells we used require IL-2 in the culture medium. This cytokine also induces ppERK but not other MAPK signals (Yu *et al*, 2000) via pathways independent of Vav1. In IL-2 starved cells the background phosphorylation is lower or absent, but induction of ERK phosphorylation upon receptor triggering is hardly detectable. An additional experimental complication arises, as the ERK signal in our system reacts very sensitive to different kinds of stress e.g. changes of the temperature and centrifugation. When we used anti-NKG2D coated beads, the induced ERK phosphorylation was very robust and showed a similar dose-response as pVav1. Probably the slower kinetic upon bead stimulation is beneficial for the specificity of the signal. As expected, relocalization of NKG2D and actin upon receptor crosslinking were not affected by MEK inhibition, excluding a negative feedback from the MAPK pathway to the actin rearrangement. The MAPK cascade offers possibilities for further amplification of the signal. It has been shown before, that the double phosphorylation of MAPK transforms incoming signals to show a steeper response or even a digital behavior (Altan-Bonnet and Germain, 2005; Huang and Ferrell, 1996). In our dose-response analysis the ppERK response shows a steeper increase than pVav1. So we assume, that this mechanism of signal amplification downstream of Vav1 also plays a role in the signaling cascade of NK cells.

The Ca^{2+} flux is initiated immediately upon activating receptor crosslinking and increases similar to the pVav1 kinetic until a plateau is reached. The peak level is in contrast to the Vav1 phosphorylation not transient, but stable for at least 20 min. The amplitude of the signal is associated with the stimulation strength, matching the pVav1 response. The dose-response of the Ca^{2+} signal is also very similar to the Vav1 phosphorylation, it increases rapidly upon activating receptor stimulation, but the signals of inhibitory receptors are dominant and can block the signal almost completely. Combined with the result, that blocking PLC-γ activity with a chemical inhibitor does not affect Vav1 phosphorylation, this suggest, that the Ca^{2+} signal is initiated downstream of pVav1. It has been proposed before, that PLC-γ recruitment to the membrane, and so the initiation of the Ca^{2+} signal, depends on pVav1 (Graham *et al*, 2006). We propose that the Ca^{2+} flux is passing the signal integrated at the level of Vav1 on, to induce downstream effects, leading to an amplification and prolongation of the activation signal.

Our hypothesis is that the activating and inhibitory signals are integrated at the level of Vav1, but how does this integration affect the cytotoxicity of the NK cells? The cytotoxic activity of NK cells shows the same dose-response as pVav1 upon differential triggering of activating and inhibitory receptors. The inhibitory signal is dominant over a large concentration range. Without inhibitory signal, low amounts of activating signal are sufficient to induce the maximal cytotoxicity. In a physiologic context, it is essential, that NK cells spare targets when they still express MHC class I to avoid autoimmune reactions damaging healthy tissues. But cells without inhibitory ligands are killed as soon as the NK cell receives activating stimulation, as loss of MHC class I is characteristic for many virus infections or transformation of the cell. The identical dose-response of cytotoxicity and pVav1 allows the conclusion that signals downstream of Vav1 are transmitted unaltered. Our data do not justify the converse argument, that there is no further signal integration, feedback loops or crosstalk between different pathways. In agreement with our hypothesis that Vav1 integrates positive and negative signals, disturbances of the signal cascade by SFK inhibition show the same effect on the level of Vav1 as on the cytotoxic activity of NK cells. The alternative explanation, that the signals are integrated simultaneously in alternative pathways, would be very uneconomic and complicated, but we cannot exclude this possibility. As we disrupted the signal upstream of pVav1 this inhibition could also affect NK cell killing via other, pVav1 independent pathways, that depend also on the activity on SFKs. The real contribution of pVav1 for the cytotoxicity of human NK cells has to be further examined by disturbing the signals directly on the level of Vav1 e.g. by silencing Vav family members with siRNA or by pharmacological inhibition of the GEF activity of Vav proteins.

5.5. Importance of Vav1 for the NK cell function

The multiple domains of Vav1 provide many interaction possibilities. It can interact via the protein Grb2 with the NKG2D signaling adapter DAP10. Vav1 can bind via its PH domain to phosphoinositides, products of PI3K, which is also able to bind to

DAP10. Who's connected first with NKG2D after stimulation: PI3K or complexes of Grb2 and Vav1? It has been suggested that the interaction of Vav1 with DAP10 is necessary to recruit PI3K, as in the absence of Vav1 stimulation of NKG2D cannot induce Akt phosphorylation (Graham *et al*, 2006). But also the reverse model has been proposed, as it is assumed that phosphoinositides are recruiting proteins with PH domains to the membrane. Therefore it has been suggested, that the products of PI3K initiate Vav1 recruitment to the receptor. Binding assays *in vitro* could show an enhancement of GEF activity after phosphatidylinositol-3,4,5-trisphosphate and a reduction after phosphatidylinositol-4,5-bisphosphate binding to Vav1 (Han *et al*, 1998; Jiang *et al*, 2000). It depends on the cell type and the signaling mechanisms of the receptor studied if Vav1 phosphorylation is independent of PI3K, or not. As in our system PI3K inhibition has no influence on Vav1 phosphorylation after NKG2D triggering we propose, that PI3K recruitment and activity is induced downstream of Vav1. We suggest that interaction of SFKs and Vav1 with the receptor initiate the pVav1 signal. The high local concentration of kinases in proximity to the receptor could allow phosphorylation of the regulatory tyrosines in the acidic region of Vav1. If these tyrosines are phosphorylated, Vav1 is released from its inactive autoinhibitory conformation. These phosphorylation events induce the GEF activity of Vav1 and enable the downstream signals.

In lymphocytes, all three Vav family members are expressed, but if each of the proteins has specific functions or if the functions are redundant is not completely understood. NK cells develop normal in Vav1 deficient mice; they have regular NK cell numbers, with an unaltered pattern of surface receptors. In contrast, T cell development is blocked at the transition from double negative to double positive thymocytes. Also when all three Vav family members are missing, NK cell development is not abrogated (Cella *et al*, 2004; Colucci *et al*, 2001). Studies with Vav1 knock out mice showed that Vav1 is important for *in vivo* tumor clearance. Further investigation revealed a severe defect in cytotoxicity mediated by various receptors including FcRγ, 2B4 and NKG2D. The IFNγ production was unaffected in these mice. In a different study the effects of all three Vav family members downstream of various receptors were investigated to elucidate possible redundancies of Vav proteins in NK cells. The signaling of NKG2D/DAP10 was largely Vav1 dependent, but in contrast to the previous study the signals of FcRγ and DAP12 were identified to be mainly mediated by Vav2 and 3. In mice the redundancy between Vav1 and the other two family members seem to depend on the cell type and the function examined. Whereas Vav1 seems to be essential in T cells for proliferation and the induction of a normal Ca^{2+} response upon TCR engagement, B cells are only affected after deletion of at least two of the three Vav proteins (Fujikawa *et al*, 2003). The studies examining redundancy of the Vav family members have been done in mice, further studies have to answer the question if Vav proteins are able to compensate the functions of each other in human NK cells. In our system stimulation of receptors transmitting the signals via DAP10, ITSM motifs and ITAM motifs induce pVav1, but we did not test the involvement of other Vav family

members. As the amino acid sequence of the acidic region of the Vav proteins is quite different the pVav1 antibody should not cross-react with Vav2 and 3, but we did not have the possibility to test this experimentally. For Vav2 and 3 the direct interaction with SHP-1 has not been shown, therefore the question arises if signals mediated by these proteins are inhibited with the same or a similar mechanism.

The studies on Vav deficient mice suggest, that the different effector functions of NK cells do not rely on the same signaling pathways. The cytokine production is not affected by the lack of Vav proteins in the same way as the cytotoxicity downstream of the same receptor. After stimulation of one specific receptor the signal is transmitted via Vav dependent and independent pathways, initiating different effector functions. But whereas the cytokine production can be unaffected under identical conditions, Vav proteins are indispensable for cytotoxicity upon engagement of various NK cell receptors.

Recently it has been shown, that also induced phosphorylation of the adapter protein CrkII contributes to the inhibition mediated by ITIM carrying receptors (Peterson and Long, 2008). Under activating conditions the scaffolding protein c-Cbl interacts with the SH2 domain of Vav1. Complexes of CrkII with c-Cbl and the GEF C3G are also detectable. Actin rearrangement and lamellipodia formation are promoted by the interaction of CrkII with c-Cbl. ITIM signals promote phosphorylation of CrkII, probably via the kinase c-Abl, leading to disruption of the complexes necessary for NK cell activation. If these events occur in parallel or downstream of the signaling events analyzed by us has to be investigated, because it is not clear if Vav1 is necessary to transmit the signals from ITIMs to CrkII.

5.6. Robust, predictive simulations of NK cell activation

Our model including the association of the kinase with the receptor offers the possibility to make realistic end point simulations of the pVav1 response of NK cells towards activating and inhibitory signals. We tested our model further because we wanted to know if the model is also able to produce realistic time course simulations. The predictions from the model that the kinetic of Vav1 phosphorylation would not change when the activating (or inhibitory, data not shown) stimulus is varied could be confirmed experimentally. Almost identically, the maximum phosphorylation is reached within 3 min after stimulation, indicating that the kinetic parameters used for our simulation are in a physiological relevant range. In our model, the level of pVav1 stays constant, once a plateau is reached, but in the experiment we observed a decrease in Vav1 phosphorylation between 5 and 10 min after stimulation. This indicates, that there exists at least one mechanism, probably a negative feedback loop, to shut off the activating signal although the initiating signal is still present. A possible mechanism to shut down signaling processes is the internalization and turnover of the respective receptor after stimulation (Alvarez-Arias and Campbell, 2007; Sandusky *et al*, 2006). Engagement of other receptors leads to a dramatic reduction of their surface expression through shedding from the surface (Grzywacz *et al*, 2007), showing that NK cell activation can be modulated on the receptor level. It

has been shown for some ligands, that they are transferred rapidly after conjugation with the target cell to the NK cell, but how these ligands are involved in modulating the NK cell activity has to be investigated (McCann *et al*, 2007). Another possible reason, why the pVav1 level gets reduced is, that as soon as the downstream effectors are also recruited, they displace Vav1 from the synapse. We did not include any mechanism in our model that could terminate the signal therefore the pVav1 level stays constant once the plateau is reached. The slope of the onset of Vav1 phosphorylation and the maximum levels can be simulated in a realistic way.

The kinetic parameters used in the model have been excessively tested by our cooperation partner, using two completely different ways of analysis. The parameter scan as well as the parameter fit could show, that the simulation results are very stable in producing a physiological response provided that kinase association is included. Models lacking this module could not be forced by parameter changes to produce this response. This reassured us, that the results of our simulations are specific for the reactions we included, as the model is not sensitive to parameter changes. By manipulating the parameters we could never cause the same impact, as by addition of the kinase association module (c). Therefore we are confident, that we could identify key concepts of the signal integration of NK cells.

It is intriguing to transfer this model to other immune cells that also receive activating and inhibitory stimulation, e.g. a subset of $CD4^+/CD8^+$ and $\gamma\delta$ T cells also express KIRs. T cells can acquire stable expression of KIRs after completion of their rearrangement of the TCR locus, and the number of KIR positive T cells increases with the age (Ugolini and Vivier, 2000). Co-ligation of the TCR and KIRs can down modulate or completely inhibit cytokine production and cytotoxicity of $CD8^+$ T cells (Phillips *et al*, 1995). The mechanism inducing the expression and the functional consequences are not fully understood. KIRs are mainly expressed on cells with a memory like phenotype, probably because they protect the cell from activation induced cell death. Maybe it is also a mechanism to maintain tolerance and prevent autoimmunity, e.g. in chronic infections. The signaling properties of the KIR receptors seem to be critically depending on the activation status of the cell. Investigating these connections by mathematical modeling could help to reveal the mechanisms causing the effects of KIR triggering on T cells.

Manipulation of the model system offers - compared to manipulations of cells - a quick and easy possibility to test the effects of perturbations on NK cell activity. We successfully predicted the effects of SFK inhibition with our model. Changing the stimulus strength did not affect the kinetic of Vav1 phosphorylation, but reducing the activity of the kinase predicted a slower increase and retarded maximum. By inhibition of SFKs we experimentally confirmed this slower kinetic. The maximum of Vav1 phosphorylation was also decreased in the simulation and in our experiment. SFK inhibition had exactly the same impact on Vav1 phosphorylation as on cytotoxicity: the amplitude was reduced, but the dose-response was not affected. Using the chemical inhibitors it is impossible to control, if we reduced the activity to the same extent as in the simulation, but this result has strong qualitative

significance. Models like this could be extremely helpful in identifying effective targets to modulate NK cell activity. For the treatment of various diseases therapeutic approaches try to utilize the power of NK cells. Most of these approaches aim at enhancing the expression of activating ligands on tumor or infected cells or to reduce interactions of inhibitory NK cell receptors with their ligands (Romagne *et al*, 2009; Vales-Gomez *et al*, 2008). To harness the cytotoxic potential of NK cells, it could be of advantage to identify effective disturbances by simulations first and then evaluating the effect experimentally. For example, our model would predict, that if we wanted to overcome the dominance of inhibitory signals it would have a small effect to target the interactions of inhibitory receptors and their ligands. Interfering with the activity of phosphatases also would not be very efficient. But a substance disrupting the interaction of inhibitory receptors and phosphatases would potently enhance NK cell activity against MHC class I low targets. Mathematical modeling is a powerful method to help us to understand complex signaling processes and to reveal key regulatory mechanisms. The insight gained about the signal integration can be used to identify new effective therapeutic strategies.

6. References

Aghazadeh B, Lowry WE, Huang XY, Rosen MK (2000) Structural basis for relief of autoinhibition of the Dbl homology domain of proto-oncogene Vav by tyrosine phosphorylation. *Cell* **102:** 625-633.

Aldridge BB, Burke JM, Lauffenburger DA, Sorger PK (2006) Physicochemical modelling of cell signalling pathways. *Nat Cell Biol* **8:** 1195-1203.

Altan-Bonnet G, Germain RN (2005) Modeling T cell antigen discrimination based on feedback control of digital ERK responses. *PLoS Biol* **3:** e356.

Alvarez-Arias DA, Campbell KS (2007) Protein kinase C regulates expression and function of inhibitory killer cell Ig-like receptors in NK cells. *J Immunol* **179:** 5281-5290.

Amarasinghe GK, Rosen MK (2005) Acidic region tyrosines provide access points for allosteric activation of the autoinhibited Vav1 Dbl homology domain. *Biochemistry* **44:** 15257-15268.

Anderson DR, Grillo-Lopez A, Varns C, Chambers KS, Hanna N (1997) Targeted anti-cancer therapy using rituximab, a chimaeric anti-CD20 antibody (IDEC-C2B8) in the treatment of non-Hodgkin's B-cell lymphoma. *Biochem Soc Trans* **25:** 705-708.

Andersson S, Fauriat C, Malmberg JA, Ljunggren HG, Malmberg KJ (2009) KIR acquisition probabilities are independent of self-HLA class I ligands and increase with cellular KIR expression. *Blood*.

Anfossi N, Andre P, Guia S, Falk CS, Roetynck S, Stewart CA, Breso V, Frassati C, Reviron D, Middleton D, Romagne F, Ugolini S, Vivier E (2006) Human NK cell education by inhibitory receptors for MHC class I. *Immunity* **25:** 331-342.

Arnon TI, Achdout H, Levi O, Markel G, Saleh N, Katz G, Gazit R, Gonen-Gross T, Hanna J, Nahari E, Porgador A, Honigman A, Plachter B, Mevorach D, Wolf DG, Mandelboim O (2005) Inhibition of the NKp30 activating receptor by pp65 of human cytomegalovirus. *Nat Immunol* **6:** 515-523.

Arnon TI, Lev M, Katz G, Chernobrov Y, Porgador A, Mandelboim O (2001) Recognition of viral hemagglutinins by NKp44 but not by NKp30. *Eur J Immunol* **31:** 2680-2689.

Avril T, Floyd H, Lopez F, Vivier E, Crocker PR (2004) The membrane-proximal immunoreceptor tyrosine-based inhibitory motif is critical for the inhibitory signaling mediated by Siglecs-7 and -9, CD33-related Siglecs expressed on human monocytes and NK cells. *J Immunol* **173:** 6841-6849.

Billadeau DD, Brumbaugh KM, Dick CJ, Schoon RA, Bustelo XR, Leibson PJ (1998) The Vav-Rac1 pathway in cytotoxic lymphocytes regulates the generation of cell-mediated killing. *J Exp Med* **188:** 549-559.

Biron CA, Nguyen KB, Pien GC, Cousens LP, Salazar-Mather TP (1999) Natural killer cells in antiviral defense: function and regulation by innate cytokines. *Annu Rev Immunol* **17:** 189-220.

Bix M, Liao NS, Zijlstra M, Loring J, Jaenisch R, Raulet D (1991) Rejection of class I MHC-deficient haemopoietic cells by irradiated MHC-matched mice. *Nature* **349:** 329-331.

Boyington JC, Brooks AG, Sun PD (2001) Structure of killer cell immunoglobulin-like receptors and their recognition of the class I MHC molecules. *Immunol Rev* **181:** 66-78.

Brandt CS, Baratin M, Yi EC, Kennedy J, Gao Z, Fox B, Haldeman B, Ostrander CD, Kaifu T, Chabannon C, Moretta A, West R, Xu W, Vivier E, Levin SD (2009) The B7 family member B7-H6 is a tumor cell ligand for the activating natural killer cell receptor NKp30 in humans. *J Exp Med*.

Brodin P, Karre K, Hoglund P (2009a) NK cell education: not an on-off switch but a tunable rheostat. *Trends Immunol* **30:** 143-149.

Brodin P, Lakshmikanth T, Johansson S, Karre K, Hoglund P (2009b) The strength of inhibitory input during education quantitatively tunes the functional responsiveness of individual natural killer cells. *Blood* **113:** 2434-2441.

Bryceson YT, March ME, Barber DF, Ljunggren HG, Long EO (2005) Cytolytic granule polarization and degranulation controlled by different receptors in resting NK cells. *J Exp Med* **202:** 1001-1012.

Caraux A, Kim N, Bell SE, Zompi S, Ranson T, Lesjean-Pottier S, Garcia-Ojeda ME, Turner M, Colucci F (2006) Phospholipase C-gamma2 is essential for NK cell cytotoxicity and innate immunity to malignant and virally infected cells. *Blood* **107:** 994-1002.

Cella M, Fuchs A, Vermi W, Facchetti F, Otero K, Lennerz JK, Doherty JM, Mills JC, Colonna M (2009) A human natural killer cell subset provides an innate source of IL-22 for mucosal immunity. *Nature* **457:** 722-725.

Cella M, Fujikawa K, Tassi I, Kim S, Latinis K, Nishi S, Yokoyama W, Colonna M, Swat W (2004) Differential requirements for Vav proteins in DAP10- and ITAM-mediated NK cell cytotoxicity. *J Exp Med* **200:** 817-823.

Cerny J, Fiserova A, Horvath O, Bezouska K, Pospisil M, Horejsi V (1997) Association of human NK cell surface receptors NKR-P1 and CD94 with Src-family protein kinases. *Immunogenetics* **46:** 231-236.

Cerwenka A, Lanier LL (2001) Natural killer cells, viruses and cancer. *Nat Rev Immunol* **1:** 41-49.

Chalifour A, Scarpellino L, Back J, Brodin P, Devevre E, Gros F, Levy F, Leclercq G, Hoglund P, Beermann F, Held W (2009) A Role for cis Interaction between the Inhibitory Ly49A receptor and MHC class I for natural killer cell education. *Immunity* **30:** 337-347.

Chavez-Galan L, Arenas-Del Angel MC, Zenteno E, Chavez R, Lascurain R (2009) Cell death mechanisms induced by cytotoxic lymphocytes. *Cell Mol Immunol* **6:** 15-25.

Chiang GG, Sefton BM (2001) Specific dephosphorylation of the Lck tyrosine protein kinase at Tyr-394 by the SHP-1 protein-tyrosine phosphatase. *J Biol Chem* **276:** 23173-23178.

Claus M, Meinke S, Bhat R, Watzl C (2008) Regulation of NK cell activity by 2B4, NTB-A and CRACC. *Front Biosci* **13:** 956-965.

Colucci F, Caligiuri MA, Di Santo JP (2003) What does it take to make a natural killer? *Nat Rev Immunol* **3:** 413-425.

Colucci F, Rosmaraki E, Bregenholt S, Samson SI, Di Bartolo V, Turner M, Vanes L, Tybulewicz V, Di Santo JP (2001) Functional dichotomy in natural killer cell signaling: Vav1-dependent and -independent mechanisms. *J Exp Med* **193:** 1413-1424.

Colucci F, Schweighoffer E, Tomasello E, Turner M, Ortaldo JR, Vivier E, Tybulewicz VL, Di Santo JP (2002) Natural cytotoxicity uncoupled from the Syk and ZAP-70 intracellular kinases. *Nat Immunol* **3:** 288-294.

Cooper JA, MacAuley A (1988) Potential positive and negative autoregulation of p60c-src by intermolecular autophosphorylation. *Proc Natl Acad Sci U S A* **85:** 4232-4236.

Cooper MA, Fehniger TA, Fuchs A, Colonna M, Caligiuri MA (2004) NK cell and DC interactions. *Trends Immunol* **25:** 47-52.

Crocker PR, Paulson JC, Varki A (2007) Siglecs and their roles in the immune system. *Nat Rev Immunol* **7:** 255-266.

Daniels KA, Devora G, Lai WC, O'Donnell CL, Bennett M, Welsh RM (2001) Murine cytomegalovirus is regulated by a discrete subset of natural killer cells reactive with monoclonal antibody to Ly49H. *J Exp Med* **194:** 29-44.

Davis DM (2002) Assembly of the immunological synapse for T cells and NK cells. *Trends Immunol* **23:** 356-363.

Davis SJ, van der Merwe PA (2006) The kinetic-segregation model: TCR triggering and beyond. *Nat Immunol* **7:** 803-809.

Degli-Esposti MA, Smyth MJ (2005) Close encounters of different kinds: dendritic cells and NK cells take centre stage. *Nat Rev Immunol* **5:** 112-124.

Dokun AO, Kim S, Smith HR, Kang HS, Chu DT, Yokoyama WM (2001) Specific and nonspecific NK cell activation during virus infection. *Nat Immunol* **2:** 951-956.

Eagle RA, Trowsdale J (2007) Promiscuity and the single receptor: NKG2D. *Nat Rev Immunol* **7:** 737-744.

Eissmann P, Beauchamp L, Wooters J, Tilton JC, Long EO, Watzl C (2005) Molecular basis for positive and negative signaling by the natural killer cell receptor 2B4 (CD244). *Blood* **105:** 4722-4729.

Eleme K, Taner SB, Onfelt B, Collinson LM, McCann FE, Chalupny NJ, Cosman D, Hopkins C, Magee AI, Davis DM (2004) Cell surface organization of stress-inducible proteins ULBP and MICA that stimulate human NK cells and T cells via NKG2D. *J Exp Med* **199:** 1005-1010.

Endt J, McCann FE, Almeida CR, Urlaub D, Leung R, Pende D, Davis DM, Watzl C (2007) Inhibitory Receptor Signals Suppress Ligation-Induced Recruitment of NKG2D to GM1-Rich Membrane Domains at the Human NK Cell Immune Synapse. *J Immunol* **178:** 5606-5611.

Eriksson M, Leitz G, Fallman E, Axner O, Ryan JC, Nakamura MC, Sentman CL (1999) Inhibitory receptors alter natural killer cell interactions with target cells yet allow simultaneous killing of susceptible targets. *J Exp Med* **190:** 1005-1012.

Fassett MS, Davis DM, Valter MM, Cohen GB, Strominger JL (2001) Signaling at the inhibitory natural killer cell immune synapse regulates lipid raft polarization but not class I MHC clustering. *Proc Natl Acad Sci U S A* **98:** 14547-14552.

Feinerman O, Veiga J, Dorfman JR, Germain RN, Altan-Bonnet G (2008) Variability and robustness in T cell activation from regulated heterogeneity in protein levels. *Science* **321:** 1081-1084.

Ferlazzo G, Munz C (2004) NK cell compartments and their activation by dendritic cells. *J Immunol* **172:** 1333-1339.

Fujikawa K, Miletic AV, Alt FW, Faccio R, Brown T, Hoog J, Fredericks J, Nishi S, Mildiner S, Moores SL, Brugge J, Rosen FS, Swat W (2003) Vav1/2/3-null mice define an essential role for Vav family proteins in lymphocyte development and activation but a differential requirement in MAPK signaling in T and B cells. *J Exp Med* **198:** 1595-1608.

Galandrini R, Palmieri G, Piccoli M, Frati L, Santoni A (1999) Role for the Rac1 exchange factor Vav in the signaling pathways leading to NK cell cytotoxicity. *J Immunol* **162:** 3148-3152.

Gassmann M, Grenacher B, Rohde B, Vogel J (2009) Quantifying Western blots: pitfalls of densitometry. *Electrophoresis* **30:** 1845-1855.

Gilfillan S, Chan CJ, Cella M, Haynes NM, Rapaport AS, Boles KS, Andrews DM, Smyth MJ, Colonna M (2008) DNAM-1 promotes activation of cytotoxic lymphocytes by nonprofessional antigen-presenting cells and tumors. *J Exp Med* **205:** 2965-2973.

Graham DB, Cella M, Giurisato E, Fujikawa K, Miletic AV, Kloeppel T, Brim K, Takai T, Shaw AS, Colonna M, Swat W (2006) Vav1 controls DAP10-mediated natural cytotoxicity by regulating actin and microtubule dynamics. *J Immunol* **177:** 2349-2355.

Grzywacz B, Kataria N, Verneris MR (2007) CD56(dim)CD16(+) NK cells downregulate CD16 following target cell induced activation of matrix metalloproteinases. *Leukemia* **21:** 356-359; author reply 359.

Han J, Luby-Phelps K, Das B, Shu X, Xia Y, Mosteller RD, Krishna UM, Falck JR, White MA, Broek D (1998) Role of substrates and products of PI 3-kinase in regulating activation of Rac-related guanosine triphosphatases by Vav. *Science* **279:** 558-560.

Herberman RB, Nunn ME, Holden HT, Lavrin DH (1975a) Natural cytotoxic reactivity of mouse lymphoid cells against syngeneic and allogeneic tumors. II. Characterization of effector cells. *Int J Cancer* **16:** 230-239.

Herberman RB, Nunn ME, Lavrin DH (1975b) Natural cytotoxic reactivity of mouse lymphoid cells against syngeneic acid allogeneic tumors. I. Distribution of reactivity and specificity. *Int J Cancer* **16:** 216-229.

Hesslein DG, Takaki R, Hermiston ML, Weiss A, Lanier LL (2006) Dysregulation of signaling pathways in CD45-deficient NK cells leads to differentially regulated cytotoxicity and cytokine production. *Proc Natl Acad Sci U S A* **103:** 7012-7017.

Hof P, Pluskey S, Dhe-Paganon S, Eck MJ, Shoelson SE (1998) Crystal structure of the tyrosine phosphatase SHP-2. *Cell* **92:** 441-450.

Hoglund P, Ohlen C, Carbone E, Franksson L, Ljunggren HG, Latour A, Koller B, Karre K (1991) Recognition of beta 2-microglobulin-negative (beta 2m-) T-cell blasts by natural killer cells from normal but not from beta 2m- mice: nonresponsiveness controlled by beta 2m- bone marrow in chimeric mice. *Proc Natl Acad Sci U S A* **88:** 10332-10336.

Huang CY, Ferrell JE, Jr. (1996) Ultrasensitivity in the mitogen-activated protein kinase cascade. *Proc Natl Acad Sci U S A* **93:** 10078-10083.

Huntington ND, Xu Y, Nutt SL, Tarlinton DM (2005) A requirement for CD45 distinguishes Ly49D-mediated cytokine and chemokine production from killing in primary natural killer cells. *J Exp Med* **201:** 1421-1433.

Jiang K, Zhong B, Gilvary DL, Corliss BC, Hong-Geller E, Wei S, Djeu JY (2000) Pivotal role of phosphoinositide-3 kinase in regulation of cytotoxicity in natural killer cells. *Nat Immunol* **1:** 419-425.

Karlhofer FM, Ribaudo RK, Yokoyama WM (1992) MHC class I alloantigen specificity of Ly-49+ IL-2-activated natural killer cells. *Nature* **358:** 66-70.

Karre K, Ljunggren HG, Piontek G, Kiessling R (1986) Selective rejection of H-2-deficient lymphoma variants suggests alternative immune defence strategy. *Nature* **319:** 675-678.

Kaufmann SH (1993) Immunity to intracellular bacteria. *Annu Rev Immunol* **11:** 129-163.

Kielczewska A, Kim HS, Lanier LL, Dimasi N, Vidal SM (2007) Critical residues at the Ly49 natural killer receptor's homodimer interface determine functional recognition of m157, a mouse cytomegalovirus MHC class I-like protein. *J Immunol* **178:** 369-377.

Kiessling R, Klein E, Pross H, Wigzell H (1975a) "Natural" killer cells in the mouse. II. Cytotoxic cells with specificity for mouse Moloney leukemia cells. Characteristics of the killer cell. *Eur J Immunol* **5:** 117-121.

Kiessling R, Klein E, Wigzell H (1975b) "Natural" killer cells in the mouse. I. Cytotoxic cells with specificity for mouse Moloney leukemia cells. Specificity and distribution according to genotype. *Eur J Immunol* **5:** 112-117.

Korbel DS, Finney OC, Riley EM (2004) Natural killer cells and innate immunity to protozoan pathogens. *Int J Parasitol* **34:** 1517-1528.

Kuepfer L, Peter M, Sauer U, Stelling J (2007) Ensemble modeling for analysis of cell signaling dynamics. *Nat Biotechnol* **25:** 1001-1006.

Lee SH, Girard S, Macina D, Busa M, Zafer A, Belouchi A, Gros P, Vidal SM (2001) Susceptibility to mouse cytomegalovirus is associated with deletion of an activating natural killer cell receptor of the C-type lectin superfamily. *Nat Genet* **28:** 42-45.

Lieberman J (2003) The ABCs of granule-mediated cytotoxicity: new weapons in the arsenal. *Nat Rev Immunol* **3:** 361-370.

Ljunggren HG, Karre K (1985) Host resistance directed selectively against H-2-deficient lymphoma variants. Analysis of the mechanism. *J Exp Med* **162:** 1745-1759.

Ljunggren HG, Karre K (1990) In search of the 'missing self': MHC molecules and NK cell recognition. *Immunol Today* **11:** 237-244.

Long EO (2008) Negative signaling by inhibitory receptors: the NK cell paradigm. *Immunol Rev* **224:** 70-84.

Long EO, Barber DF, Burshtyn DN, Faure M, Peterson M, Rajagopalan S, Renard V, Sandusky M, Stebbins CC, Wagtmann N, Watzl C (2001) Inhibition of natural killer cell activation signals by killer cell immunoglobulin-like receptors (CD158). *Immunol Rev* **181:** 223-233.

Lou Z, Jevremovic D, Billadeau DD, Leibson PJ (2000) A balance between positive and negative signals in cytotoxic lymphocytes regulates the polarization of lipid rafts during the development of cell-mediated killing. *J Exp Med* **191:** 347-354.

Lu W, Gong D, Bar-Sagi D, Cole PA (2001) Site-specific incorporation of a phosphotyrosine mimetic reveals a role for tyrosine phosphorylation of SHP-2 in cell signaling. *Mol Cell* **8:** 759-769.

Luci C, Reynders A, Ivanov, II, Cognet C, Chiche L, Chasson L, Hardwigsen J, Anguiano E, Banchereau J, Chaussabel D, Dalod M, Littman DR, Vivier E, Tomasello E (2009) Influence of the transcription factor RORgammat on the development of NKp46+ cell populations in gut and skin. *Nat Immunol* **10:** 75-82.

Malmberg KJ, Ljunggren HG (2009) Spotlight on IL-22-producing NK cell receptor-expressing mucosal lymphocytes. *Nat Immunol* **10:** 11-12.

Mandelboim O, Lieberman N, Lev M, Paul L, Arnon TI, Bushkin Y, Davis DM, Strominger JL, Yewdell JW, Porgador A (2001) Recognition of haemagglutinins on virus-infected cells by NKp46 activates lysis by human NK cells. *Nature* **409:** 1055-1060.

McCann FE, Eissmann P, Onfelt B, Leung R, Davis DM (2007) The activating NKG2D ligand MHC class I-related chain A transfers from target cells to NK cells in a manner that allows functional consequences. *J Immunol* **178:** 3418-3426.

McFarland BJ, Strong RK (2003) Thermodynamic analysis of degenerate recognition by the NKG2D immunoreceptor: not induced fit but rigid adaptation. *Immunity* **19:** 803-812.

McNeill L, Salmond RJ, Cooper JC, Carret CK, Cassady-Cain RL, Roche-Molina M, Tandon P, Holmes N, Alexander DR (2007) The differential regulation of Lck kinase phosphorylation sites by CD45 is critical for T cell receptor signaling responses. *Immunity* **27:** 425-437.

Moretta A (2002) Natural killer cells and dendritic cells: rendezvous in abused tissues. *Nat Rev Immunol* **2:** 957-964.

Moretta A, Bottino C, Vitale M, Pende D, Cantoni C, Mingari MC, Biassoni R, Moretta L (2001) Activating receptors and coreceptors involved in human natural killer cell-mediated cytolysis. *Annu Rev Immunol* **19:** 197-223.

Moretta A, Vitale M, Bottino C, Orengo AM, Morelli L, Augugliaro R, Barbaresi M, Ciccone E, Moretta L (1993) P58 molecules as putative receptors for major histocompatibility complex (MHC) class I molecules in human natural killer (NK) cells. Anti-p58 antibodies reconstitute lysis of MHC class I-protected cells in NK clones displaying different specificities. *J Exp Med* **178:** 597-604.

Murphy JW, McDaniel DO (1982) In vitro reactivity of natural killer (NK) cells against Cryptococcus neoformans. *J Immunol* **128:** 1577-1583.

Orange JS (2008) Formation and function of the lytic NK-cell immunological synapse. *Nat Rev Immunol* **8:** 713-725.

Paster W, Paar C, Eckerstorfer P, Jakober A, Drbal K, Schutz GJ, Sonnleitner A, Stockinger H (2009) Genetically encoded Forster resonance energy transfer sensors for the conformation of the Src family kinase Lck. *J Immunol* **182:** 2160-2167.

Peterson ME, Long EO (2008) Inhibitory receptor signaling via tyrosine phosphorylation of the adaptor Crk. *Immunity* **29:** 578-588.

Phillips JH, Gumperz JE, Parham P, Lanier LL (1995) Superantigen-dependent, cell-mediated cytotoxicity inhibited by MHC class I receptors on T lymphocytes. *Science* **268:** 403-405.

Pogge von Strandmann E, Simhadri VR, von Tresckow B, Sasse S, Reiners KS, Hansen HP, Rothe A, Boll B, Simhadri VL, Borchmann P, McKinnon PJ, Hallek M, Engert A (2007) Human leukocyte antigen-B-associated transcript 3 is released from tumor cells and engages the NKp30 receptor on natural killer cells. *Immunity* **27:** 965-974.

Rajagopalan S, Long EO (1997) The direct binding of a p58 killer cell inhibitory receptor to human histocompatibility leukocyte antigen (HLA)-Cw4 exhibits peptide selectivity. *J Exp Med* **185:** 1523-1528.

Ranson T, Vosshenrich CA, Corcuff E, Richard O, Muller W, Di Santo JP (2003) IL-15 is an essential mediator of peripheral NK-cell homeostasis. *Blood* **101:** 4887-4893.

Reff ME, Carner K, Chambers KS, Chinn PC, Leonard JE, Raab R, Newman RA, Hanna N, Anderson DR (1994) Depletion of B cells in vivo by a chimeric mouse human monoclonal antibody to CD20. *Blood* **83:** 435-445.

Rehm M, Huber HJ, Hellwig CT, Anguissola S, Dussmann H, Prehn JH (2009) Dynamics of outer mitochondrial membrane permeabilization during apoptosis. *Cell Death Differ* **16:** 613-623.

Romagne F, Andre P, Spee P, Zahn S, Anfossi N, Gauthier L, Capanni M, Ruggeri L, Benson DM, Jr., Blaser BW, Della Chiesa M, Moretta A, Vivier E, Caligiuri MA, Velardi A, Wagtmann N (2009) Pre-clinical characterization of 1-7F9, a novel human anti-KIR therapeutic antibody that augments NK-mediated killing of tumor cells. *Blood*.

Saez-Borderias A, Romo N, Magri G, Guma M, Angulo A, Lopez-Botet M (2009) IL-12-dependent inducible expression of the CD94/NKG2A inhibitory receptor regulates CD94/NKG2C+ NK cell function. *J Immunol* **182:** 829-836.

Salazar-Mather TP, Orange JS, Biron CA (1998) Early murine cytomegalovirus (MCMV) infection induces liver natural killer (NK) cell inflammation and protection through macrophage inflammatory protein 1alpha (MIP-1alpha)-dependent pathways. *J Exp Med* **187:** 1-14.

Sandusky MM, Messmer B, Watzl C (2006) Regulation of 2B4 (CD244)-mediated NK cell activation by ligand-induced receptor modulation. *Eur J Immunol* **36:** 3268-3276.

Sanos SL, Bui VL, Mortha A, Oberle K, Heners C, Johner C, Diefenbach A (2009) RORgammat and commensal microflora are required for the differentiation of mucosal interleukin 22-producing NKp46+ cells. *Nat Immunol* **10:** 83-91.

Schilling M, Maiwald T, Bohl S, Kollmann M, Kreutz C, Timmer J, Klingmuller U (2005) Computational processing and error reduction strategies for standardized quantitative data in biological networks. *FEBS J* **272:** 6400-6411.

Shenoy-Scaria AM, Gauen LK, Kwong J, Shaw AS, Lublin DM (1993) Palmitylation of an amino-terminal cysteine motif of protein tyrosine kinases p56lck and p59fyn mediates interaction with glycosyl-phosphatidylinositol-anchored proteins. *Mol Cell Biol* **13:** 6385-6392.

Smyth MJ, Thia KY, Street SE, Cretney E, Trapani JA, Taniguchi M, Kawano T, Pelikan SB, Crowe NY, Godfrey DI (2000) Differential tumor surveillance by natural killer (NK) and NKT cells. *J Exp Med* **191:** 661-668.

Stebbins CC, Watzl C, Billadeau DD, Leibson PJ, Burshtyn DN, Long EO (2003) Vav1 Dephosphorylation by the Tyrosine Phosphatase SHP-1 as a Mechanism for Inhibition of Cellular Cytotoxicity. *Mol Cell Biol* **23:** 6291-6299.

Tabiasco J, Rabot M, Aguerre-Girr M, El Costa H, Berrebi A, Parant O, Laskarin G, Juretic K, Bensussan A, Rukavina D, Le Bouteiller P (2006) Human decidual NK cells: unique phenotype and functional properties -- a review. *Placenta* **27 Suppl A:** S34-39.

Trinchieri G, Valiante N (1993) Receptors for the Fc fragment of IgG on natural killer cells. *Nat Immun* **12:** 218-234.

Ugolini S, Vivier E (2000) Regulation of T cell function by NK cell receptors for classical MHC class I molecules. *Curr Opin Immunol* **12:** 295-300.

Upshaw JL, Arneson LN, Schoon RA, Dick CJ, Billadeau DD, Leibson PJ (2006) NKG2D-mediated signaling requires a DAP10-bound Grb2-Vav1 intermediate and phosphatidylinositol-3-kinase in human natural killer cells. *Nat Immunol* **7:** 524-532.

Vales-Gomez M, Chisholm SE, Cassady-Cain RL, Roda-Navarro P, Reyburn HT (2008) Selective induction of expression of a ligand for the NKG2D receptor by proteasome inhibitors. *Cancer Res* **68:** 1546-1554.

Valiante NM, Uhrberg M, Shilling HG, Lienert-Weidenbach K, Arnett KL, D'Andrea A, Phillips JH, Lanier LL, Parham P (1997) Functionally and structurally distinct NK cell receptor repertoires in the peripheral blood of two human donors. *Immunity* **7:** 739-751.

Vanherberghen B, Andersson K, Carlin LM, Nolte-'t Hoen EN, Williams GS, Hoglund P, Davis DM (2004) Human and murine inhibitory natural killer cell receptors transfer from natural killer cells to target cells. *Proc Natl Acad Sci U S A* **101:** 16873-16878.

Veillette A (2006) NK cell regulation by SLAM family receptors and SAP-related adapters. *Immunol Rev* **214:** 22-34.

Wagtmann N, Biassoni R, Cantoni C, Verdiani S, Malnati MS, Vitale M, Bottino C, Moretta L, Moretta A, Long EO (1995a) Molecular clones of the p58 NK cell receptor reveal immunoglobulin-related molecules with diversity in both the extra- and intracellular domains. *Immunity* **2:** 439-449.

Wagtmann N, Rajagopalan S, Winter CC, Peruzzi M, Long EO (1995b) Killer cell inhibitory receptors specific for HLA-C and HLA-B identified by direct binding and by functional transfer. *Immunity* **3:** 801-809.

Wahle JA, Paraiso KH, Kendig RD, Lawrence HR, Chen L, Wu J, Kerr WG (2007) Inappropriate recruitment and activity by the Src homology region 2 domain-containing phosphatase 1 (SHP1) is responsible for receptor dominance in the SHIP-deficient NK cell. *J Immunol* **179:** 8009-8015.

Walzer T, Blery M, Chaix J, Fuseri N, Chasson L, Robbins SH, Jaeger S, Andre P, Gauthier L, Daniel L, Chemin K, Morel Y, Dalod M, Imbert J, Pierres M, Moretta A, Romagne F, Vivier E (2007a) Identification, activation, and selective in vivo ablation of mouse NK cells via NKp46. *Proc Natl Acad Sci U S A* **104:** 3384-3389.

Walzer T, Jaeger S, Chaix J, Vivier E (2007b) Natural killer cells: from CD3(-)NKp46(+) to post-genomics meta-analyses. *Curr Opin Immunol* **19:** 365-372.

Watzl C (2003) The NKG2D receptor and its ligands-recognition beyond the "missing self"? *Microbes Infect* **5:** 31-37.

Watzl C, Long EO (2003) Natural killer cell inhibitory receptors block actin cytoskeleton-dependent recruitment of 2B4 (CD244) to lipid rafts. *J Exp Med* **197:** 77-85.

Watzl C, Stebbins CC, Long EO (2000) NK cell inhibitory receptors prevent tyrosine phosphorylation of the activation receptor 2B4 (CD244). *J Immunol* **165:** 3545-3548.

Welte S, Kuttruff S, Waldhauer I, Steinle A (2006) Mutual activation of natural killer cells and monocytes mediated by NKp80-AICL interaction. *Nat Immunol* **7:** 1334-1342.

Yokoyama WM, Kim S (2006) Licensing of natural killer cells by self-major histocompatibility complex class I. *Immunol Rev* **214:** 143-154.

Yu TK, Caudell EG, Smid C, Grimm EA (2000) IL-2 activation of NK cells: involvement of MKK1/2/ERK but not p38 kinase pathway. *J Immunol* **164:** 6244-6251.

Zhang Y, Wallace DL, de Lara CM, Ghattas H, Asquith B, Worth A, Griffin GE, Taylor GP, Tough DF, Beverley PC, Macallan DC (2007) In vivo kinetics of human natural killer cells: the effects of ageing and acute and chronic viral infection. *Immunology* **121:** 258-265.

7. Abbreviations

ADCC	antibody-dependent cellular cytotoxicity
CD	cluster of differentiation
CRACC	CD2-like receptor-activating cytotoxic cells
CTX	Choleratoxin
DAP	DNAX activation protein
DC	dendritic cells
DMSO	Dimethylsulfoxide
E.coli	*Escherichia coli*
ERK	Extracellular signal-regulated kinase
GEF	guanine exchange factor
GM-CSF	granulocyte-macrophage colony-stimulating factor
GST	glutathione-S-transferase
GTPases	guanosine triphosphatase
HLA	human leukocyte antigen
IFN	interferon
Ig	Immunoglobulin
IL	interleukin
IS	immunological synapse
ITAM	immunoreceptor tyrosine-based activation motif
ITIM	immunoreceptor tyrosine-based inhibition motif
ITSM	immunoreceptor tyrosine-based switch motif
KIR	killer cell Ig-like receptors
Klra	killer cell lectin-like receptor family a
LFA	lymphocyte function-associated antigen
LILR	leukocyte immunoglobulin like receptor
MAPK	mitogen activated protein kinase
MEK	mitogen-activated protein kinase kinase
MFI	mean fluorescence intensity
MHC	major histocompatibility complex
MICA/B	MHC class I related chain A and B
m**in**	minute
MTOC	microtubule-organizing center

NCR	natural cytotoxicity receptors
NK	Natural killer
PBL	peripheral blood lymphocytes
PI3K	phosphatidylinositol-3-kinase
PLC	phospholipase C
SDS-PAGE	sodium dodecyl sulfate polyacrylamide gel electrophoresis
SFK	Src family kinases
SHP	SH2 containing protein tyrosine phosphatases
Siglecs	sialic-acid-binding immunoglobulin-like lectins
SLAM	signaling lymphocyte activation molecule
SRR	SLAM related receptors
TNF	tumor necrosis factor